Characterizing Turbulent Spray Deposition from Self-Propelled Sprayers

CARP Project 2016.8

Final Report

Tom Wolf, Ph.D.
Agrimetrix Research & Training

11/30/2021

Agrimetrix

Table of Contents

Executive Summary

Field tests were done to document the deposition variability of sprays from self-propelled sprayers. Several approaches were taken. First, deposition data from historical drift trials using petri plates were analyzed to identify trends with application method. Second, the effect of boom stability on deposit patternation was tested for a number of travel speeds and boom heights. Third, the effect of spray quality, boom height, and travel speed on boom-wide spray deposits was quantified across and along the direction of travel using a 2 mm diameter monofilament string. Finally the aerodynamic turbulence caused by a sprayer was evaluated using computational fluid dynamics (CFD).

Overall, deposit variability as measured by Coefficient of Variation (CV) was higher than expected, averaging 16% for the historical data (min=9%, max= 37%), 22% for the straw collector data (min=12%, max=49%) and 31% for the string data (min=18%, max= 56%). For the string data, a CV of 31% corresponded to a ratio of the highest to the lowest deposit of that particular pattern of about 7-fold.

Deposition was less uniform across the width of the boom as it was along the direction of travel. Higher wind speeds increased variability, as did a combination of higher booms and faster travel speeds. Finer sprays also tended to deposit less uniformly.

Deposit patterns, and the magnitude of the associated variability, were only moderately repeatable, but some similar trends were apparent. The first was the downwind displacement of the edges of the spray swath. The second was the overall lower deposition in the wake of the sprayer wheel tracks. The final common observation was the greater variability of the deposit in the centre of the spray boom, behind the tractor unit, than on either of the left or right spray boom wings.

Efforts to reduce the variability using lower booms, lower speeds, and coarser sprays met with some success. However, even the “best” configuration of sprayer (low boom, slow travel speed, and coarser spray) was only somewhat more uniform compared to the alternative (high boom, fast speed, and finer sprays), improving the CV by about 5% each time one such variable was changed. Benefits did not accumulate when all improvements were made. Only in the 2020 set of trials did the deposit CV improve by more, in this case 15%, from “High & Fast” to “Low & Slow”.

Computational Fluid Dynamics studies showed that disturbances in the flow field were increased with travel speed and boom height Both upward and lateral components were increased similarly, increasing the potential for spray droplets to be directed off target.

Tire width had an impact on flow field disturbances. Not only was greater turbulence observed in the wake of the wider tires, the width of the tire-induced wake was several tire widths more than the width of the tractor unit.

The overall influence of flow field disturbance extended to simple boom structural components, although the downfield reach of these was less extensive than of the tractor unit wake. Nonetheless, the upward and horizontal flows that were generated have the capacity to displace the small droplets in a spray cloud, affecting spray deposition and airborne movement beyond what is predicted by a static pattern test.

Introduction

The uniformity of a spray deposit is fundamental to a successful spray application. Spray dosage is directly related to pesticide performance. Regions of under-dosing represent poor pest control, whereas over-dosing represent waste. As a result, the spray industry has used a benchmark of 5% variation in flow rate for nozzles, and 15% coefficient of variation (CV) for the deposit under the boom.

Initial studies on deposit uniformity focused on single or multiple nozzles positioned over a patternator, a collection device with multiple troughs that separate the spray pattern into various channels of, say, 1 to 5 cm resolution (Ozkan and Ackerman, 1992). By collecting the spray for a period of time, the volume in each channel is recorded and the variability calculated. This "static patternation" was done under lab conditions with a fixed boom and patternator and is still used by nozzle manufacturers to assure the proper design and operation of their nozzles and can also be used to study boom movement and wind displacement.

The parameter used to quantify variability was suggested to be the "coefficient of variation" or CV. It is defined as the standard deviation of a set of measurements expressed as a percentage of the mean of those same observations.

$$CV\ (\%) = \frac{Standard\ Deviation}{Mean} * 100$$

Smith (1992) identified other possible variables to predict deposit variability and found the range between maximum and minimum values to be closely correlated to CV. This did not, however, provide an opportunity to reduce the number of measurements required to characterize a deposit, and CV has remained the standard parameter. Smith found benchmarks of 15% and 30% CV to have the ratio of maximum to minimum deposits to be about 1.5 and 2.7, respectively.

The "span" of a distribution may also be a way to describe its characteristics. By definition, span is the difference between the 90th and 10th percentile divided by the 50th percentile.

$$Span = \frac{90th\ percentile - 10th\ percentile}{50th\ percentile}$$

Span values may be zero for a perfectly uniform distribution, or approach 2 or more for very variable distributions. For both Span and CV, the values will depend on the number of observations. Similar minimum, maximum, and average deposit values will result in the same CVs, but methods that have more observations in the dataset that fill in the intermediate values will have lower CVs (Table 1). As a result, it is not accurate to compare variation between differing methodologies.

Table 1: Effect of numerical sample characteristics on descriptive parameters.

Location	Dataset 1	Dataset 2	Dataset 3	Dataset 4
1	1	1	1	1
2	9	5	3	2
3	17	9	5	3
4		13	7	4
5		17	9	5
6			11	6
7			13	7
8			15	8
9			17	9
10				10
11				11
12				12
13				13
14				14
15				15
16				16
17				17
Min	1	1	1	1
Max	17	17	17	17
Range	16	16	16	16
Ratio	17	17	17	17
Mean	9.0	9.0	9.0	9.0
Std. Dev.	6.5	5.7	5.2	4.9
CV	**72.6**	**62.9**	**57.4**	**54.4**
10^{th} Perc.			1.0	1.8
50th Perc.			9.0	9.0
90th Perc.			17.0	16.2
Span			**1.78**	**1.60**

Research increasingly focused on the impact of boom stability on pattern uniformity. In one such study, Krishnan *et al.* (2005) simulated boom sway in accordance with separate field observations and reported acceptable deposit variability, with CV values ranging from 8.5 to 13%. Herbst and Wolf (2001) recognized that field conditions introduced weather variability that made fair, standardized tests very difficult to reproduce. They developed a servo-hydraulic vibration test bench system in which a sprayer was parked, simulating bumpy terrain. Spray deposits were measured on a moving conveyor under the boom. As a result, dynamic boom movements could be evaluated without the confounding effects of variable weather conditions, however, forward travel speed could not be simulated. Tests along the boom of trailed and mounted sprayers gave deposit CV results from 10 to 22%. In field tests evaluating the direction of travel, CV values ranged from 10 to 20%, with greater variability further out from the sprayer body, as expected.

Lardoux *et al.* (2007) similarly studied the impact of boom movements on spray distribution with a conveyor and shaking platform under laboratory conditions. Static and dynamic distributions had the same overall response to boom height, boom speed, and nozzle type in dynamic conditions, but the magnitude of the variability was greater under dynamic testing. Both roll and yaw increased unevenness. For roll movements, changes in nozzle heights explained the variations.

Although easier to implement, stationary booms could not adequately simulate the variability under field conditions, where variability was additionally impacted by forward travel speed as well as ambient weather conditions. Aerial application, for which static patternation was not possible because atomization and distribution depended on flight speed, provided the necessary tools. "Dynamic patternation" studies were developed by Yates (1962, using plexiglass plates as collectors and tracer metals in the spray tank that were quantified using flame ionization. Aircraft sprayed a tracer-dye as they flew over a collector system, most commonly string or water-sensitive paper, as described by Whitney and Roth (1985). A cotton sting with a diameter of about 1 mm was considered an optimal collector. Carlton *et al.* (1990) studied monofilament line as a collector and found inconclusive results regarding the preferred diameter, with lines as small as 0.18 mm and lines as thick as 3.18 mm showing acceptable capture of a variety of spray qualities.

Dynamic methods permitted the evaluation of moving ground sprayers. Smith (1992) showed that deposit variation was greater under field than laboratory conditions. Of 36 separate spray passes in the field, 13 (36%) had CV values less than 15%, and when the nozzles were pointed back, five of 24 passes had CV values less than 15%. Under lab conditions, 77% and 96% of runs, respectively, had acceptably low CV values. Higher water volumes tended to improve deposit uniformity.

Womac *et al.* (2001) studied two sprayer nozzles at various travel speeds under calm wind conditions and concluded that field applied CV values of coverage on water-sensitive cards ranged from 13% to 21% for all nozzles compared to 4% to 16% for a static spray pattern uniformity test. They concluded that acceptable coverage could be achieved with a sprayer travelling between 6.4 and 27.9 km/h.

Moving booms create characteristic wake effects, not only from the boom components themselves, but also from the spray pattern created by the nozzles. Young (1990) showed that the spray pattern blocks air movement, forcing air to flow around the spray sheet. This draws fine droplets away from the center of the spray pattern. Even slow travel speeds were able to displace spray from the centre of a single nozzle and re-distribute it at the edges of the pattern, altering the deposited dose directly underneath the nozzle (Wolf *et al.*, 1997). In wind tunnel studies, Farooq *et al.* (2001) showed that the turbulent wake of the spray pattern altered the flight path of droplets in accordance with their size class. Droplets >200µm retained their vertical trajectory, whereas droplets between 50 and 200 µm were swept back significantly. Droplets less than 50 µm moved in a variety of directions, including back towards the spray plume. Thistle *et al.* (2004) showed that small (50 µm) droplets introduced into an ambient vortex moved in a circular motion, whereas larger (350 µm) droplets moved in a linear fashion. This has implication not just for initial displacement, but for longer susceptibility to in-flight evaporation, resulting in reductions in size and propensity for further displacement.

Aerodynamic turbulence was purposely generated with a bluff plate sprayer by Furness *et al.* (2001). Their study evaluated various spray volumes, spray qualities, and travel speeds on spray deposition. The study showed significant increases in spray deposit resulting from the bluff-plate (a wedge-shaped shield installed in front of the spray boom) but also an apparent (though not quantified) increase in deposit variability. This study illustrated the greater sensitivity of finer sprays to turbulent displacement, as expected, with both

positive (greater deposition on spray targets) and negative (greater variability) effects that need to be balanced.

Whereas the spray pattern created a unique set of aerodynamic conditions, the sprayer and boom itself has the potential to add to this complexity. Teske *et al.* (2015) measured the air velocities of a scaled sprayer model in a wind-tunnel and documented significant variation on the velocity characteristics as measurements proceeded from the centre of the sprayer (behind the tractor unit) to the boom. They concluded that the turbulence translated into additional time spent aloft by the particles. In addition to any crosswind behind the tractor/boom model, their results suggested that the tractor/boom wake could increase airborne particle drift (especially for smaller particles).

Landry and Wolf (2019) measured aerodynamic turbulence behind a moving sprayer using sonic anemometry. Total Kinetic Energy (TKE) was impacted significantly by location of measurement (open boom vs wheel plus boom), travel speed, and distance behind boom. TKE was not affected by the presence of a spray. However, the impact of the airflow on the spray pattern was not evaluated. The lack of aerodynamic influence of the spray patterns was also found by Teske *et al.* (2015) in a wind tunnel study.

Computational Fluid Dynamics (CFD) was first shown to be a useful tool for simulating aerodynamic behaviour of pesticide spray particles by Reichard *et al.* (1992). They validated the predicted drift distance of droplets of various sizes with FLUENT using wind tunnel test and found them to be in general agreement. Tsay *et al.* (2002) evaluated six shield designs on a spray boom using Fluent and was able to assess their effects on spray drift potential of a range of droplet sizes. Their results had agreement with subsequent wind tunnel tests of some similar designs by Sidahmed *et al.* (2004). In both cases, the evaluations focused on sections of the boom in the absence of a cross wind or a tractor unit and did not study the uniformity of the resulting deposit.

Previous Data

Spray Drift Trials

Spray drift trials often include information about the on-swath deposition of spray to arrive at a mass balance. Agriculture and Agri-Food Canada (AAFC) and the Saskatchewan Research Council (SRC) collaborated in spray drift trials between 1986- and 1992 (Wolf at al, 1991, Grover at al., 1995), and these historical data were added to more recent datasets continuing until 2011 to arrive at 154 trials for which on-swath deposit was available. Never having been analyzed before, these trials included a variety of spray qualities, boom heights, travel speeds, wind speeds, and boom shrouds.

In all trials, 24 petri plates were positioned on the spray swath in a grid, 6 positions along the swath, and 4 positions across the swath (Figure 1). The variability in the amount of spray that deposited could be calculated for each trial. Although this array was measured and repeated with approximately 25 cm location accuracy, it did not correspond to any specific boom location and should be viewed as a random sample of deposition. It is nonetheless useful to use the datasetto identify some relationships.

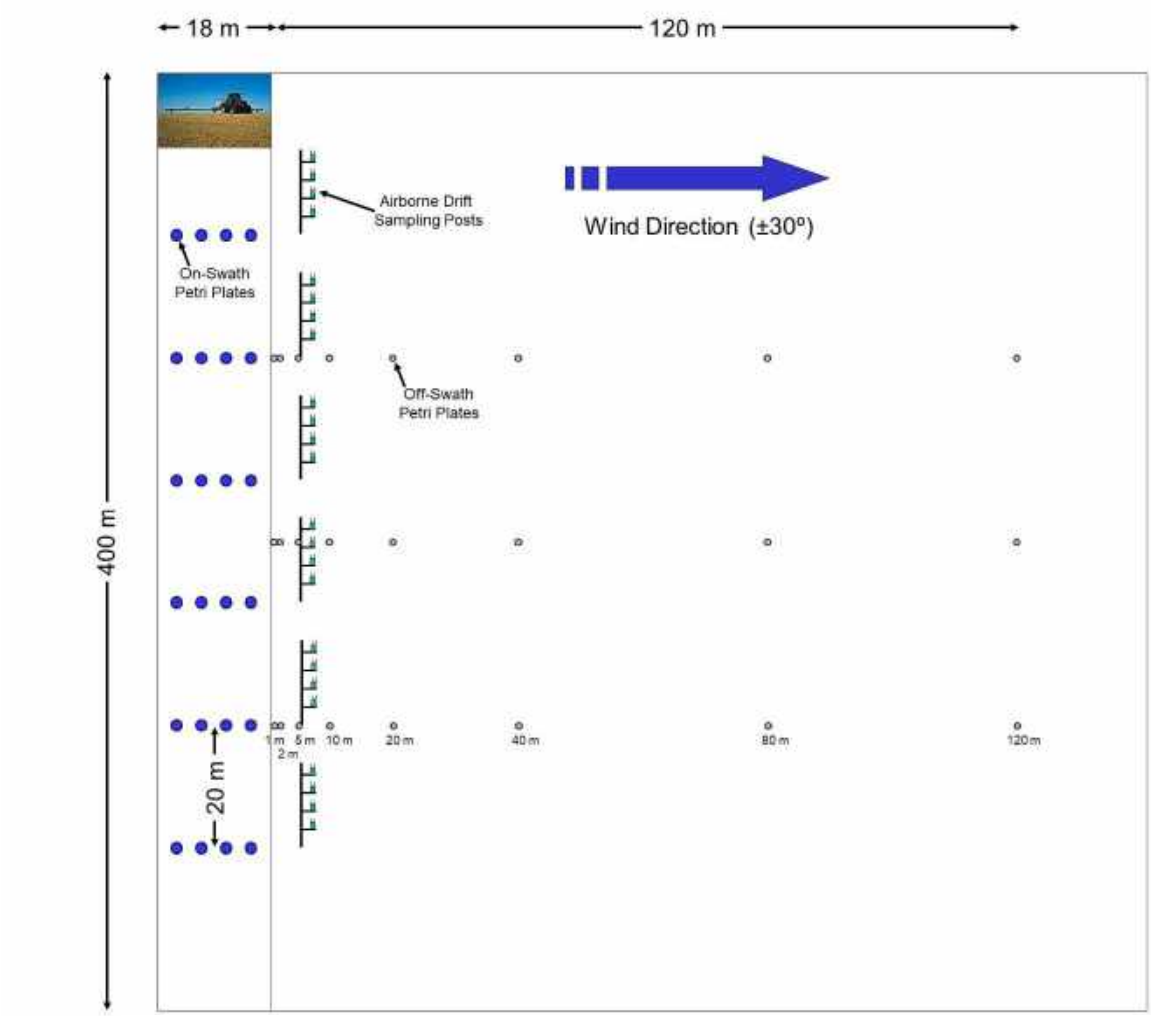

Figure 1: Sampler layout for spray drift trials. The array of on-swath petri plates can be used to calculate spray deposit amount and its variability.

Effect of Wind Speed on Deposit CV

Shrouded booms were removed from this analysis. Overall deposit variability from 5% to 40% was observed in 112 trials (Figure 2). There was a trend for deposit CV to increase with wind speed, although with considerable variability in this response. The R-squared value of 0.166 indicating that wind speed was unable to account for the majority of the variation in response. Nonetheless, it makes sense that higher wind speeds may result in higher CVs due to the associated turbulence and gusting that can displace sprays from their intended path.

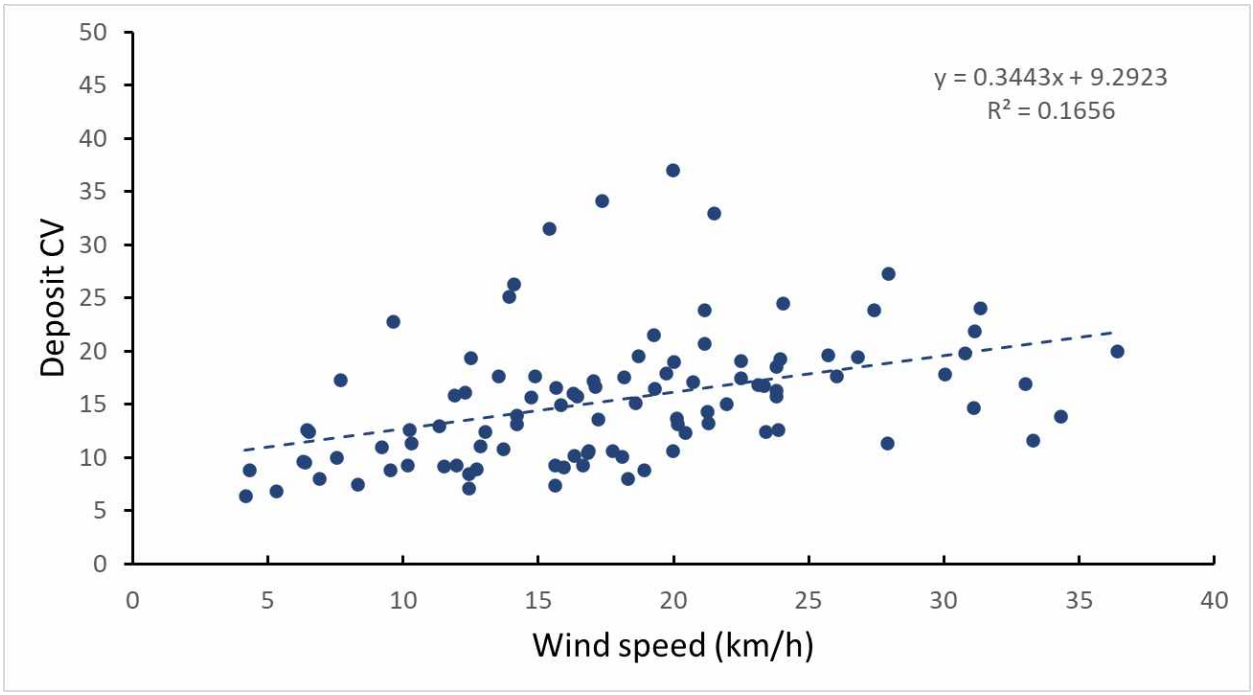

Figure 2: Relationship of wind speed and deposit CV for 112 drift trials

Effect of Spray Quality on Deposit CV

Five spray qualities were identified for the drift trials. There were no strong trends with spray quality, except that the Fine sprays tended to have higher CVs than the coarser sprays (Figure 3).

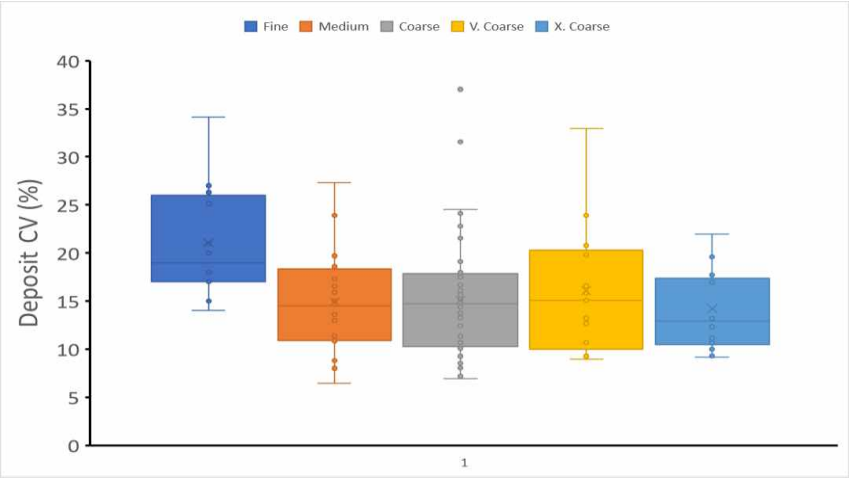

Figure 3: Effect of spray quality on deposit CV

Effect of Boom Height and Travel Speed

The data were separated into two broad groups, one of which was sprayers that had high booms (>50 cm) and travelled fast (> 16 km/h), and another group with lo booms (<=50 cm) that travelled slowly (8-16 km/h). For both groups of conditions, deposit CVs increased with wind speed, as before. However, the "Low and Slow" configuration had overall lower CVs than the "High and Fast" configuration (Figure 4). The advantage was about 3% CV lower for the "Low and Slow" setup.

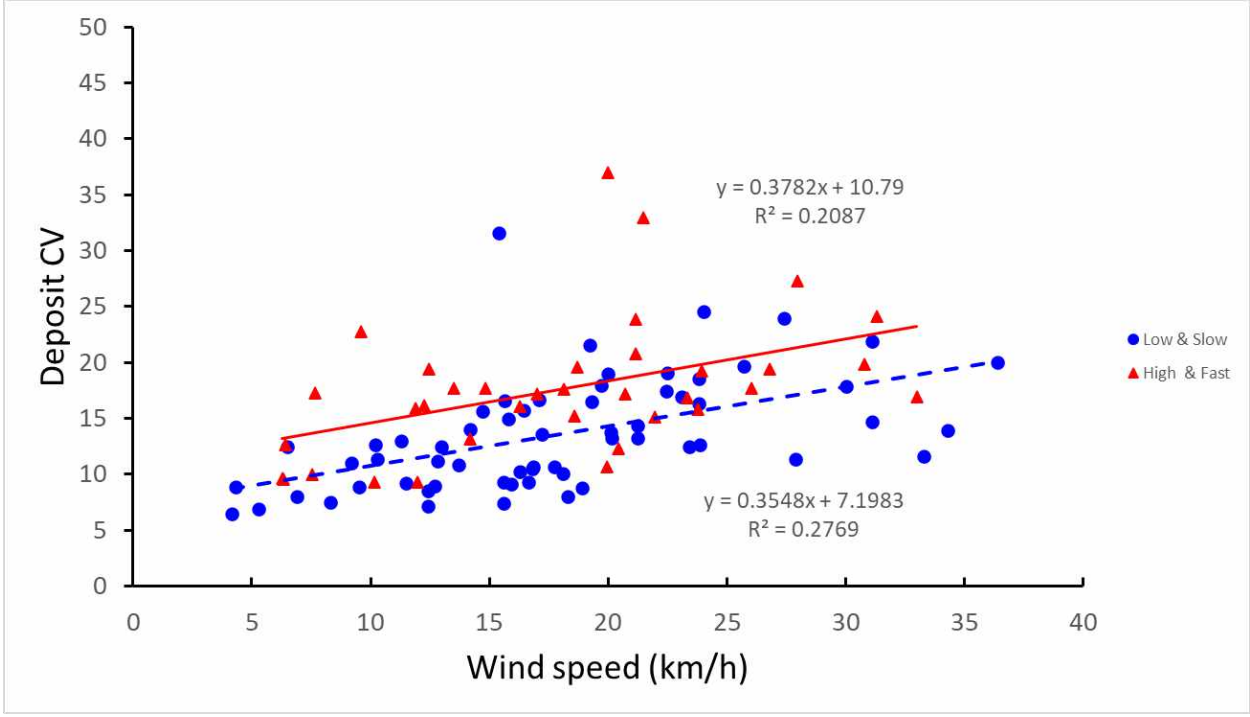

Figure 4: Effect of boom height and travel speed on deposit CV

Effect of Shrouds

The dataset for sprayers with shrouds was small in comparison to the other dataset, and sprayer configurations without shrouds were limited to those that matched the shrouds in spray quality and travel speed. The shrouds (a combination of AgShield, Flexi-Coil, and Brandt) seemed to increase deposit CVs at the higher wind speeds (Figure 5). These shrouds were designed to reduce spray drift, and any impact on deposit uniformity would not have been intended. Aerodynamic impacts on deposition may need to be considered separately.

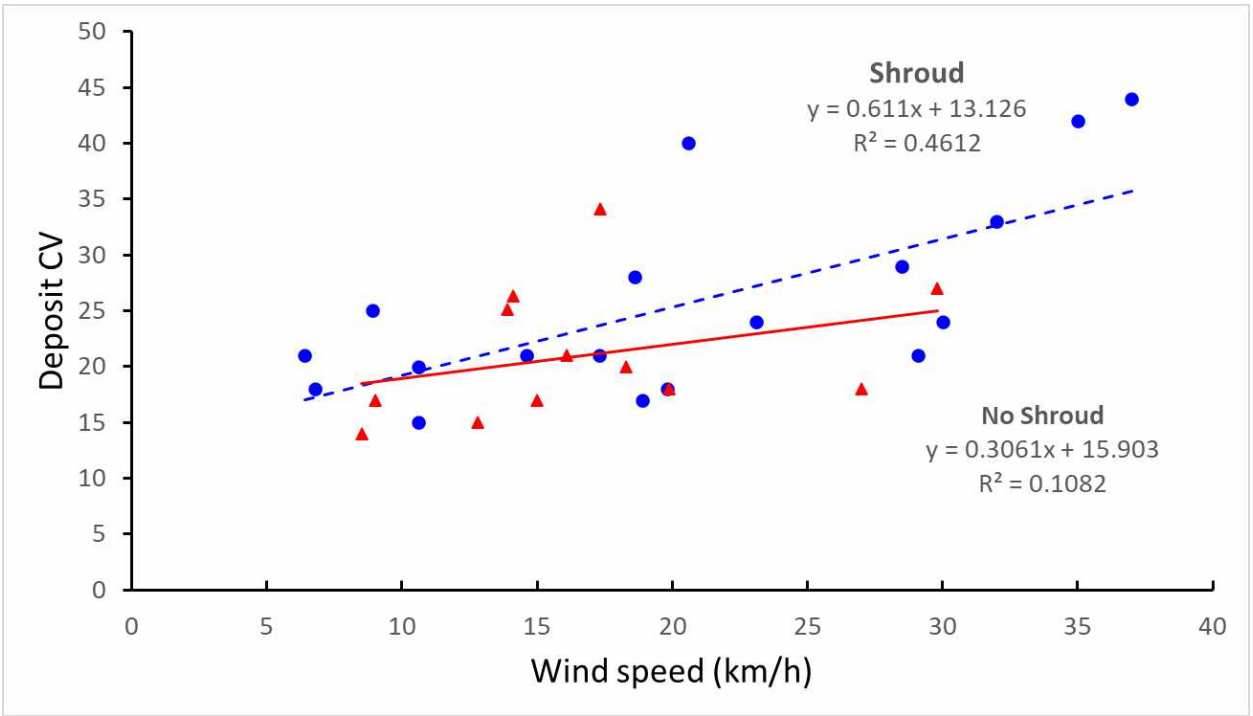

Figure 5: Effect of protective shrouds on deposit CV

Aerodynamic Foils

As part of a student design project, spray deposition from three boom configurations were evaluated. But rather than focusing on the variability under the boom, the students studied displacement from the intended spray swath on either side. They measured this displacement starting at the edge of the spray swath and continued a further 60 cm outward from there.

The three spray booms tested were an unmodified boom (Figure 65), one that contained a downward turned foil (Figure 66), and a third that contained a horizontal "Splitter" designed to reduce vortex shedding (Figure 67).

This small study showed that the moving boom caused a re-direction of the airflow down toward the ground. This compressed the air under the passing boom, prompting the high pressure air to escape outward towards the boom edge. As a result, any entrained spray in that airmass also moved out from under the boom, as shown by the higher deposits on both sides of the swath, and a somewhat lower deposit under the centre. Although this effect was small in magnitude, and was also possibly an artifact of the testing conditions, this displacement of the spray showed the sensitivity of altered airflow in the wake of a boom containing a structure capable of modifying airflow.

Current studies

Objectives

The objective of this project was to document the spray deposit distribution of a high-clearance spray boom under a variety of test conditions with a view to identifying means of improving deposition uniformity.

Deviations

Initially, the project proposed to test a large number of configurations of sprayers to define the ideal way to minimize deposit variability. On conducting and evaluating the data from the initial trials, it became apparent that the variability of deposits was much greater than had been published in the scientific literature, and that changes in sprayer configuration did not translate into predictable deposit patterns. As a result, the emphasis became to try to understand the basic components of the deposit profile with a view to identify sprayer design features that may contribute to the observed variability. Sampling focused on high resolution documentation of pattern (120 30 cm increments across a 36 m boom) in place of subsampling the deposits in a smaller number of locations.

There were two phases in the study (revised from three). In the first phase, the deposit assessments provided insight into possible sources of deposit variation. In the second phase, computational fluid dynamics (CFD) was used to compare two main configurations that were evaluated, and to evaluate the possible impacts that the sprayer wheels may have on spray deposition. The third phase, to test an optimized sprayer based on the experience with CFD, was deleted from the study with the approval of the CARP project manager.

The CFD portion of this study was contracted to PAMI and was planned and analyzed in consultation. The PAMI report will be treated as a stand-alone portion of the project and will not be discussed in this portion of the report.

Methods

Study 1: The effect of boom height and travel speed on spray deposition

Studies were conducted on September 5, 2016 to assess the impact of several application variables on spray deposition from a high-clearance sprayer (Rogator RG1100B) equipped with a 36 m boom. Collaborators in the study were PAMI and NORAC. The trials were conducted on a farm field near Humboldt, SK between 11 am and 4 pm. Conditions were calm, with occasional small wind gusts (Table 2).

Table 2: Details for 2016 trials

Time	Air Temperature (°C)	Relative Humidity (%)	Wind Gusts (km/h)	Wind direction (°)
11:00	11 - 12	61-77	7-13	40-90

The spray boom was fitted with Greenleaf AirMix 11004 nozzles spaced at 20” and operated at 40 psi, producing a Coarse spray quality. Experimental variables were four boom heights (8”, 16”, 32”, and 64” above target) and three travel speeds (8, 14, and 20 mph). Treatments were replicated three times. A total of 36 sprayer runs were scheduled to be conducted, but the high speed, low boom treatments were eliminated because the boom wayed slightly from its set height and knocked over the sampling posts.

Spray deposits were collected at three locations under the boom (inner, middle, and outer section of the left wing) distanced 4 m, 10 m, and 16 m from the centre of the sprayer. A 1-m wide array of samplers was located at each location. The samplers were plastic drinking straws measuring 1.25 cm in diameter and 11.25 cm length. Five samplers were fitted onto a sampling pole with a 1-m long horizontal bar that held samplers at 25 cm intervals (Figure 6). Two parallel rows of these sampler sections were separated by 3 m, comprising a total of 6 m sampled using 30 samplers were used for each spray pass. A total of 1020 samplers were exposed to dye in these trials and analyzed by fluorimetry.

Figure 6: One m wide sampling pole with samplers spaced 25 cm apart

The sprayer tank contained a fluorescent dye (Rhodamine WT) at 0.1% v/v as well as a non-ionic surfactant (AgSurf) at 0.2% v/v to simulate the surface tension of a pesticide formulation.

Immediately after a spray pass, samplers were removed from their holders and placed into borosilicate cuvettes for later analysis.

Figure 7: Spray pass over sample array

In the lab, 20 mL of 95% ethanol was added to each cuvette and analyzed by fluorimetry. On data reduction, dye deposits could be expressed as L/ha and related to the emitted spray amounts.

The data were used to measure the total spray deposit amount and the variability of that deposit (CV). The CV of the spray under various parts of the boom could be compared, and the impact of travel speed and boom height could be assessed.

Actual boom height at the sampling locations varied from the intended settings due to natural movement of the boom. A laser height sensor was employed to assess the actual boom height and relate it to the location of the samplers.

Study 2: Spray deposit variability as influenced by travel speed, boom height and spray quality

Studies were conducted in 2017, 2019, and 2020 using similar methodology but different sprayers and variables.

To measure deposition, a sampling method that allowed a sprayer wheel to pass over the sampler prior to the spray was needed. A 40 m long 2 mm diameter polyethylene line was used as the collector. The line was stretched across the spray swath, perpendicular to the direction of travel, and held 10 cm above ground by supporting wire frames placed at 9 m intervals. The sprayer wheels were thus able to pass over the string as it returned to its sampling height prior to being exposed to the spray. Each line was marked at 0, 18, and 36 m to indicate the locations of the swath centreline and its edges. The centreline of the field swath was also marked with coloured flags to assist the driver in navigating accurately. Based on observations during the trials, navigation accuracy of 15 cm could be achieved fairly consistently. Nonetheless, superimposition of subsequent spray passes should not be expected to exceed that level of accuracy.

The first study was conducted on October 11, 2017 to identify the impact of two spray qualities (Coarse and Extremely Coarse), travel speeds (15 and 7.5 mph), and boom heights (25" and 35") on spray deposition uniformity across the entire 36 m boom width of a John Deere r4045 sprayer fitted with 380/105 R50 tires. Eighteen trial runs were collected, exposing 28 strings to spray deposits (Table 3). Collaborators in the study were John Deere (Pattison Agriculture) who supplied the equipment and site.

Table 3: Details for 2017 trials

String	Line Location	Time	Nozzle	Pressure (psi)	Boom (in)	Speed (mph)	Wind (km/h)	Air Temp (C)
17-01	90°	14:06:00	LDX11004	60	25	15	17.7	17
17-02	90°	14:22:17	LDX11004	60	25	15	19.5	17
17-03	90°	14:37:17	ULD11004	60	25	15	17.5	17
17-04	90º	14:47:17	ULD11004	60	25	15	10.2	17
17-13	90°	16:24:40	ULD11004	60	25	15	5.0	17
17-14	90°	16:30:57	LDX11004	60	25	15	5.8	17
17-15 A	180° 14 m	12:15:00	ULD11004	60	25	15	7.9	10
17-16 B	180° 7 m	12:15:00	ULD11004	60	25	15	7.9	10
17-17 C	180° 0.5 m downwind of wheel	12:15:00	ULD11004	60	25	15	7.9	10
17-18 D	180° mid track	12:15:00	ULD11004	60	25	15	7.9	10
17-19 E	180° 0.5 m upwind of wheel	12:15:00	ULD11004	60	25	15	7.9	10
17-20 F	90º	12:15:00	ULD11004	60	25	15	7.9	11
17-21 G	180° 14 m	12:31:00	LDX11004	60	25	15	20.0	11
17-22 H	180° 7 m	12:31:00	LDX11004	60	25	15	20.0	11
17-23 I	180° 0.5 m downwind of wheel	12:31:00	LDX11004	60	25	15	20.0	11
17-24 J	180° mid track	12:31:00	LDX11004	60	25	15	20.0	11
17-25 K	180° 0.5 m upwind of wheel	12:31:00	LDX11004	60	25	15	20.0	11
17-26 L	90°	12:31:00	LDX11004	60	25	15	20.0	11
17-27 M	90°	12:48:00	LDX11004	60	25	7.5	16.5	12
17-28 N	90°	12:55:00	LDX11004	60	25	7.5	19.7	12
17-29 O	90°	13:01:00	LDX11004	60	25	7.5	7.9	12
17-31 Q	90°	13:16:20	LDX11004	60	35	15	17.4	12
17-32 R	90°	13:21:50	ULD11004	60	35	15	14.5	12
17-33 S	90°	13:27:00	ULD11004	60	35	15	9.1	12
17-34 T	90°	13:33:40	LDX11004	60	35	15	16.5	12
17-35 U	90°	13:41:30	ULD11004	60	35	15	6.0	12
17-36 V	90°	13:46:30	LDX11004	60	35	15	10.5	12

Two of the sprayer passes differed from the others. In these, the deposition pattern in the direction of travel was compared to that along the width of the boom for two spray qualities (LDX11004, Coarse, and ULD11004, Extremely Coarse). Five strings were placed parallel to the direction of travel. One was located 4 m downwind from the left boom end, a second 11 m downwind from the end, and a third 15.5 m (0.5 m upwind from the upwind edge of the upwind wheel). Two additional strings were placed under the centre of the sprayer and 0.5 m downwind of the downwind edge of the downwind sprayer wheel. A sixth string was placed perpendicular to the direction of travel (Figure 8).

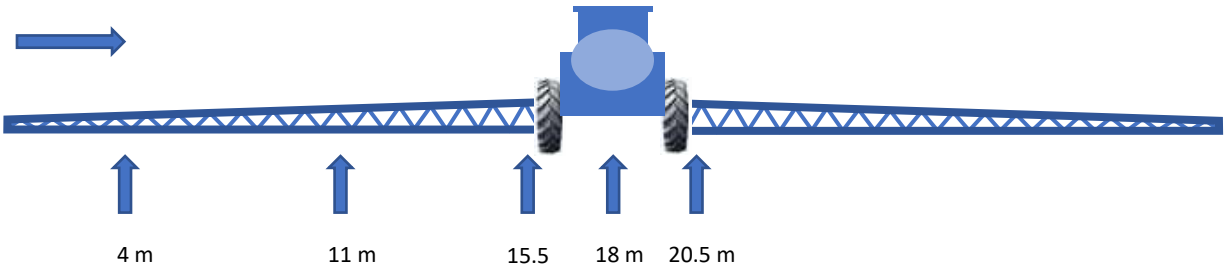

Figure 8: Perpendicular string layout positions. Horizontal arrow shows wind direction.

The second study was conducted on July 3, 2019 at a site near Dundurn, SK. Collaborators were PAMI and the University of Saskatchewan. The land owner, Ben Vanderkooi, supplied the sprayer, a John Deere R4045 with 120' boom and fitted with 380/105 R50 tires. Due to an unexpected shower, this study had to be aborted and only one pass, with two sampler strings, was completed.

Table 4: Details for 2019 trials

String	Orientation	Time	Nozzle	Pressure (psi)	Boom ht (in)	Speed (mph)	Wind (km/h)	Temp (C)
19-02 (L1,2,3)	90°	13:37	LDX11002	80	24	17	9.1	19.1
19-03 (L1,2,3)	90°	13:34	LDX11004	80	24	17	6.4	21.5
19-04 (L1,2,3)	90°	14:13	LDX11004	80	40	17	14.1	23.2
19-05 (L1,2,3)	90°	14:55	LDX11004	80	40	7.3	14.2	23.5
19-06 (L1,2,3)	90°	15:37	LDX11004	80	24	7.3	13.0	24.0

The site was re-visited shortly afterward, with four studies conducted on July 12, 2019. The effect of travel speed (18 and 7.3 mph) and boom height (24" and 40") was evaluated with a "Medium" spray quality, with three variability measurements for each treatment resulting in 12 exposed strings (Table 4).

The third study was conducted near Saskatoon on October 21, 2019. Collaborators were Cervus Equipment, who provided the site and sprayer, a John Deere 4830 with 100' boom. Six sprayer configurations, consisting of two boom heights (28" and 45") each at three travel speeds (8.9, 13.4, and 20 mph) were tested. The collector was a grid of strings 6 m long x 6 m wide. A string was stretched every 2 m, resulting in four 6 m long strings parallel to the boom (X-direction) and four 6 m long strings in the direction of travel (Y-direction). String was cut into 15 cm segments which were analyzed

individually. The resulting grid had 40 measurements for each 6 m line, for 320 segments per treatment, 1920 samples in total.

The fourth study was conducted on July 15, 2020 at a site near Delmas, SK. The farmer cooperator was Martin Prince, who provided use of his sprayer, a John Deere 4830 with 100' boom fitted with LDA120035 nozzles. Tires were 320/90/R50, fitted with row dividers on all four wheels. Two treatments were evaluated, high booms (35") and fast travel speed (18 mph) and low boom (20") and slow travel speed (9 mph). Two strings were exposed for each treatment (Table 5).

Table 5: Details for 2020 trials

String	Orientation	Time	Nozzle	Pressure (psi)	Boom ht (in)	Speed (mph)	Wind (km/h)	Temp (C)
20-01 (L2,3)	90°	14:03	LDA120035	60	35	18	16.0	19.1
20-02 (L1,3)	90°	15:29	LDA120035	60	20	9	22.5	20.7

As before, the spray tank contained a fluorescent dye so that the spray deposit could be quantified by fluorimetry.

After a spray pass, the droplets captured on the line were allowed to dry and the line was stored on reels in the dark, awaiting analysis. Previous work had established that the spray deposits on the line did not transfer to other parts of the line on contact when stored on the reels.

In the lab, each string was cut into two 15 cm segments, usually two of which were placed into a borosilicate tube labelled with the treatment and sample numbers. The deposits along the 36 m string were therefore analyzed at 120 locations at 30 cm intervals. Twenty-five mL of 95% ethanol was added to each tube using a re-pipetter, and the tubes were stoppered and agitated to dissolve the dye. The tubes were placed into trays that allowed them to be used with an autosampler to feed the fluorimeter, a Model RF-1501 spectrofluorometer equipped with Model ASC-5 auto-sampler (Shimadzu Instruments, Inc., Columbia MD). Autosampler trays could hold up to 60 samples, and each tray contained vials with known amounts of dye to confirm the standard curve. In addition, blank ethanol vials were used confirm return of the sipper cell to a zero reading at regular intervals.

Instrument sensitivity, and corresponding standard curves, were selected according to the amount of dye in the sampler. When readings were outside of the instrument range, samples were diluted by a factor of 2x and re-analyzed.

Counting all the trials, a grand total of 130 strings were exposed to spray in 68 spray passes, resulting in approximately 7,800 samples analyzed by fluorimetry.

Results

One of the differences between the two main experimental designs was the type of samplers used. In Study 1, each drinking straw represented a relatively large sampling area (22 cm^2 of surface area directly exposed to the spray) and were oriented in the direction of travel. Each straw therefore sampled a strip of the spray swath that was 1.25 cm wide and 11.25 cm long. This meant that in the direction of travel, variations that might occur were integrated (averaged) over the 11.25 cm distance, resulting in a deposit measurement that was less susceptible to subtle changes in deposition that might occur within the distance. Furthermore, the sampler size meant that they were well suited to capturing the larger, less abundant droplets in the spray cloud that make up a significant portion of the spray volume.

In comparison, the samplers used in Study 2 was a 2 mm diameter plastic line oriented parallel to the boom, perpendicular to the direction of travel. 30 cm segments of this line represented a total collection area of about 9 cm^2 per sample. The orientation parallel to the boom made these samplers very sensitive to small differences in the deposit that presented itself in the direction of travel. The sampler size was also better suited to capturing and retaining the smaller droplets, and could miss some of the less abundant large droplets entirely (Figure 9).

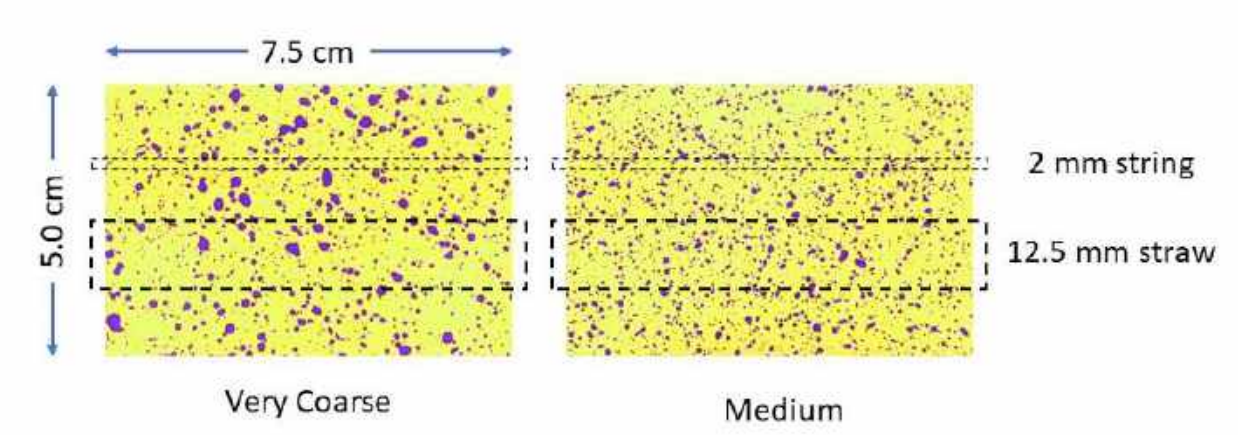

Figure 9: The size of two samplers used in this project relative to the spray deposits of two spray qualities.

The result interpretations that follow need to be placed in the context of these sampler differences. Study 1 results best depict the actual average mass deposited by the sprayer, and this mass could be extrapolated to larger scales to represent the dosage received by a portion of soil or plant of similar width and length. Study 2 is a smaller sample, and best represents a smaller target such as an emerging weed or a small insect. It is less accurate to extrapolate the string sampler results to larger areas, and the results that follow will show significant deviations from average deposits with each individual sampling line. The string, being more sensitive to variation and with a better collection efficiency for smaller droplets, was considered the preferred collector to document the effects of aerodynamic turbulence during the spray operation. It was also possible to drive the sprayer directly over the string during a trial without destroying its integrity or impacting its ability to collect spray immediately after.

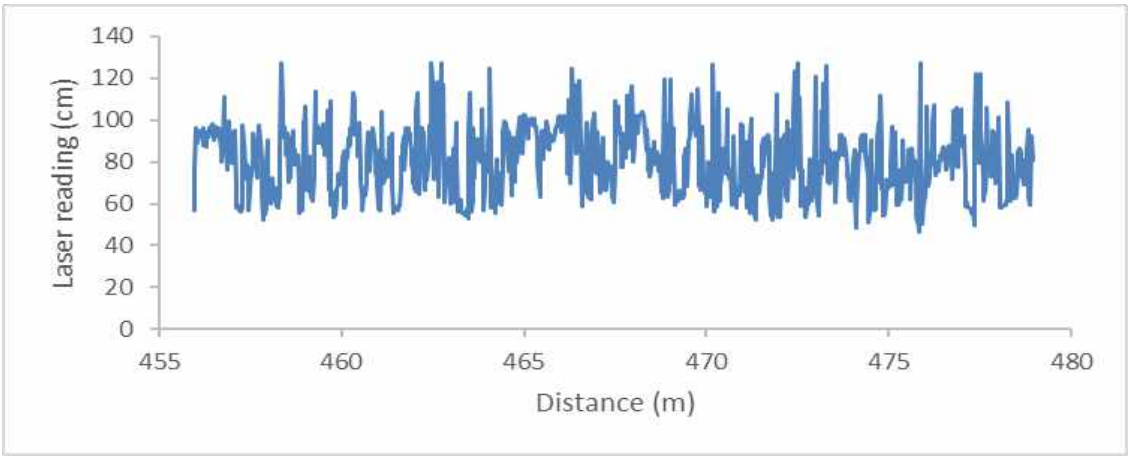

Figure 10: Laser height readings (ground and canopy)

Study 1: The effect of boom height and travel speed on spray deposition

Boom height varied considerably from the intended height settings. Average laser sensor height indications for a typical spray pass showed that the boom height variability was an average of 17% compared to the boom setting (

Figure 10). This complicated efforts to attribute deposit uniformity to a specific height setting. As a result, the 8" boom height could not be achieved at 20 mph, knocking the sampling arrays over. At 14 mph, some of the arrays were knocked over, reducing the available dataset.

Deposition CV ranged from12 to 49% when averaged over the two sampling lines and three reps per treatment, with a CV of 22% when all treatments were averaged (Table 6). The higher CVs were associated with the low boom heights of 8" and 16", but not with faster travel speeds. The value of ratios of highest to lowest deposit amounts were also associated with boom height, with the lowest boom heights resulting in the highest ratios. This was the direct result of lower than ideal boom heights leaving unexposed samplers between nozzles. Where boom height was sufficient for pattern overlap, both CVs and deposit ratios remained below 20% and 3, respectively.

*Table 6: Deposit statistics for various boom heights and travel speeds, Humboldt, 2016. Each value was the result of 90 observations (3 reps * 2 lines/rep * 15 samplers/line).*

Speed (mph)	Height (in)	Mean	Min	Max	Range	Ratio	CV (%)	10th percentile	50th percentile	90th percentile	Span
8	8	78	3	180	177	62.5	44	30	83	118	1.06
8	16	98	51	131	81	2.6	16	80	98	114	0.34
8	32	105	79	145	65	1.8	15	86	103	130	0.43
8	64	96	63	123	60	1.9	12	82	96	111	0.30
14	8	97	29	158	129	5.5	49	32	104	150	1.14
14	16	98	6	213	207	34.5	31	66	101	122	0.56
14	32	95	73	131	58	1.8	12	82	95	110	0.29
14	64	94	56	139	83	2.5	16	77	95	110	0.36
20	16	109	78	159	82	2.1	13	91	107	125	0.31
20	32	106	70	138	68	2.0	14	88	105	128	0.38
20	64	98	62	138	76	2.2	17	76	96	120	0.46
Mean		**98**	**52**	**150**	**99**	**11**	**22**	**72**	**99**	**122**	**0.51**

Effect of Boom Height

Spray deposit variability was sensitive to boom height. The most detrimental aspect of boom height was the poor pattern overlap at the suboptimal boom height of 8", as expected (Figure 11). In fact, the natural sway of the boom tended to be downward at the sampler location, knocking the sampling poles over and making it impossible to collect this low boom height at the faster travel speeds. Higher boom heights improved deposit uniformity at all speeds, as the proper pattern overlap was allowed to form prior to spray collection. The coarse nature of the spray and the type of collector made these tests relatively insensitive to turbulent spray displacement.

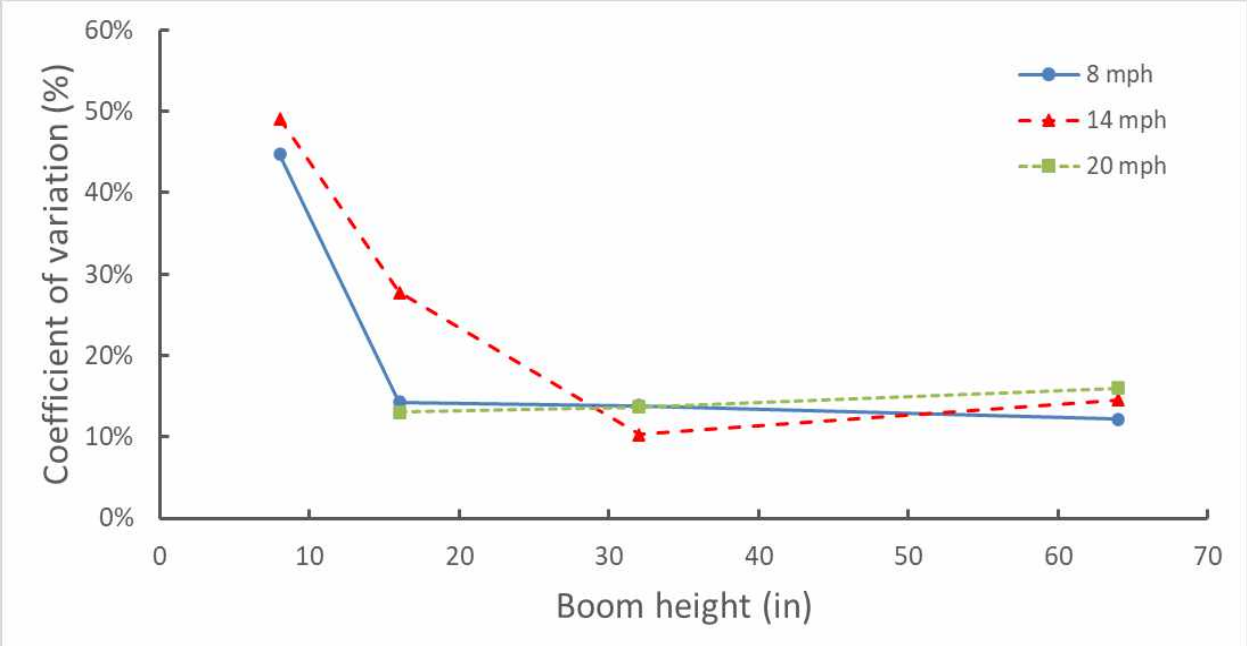

Figure 11: Effect of boom height on spray pattern uniformity at three travel speeds (average of three replicate runs).

Effect of Travel Speed

Spray deposit variability was less sensitive to travel speed than it had been to boom height. Deposit VSs stayed below 20% for all travel speeds for boom heights of 16" and greater (Figure 12). The 8" boom height again showed much higher CVs due to the insufficient pattern overlap at that height, resulting in gasp in spray deposition. The greater travel speed would have been expected to displace the spray more, but this was not borne out in the trial. In fact, even the very high boom of 64" at the 20 mph travel speed still had acceptable uniformity. Again, a contributing factor would be the relatively coarse spray used and the calm weather conditions that would reduce displacement and drift. At the 16" height, the 14 mph speed had poor uniformity while the other speeds maintained acceptable CVs. This could be attributed to the sprayer track, which caused a dip in the boom, lowering it just as it reached the sampler locations, but only at the 14 mph speed. At other speeds, the boom did not dip in this region.

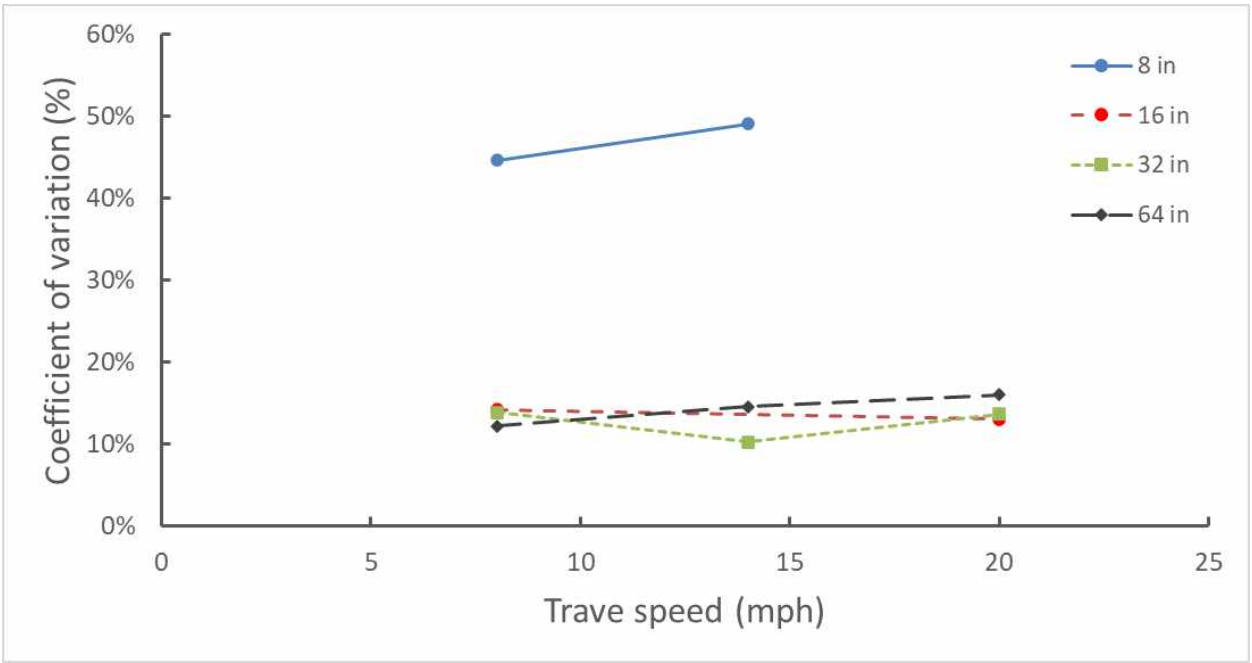

Figure 12: Effect of travel speed at four boom heights on spray pattern uniformity (average of three replicate runs).

Effect of Boom Region Sampled

There was a trend for the deposit to become more variable as the sampling moved from the point of attachment of the spray boom wing to the centre rack, to its outer edge (Figure 13). Due to the type of height control based on a single articulation at the centre rack, any sway (up and down) and yaw (fore and aft) movement would be amplified towards the outer edge of the boom.

The overall raw datasets of each treatment are shown in Appendix 1 (Figure 77 to Figure 84). Each row, from left to right, shows the five plastic straw samplers on each of the three sampling towers, for a total of 15 samplers per row. Each spray pass contained two such rows, and each spray pass was replicated three times. All individual sampler values for a treatment are listed on a single figure.

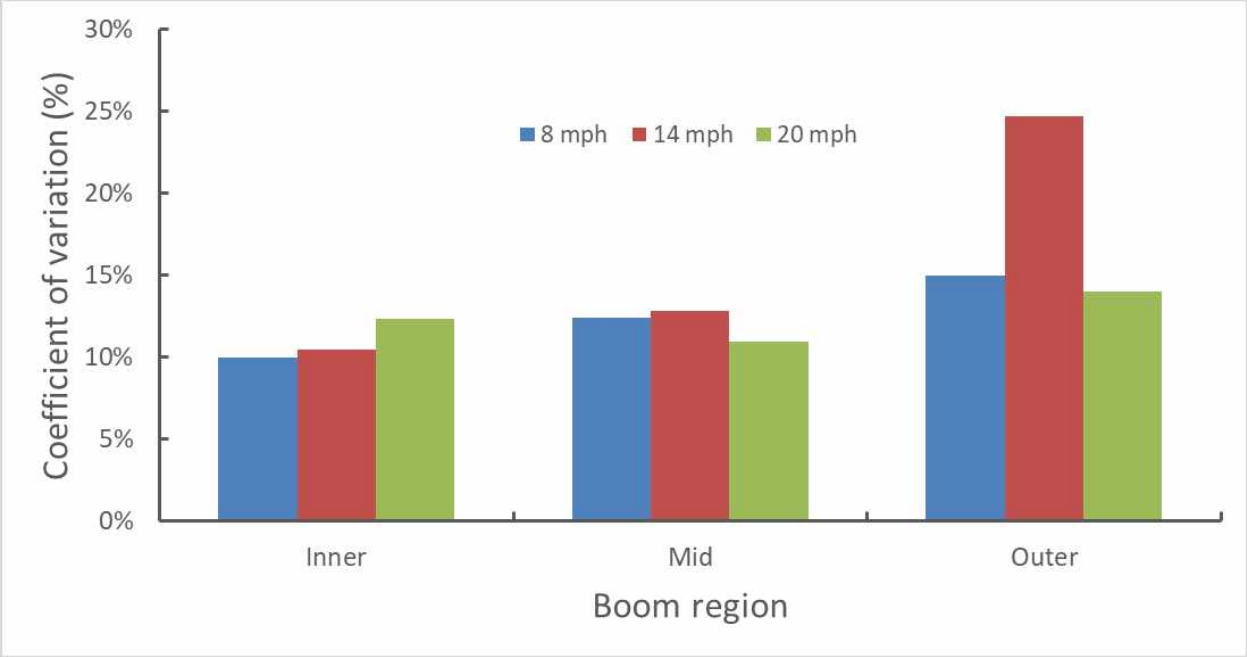

Figure 13: Deposit CV averages under three regions of the spray boom.

Study 2: Spray deposit variability as influenced by travel speed, boom height and spray quality

The use of the string sampler offered a different perspective on spray deposition compared to the straw collectors used in Study #1. The small-diameter string provided better collection efficiency of smaller droplets, and poor efficiency in the collection of the larger droplets. Under field conditions, the string would mimic smaller objects such as canola pods, petioles, seedling grassy weeds, or cotyledons of just-emerged broadleaf weeds. All of these types of objects are aerodynamically better suited for the capture of smaller particles, whereas the relatively less abundant larger droplets may miss these types of targets altogether.

The larger collector in Study 1 integrated a larger area of deposition and was therefore not able to simulate deposition on a target smaller than the collector.

The three main advantages of the smaller collector were the ability to place the string across the entire width of the sprayer and therefore capture deposits anywhere along the spray boom's width. The second advantage was the ability of the small diameter of the string to efficiently capture the smaller droplets, those most susceptible to aerodynamic displacement. Thirdly, the string permitted wheels to travel over the sampling region without destroying the sampler. After wheel passage, the string, which was under tension, simply returned to its original heights and collected the spray.

An important disadvantage of the string collector was the erratic nature of its collection of larger droplets. Large droplets are relatively rare in sprays, therefore the statistical probability that they will impact on a small target is low. But when they do, they carry a large dosage that will affect the overall size of the deposit on that section of string. As a result, some of the variability seen on these strings will be due to aerodynamic turbulence, and some may be due to occasional larger droplets. Nonetheless, the simulation by this string of small biological targets, as described earlier, provided a realistic setting for this method.

Specific and overall appearance of string deposit information

Thirty-two trials were summarized in a graphical format to identify common features and overall trends. The appearance of the deposits varied widely. In some cases, deposits were highly variable, with very pronounced deviations from the average application amount (Figure 14).

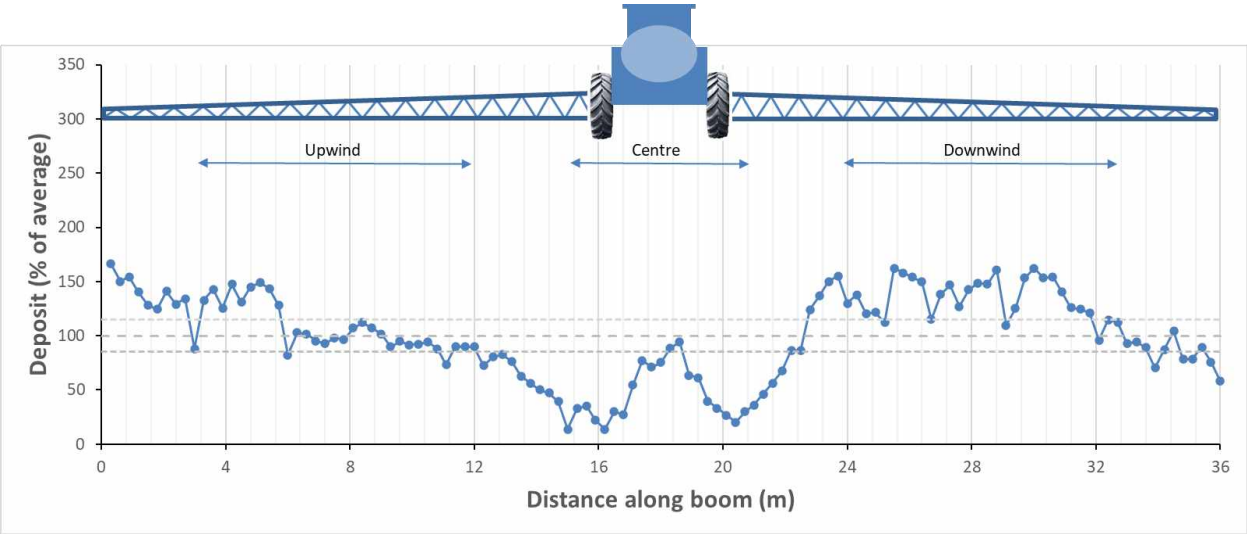

Figure 14: Example of a deposit with overall CV of 40% (Trial 19-04 L2).

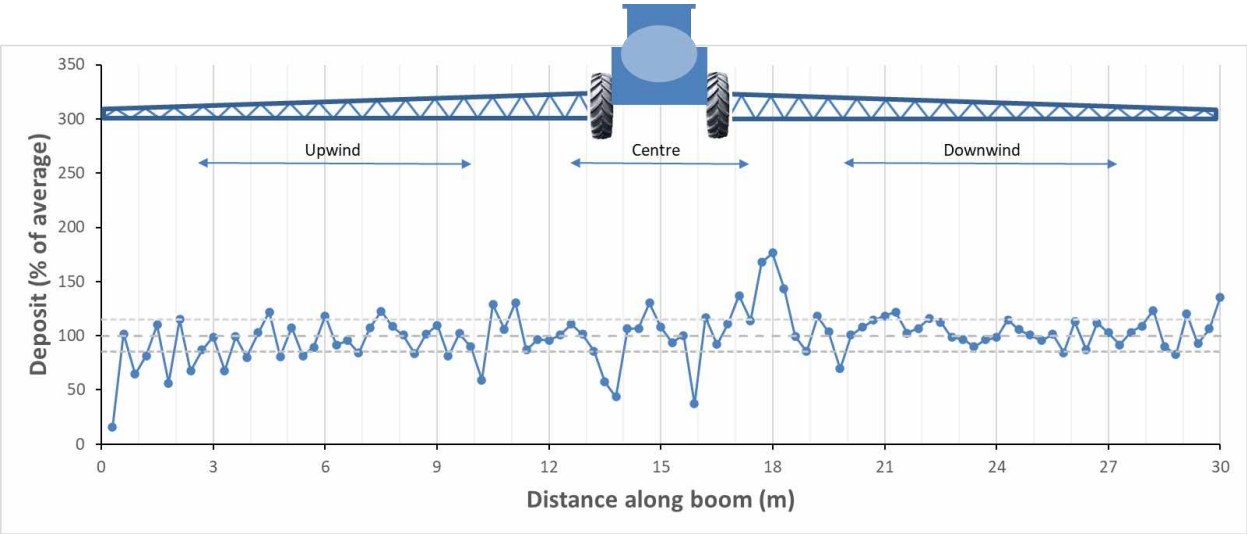

Figure 15: Example of a deposit with overall CV of 23% (Trial 20-02 L3).

In other cases, variation remained apparent but did not deviate as much from the average recovered amount (Figure 15).

Overall spray deposit variability was significantly greater for the string collector than for the straw collectors in the previous trial. Part of the reason may be the much wider range of conditions sampled with the string (i.e., wheel tracks) compared to only the upwind boom in Study 1.

Common features in a number of trials could become more obvious if their distributions were averaged (Figure 16). When eleven of deposits collected the same day in 2017 were represented, it was noted that three features remained noticeable.

1. The average deposits were low on the left side, which was the side from which the wind entered the pattern in all studies. This characteristic is common in spraying and is called “swath displacement”. It is common for aerial application where the spray is released from 3 to 5 m above ground, resulting in the windward movement of the entire spray cloud prior to impaction. The displacement is accounted for with subsequent upwind passes that fill in the gaps, assuming similar wind conditions, boom height, and spray quality.
2. The spray deposits dipped at the wheel locations. Although the exact location and magnitude of the dip varied with each spray pass on account of the variable weather conditions that accompany any spray trial, the reduction in deposits at each wheel location remained noticeable, about 15 to 20% less than the average deposition across the entire boom.
3. The deposit tended be most uniform in the middle of each boom wing. At these locations, deposits were very close to the sprayer average, and deviations only rarely exceeded 15% from the average. This suggested that any of the larger deviations observed in individual sprayer runs were not related to a specific location along the boom, and the more or less random ups and downs of an individual distribution were moderated as runs were added.

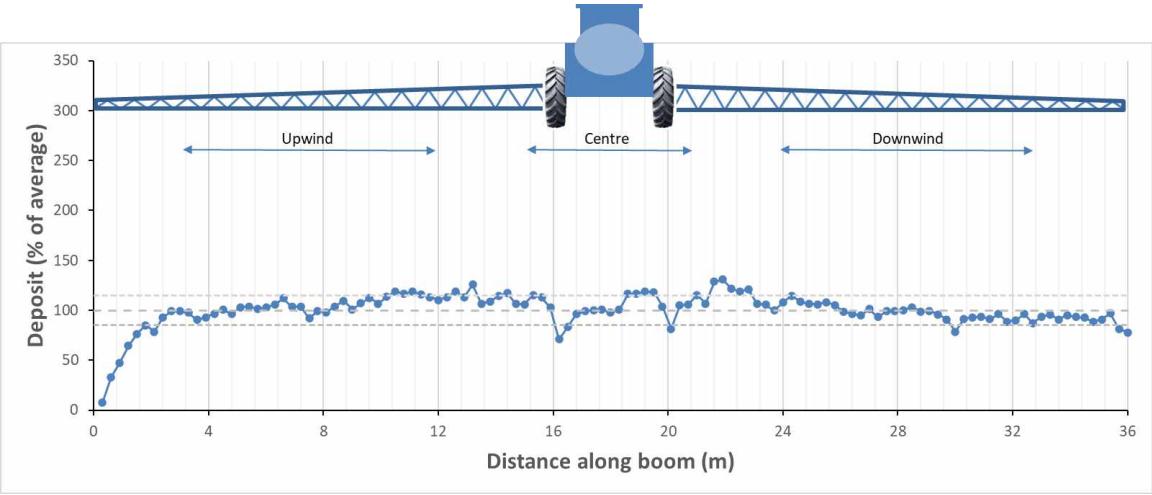

Figure 16: Average of 11 string deposits over a variety of spray qualities, boom heights, and travel speeds. Wind is from left. Note the displacement of the spray due to the wind as well as the signature of the sprayer wheel tracks.

Relationship of Variability Parameters

The CV was compared to other parameters that could be derived from the dataset. Both span and deposit ratio were calculated and compared to the CV for the same deposit data. Because the entire spray deposit was usually displaced downwind, resulting in the most upwind part of the collector to be less exposed, it was decided to eliminate the outer 2 m on either side of the pattern from analysis.

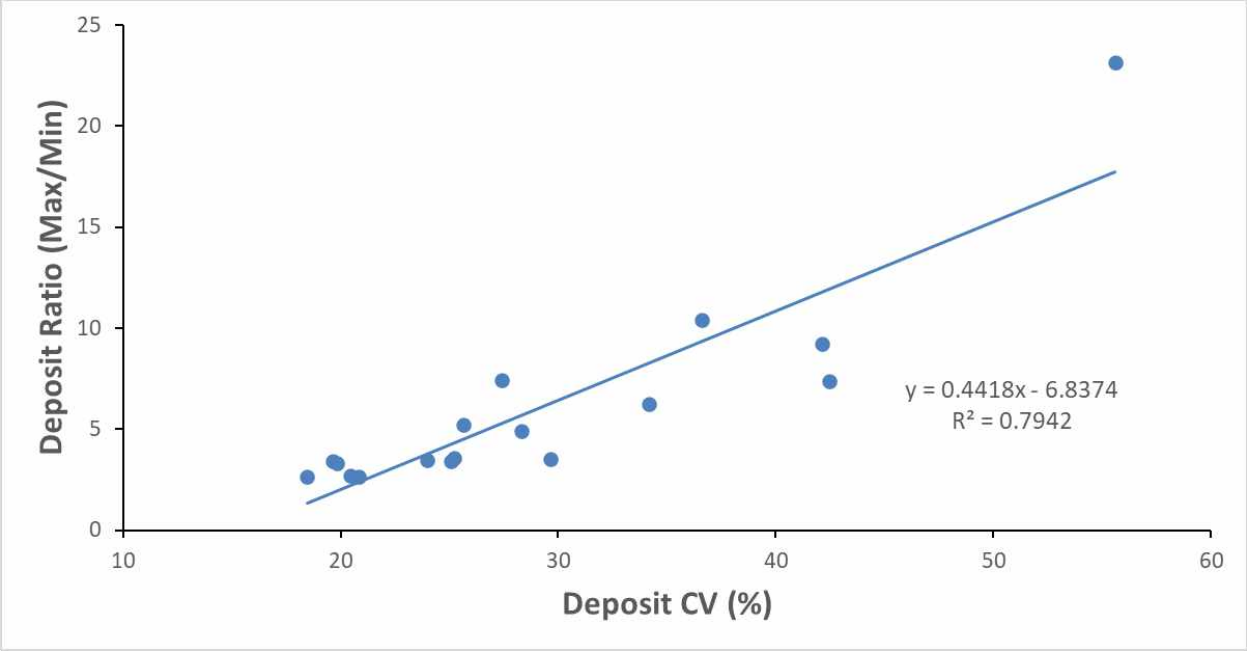

Figure 17: Relationship between the deposit CV and the range of observed values within the inner 32 m of a 36 m boom

The CV of the 36 distributions quantified for thus study averaged ranged from 22 to 57% with an average of 33% when the entire swath width was considered. These values were reduced slightly to a range of 19% to 56% with an average of 31% when the outer 2 m were eliminated from the calculations (Table 7; Figure 18). The practical meaning of these CV values can be seen in Figure 17. A CV of about 20% meant that the ratio of the highest to the lowest deposit values was about five-fold. For a 35% CV, this ratio increased to approximately ten-fold. This range was unexpectedly large, as it means that some regions of the swath only received one-third of the intended dose, whereas others received three-fold. Variability therefore represents a not only waste of product where it is over-applied, but it also risks poor control where the lowest doses are recorded. To prevent the underdosed regions from exhibiting poor control, higher pesticide doses may be required.

Table 7: Summary statistics for 36 deposition measurements where sampling was done across width of boom

Trial	Spray Quality	Speed (mph)	Height (in)	Wind (km/h)	Mean	Range (Max-Min)	Ratio (Max / Min)	CV (%)	10th percentile	50th percentile	90th percentile	Span (90^{th}-10^{th}) /50th
17-01	C	15	25	16	107	273	9.2	42	55	108	147	0.86
17-02	C	15	25	16	104	155	7.4	42	52	87	163	1.27
17-03	XC	15	25	16	103	155	6.3	34	61	104	152	0.87
17-04	XC	15	25	16	105	279	23.2	56	44	93	204	1.72
17-13	XC	15	25	16	104	178	10.4	37	55	98	155	1.02
17-14	C	15	25	16	103	114	3.5	24	69	105	134	0.63
17-27 M	C	7.5	25	16.5	103	165	5.2	26	70	101	133	0.62
17-28 N	C	7.5	25	19.7	102	123	3.6	25	72	98	138	0.67
17-29 O	C	7.5	25	7.9	103	98	2.6	18	81	101	129	0.48
17-31 Q	C	15	35	17.4	102	96	2.7	20	75	99	130	0.55
17-32 R	XC	15	25	14.5	103	128	3.4	20	80	101	125	0.45
17-33 S	XC	15	35	9.1	105	164	7.4	27	68	106	143	0.70
17-34 T	C	15	35	16.5	105	142	4.9	28	71	98	148	0.78
17-35 U	XC	15	35	6	104	106	2.6	21	77	102	133	0.55
17-36 V	C	15	35	10.5	105	143	3.5	30	71	99	148	0.78
17-20 F	XC	15	25	7.9	102	119	3.4	25	72	99	140	0.69
17-26 L	C	15	25	20	103	112	3.3	20	77	102	127	0.48
19-02 L1	M	17	24	9.1	99	150	10.1	37	35	107	140	0.98
19-02 L2	M	17	24	9.1	98	169	24.5	43	35	106	150	1.08
19-02 L3	M	17	24	9.1	101	149	7.1	38	45	104	148	0.98
19-03 L1	M	17	24	6.4	100	149	15.1	32	50	105	136	0.82
19-03 L2	M	17	24	6.4	100	170	14.1	38	38	109	144	0.98
19-03 L3	M	17	24	6.4	100	145	9.2	33	43	104	143	0.97
19-04 L1	M	17	40	14.1	99	167	15.8	42	36	105	148	1.06
19-04 L2	M	17	40	14.1	99	149	11.7	41	35	96	150	1.20
19-04 L3	M	17	40	14.1	101	148	16.4	36	34	110	140	0.96
19-05 L1	M	7.3	40	14.2	100	135	8.4	27	65	103	133	0.65
19-05 L2	M	7.3	40	14.2	99	145	19.0	26	68	102	130	0.61
19-05 L3	M	7.3	40	14.2	103	146	7.7	24	75	106	130	0.52
19-06 L1	M	7.3	24	13	103	169	9.4	28	68	102	147	0.78
19-06 L2	M	7.3	24	13	103	175	8.9	41	42	103	165	1.19
19-06 L2	M	7.3	24	13	101	121	5.3	29	61	102	134	0.71
20-01 L2	C	18	35	16	107	241	9.5	45	57	96	188	1.36
20-01 L3	C	18	35	16	103	186	4.7	29	76	98	133	0.58
20-02 L1	C	9	20	22.5	104	141	3.2	23	79	100	134	0.54
20-02 L3	C	9	20	22.5	102	139	4.7	21	81	101	123	0.41
Average		**13.4**	**28.9**	**13.6**	**102**	**154**	**8.5**	**31**	**60**	**102**	**143**	**0.82**

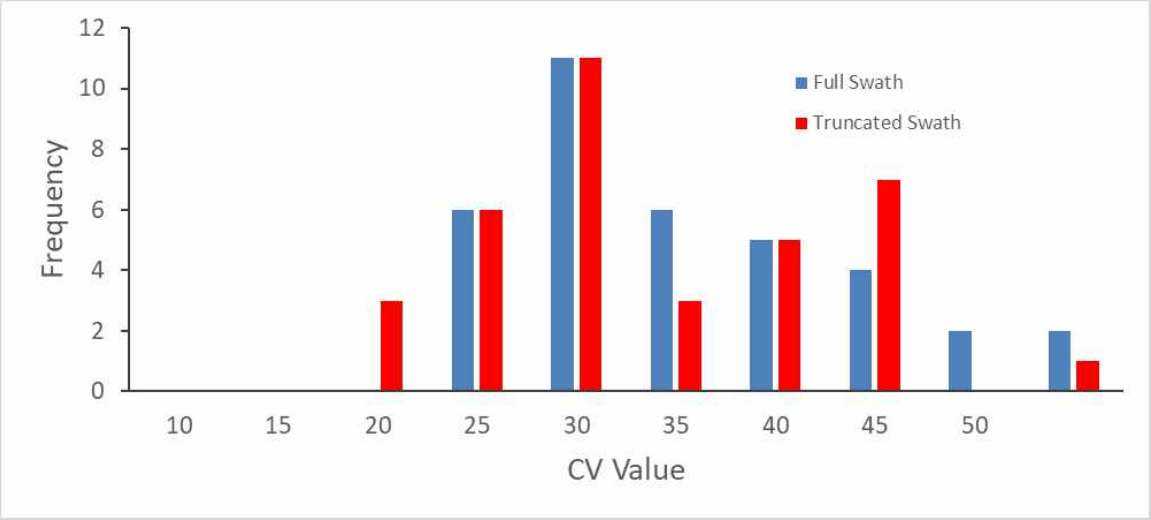

Figure 18: Frequency distribution of CV for 36 trials, taking the entire swath width or width truncated 2 m on both sides.

Repeatability of Deposit

The repeatability of the observed deposit was evaluated in two ways. The same spray pass was sub-sampled with three strings separated by 25 m down the swath. The alternate was to apply the same treatment in three separate passes, each time sampling with one string.

Both scenarios were tested, but in separate years. In 2017, the LDC11004 tip was tested at 15 mph and 35“ boom height in three separate passes.

Table 8: Deposit uniformity statistics for three successive spray passes using the same sprayer settings

	17-31 Q	17-31 T	17-31 V
Mean	102.2	104.8	105.5
Min	56.8	36.2	57.1
Max	152.5	177.9	200.6
Range (Max-Min)	95.8	141.7	143.4
Ratio (Max/Min)	2.7	4.9	3.5
CV	20.5	28.3	29.6

Looking at the statistics for the deposit, it’s difficult to determine how similar the deposits are. The overall CV ranged from 20 to 30%, yet the range of deposit amounts differed by a factor of almost two between them (Table 8).

The visual representation is much more telling (Figure 19). Even at the same location on the boom, deposits sometimes diverged, with one pass trending downward and another upward in the same region. Although there are also some regions where the three passes are almost perfectly superimposed (6 to 8 m and 27 to 30 m), these are more likely to be coincidences than patterns.

Repeatability appeared better when the same sprayer pass was sub-sampled with several strings separated by 25 m (Table 9). This time, depicting the three passes on the same graph shows the commonalities in their deposit behaviour (Figure 20).

On calculating the standard deviation of deposit measurements at each location for both methods, the average standard deviation was identical for both approaches, at 16% of the mean. However, the distribution of the variability seems to follow no obvious pattern, with high and low variation being evident both under the boom wings and behind the tractor unit (Figure 21).

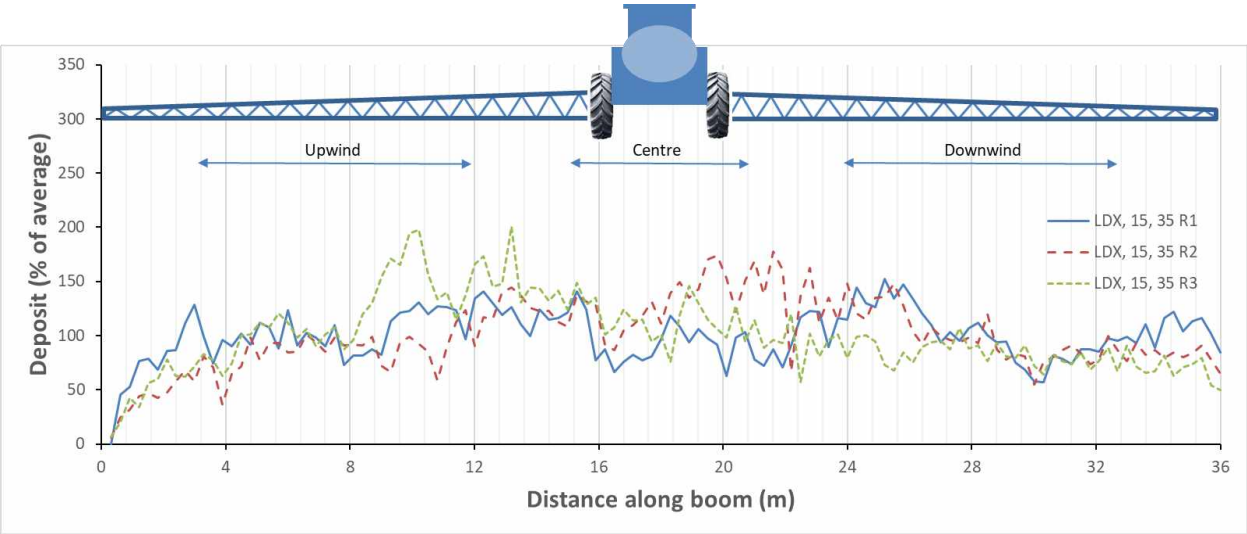

Figure 19: Three successive measurements of a spray pattern using the same spray configuration. Time elapsed for all passes was 30 min.

Table 9: Deposit uniformity statistics for three sampling lines of the same spray pass

	19-05 L1	19-05 L2	19-05 L3
Mean	99.6	98.6	102.9
Min	18.2	8.1	21.9
Max	153.5	153.6	168.4
Range (Max-Min)	135.3	145.5	146.5
Ratio (Max/Min)	8.4	19.0	7.7
CV	27.0	26.4	23.8

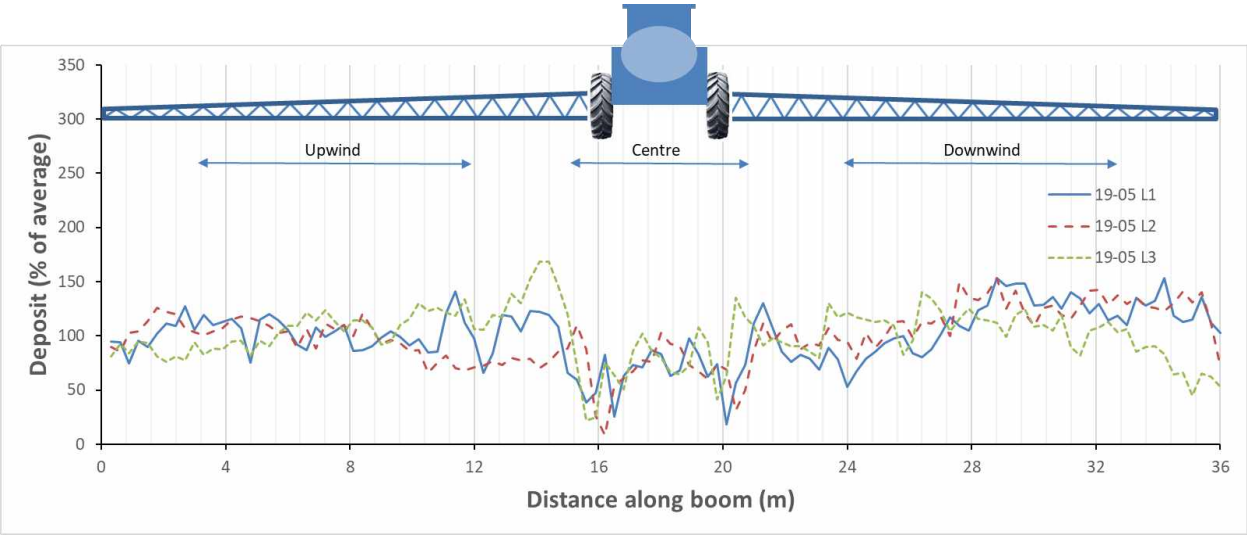

Figure 20: Three spray patterns from the same spray pass. Lines were separated by 25 m.

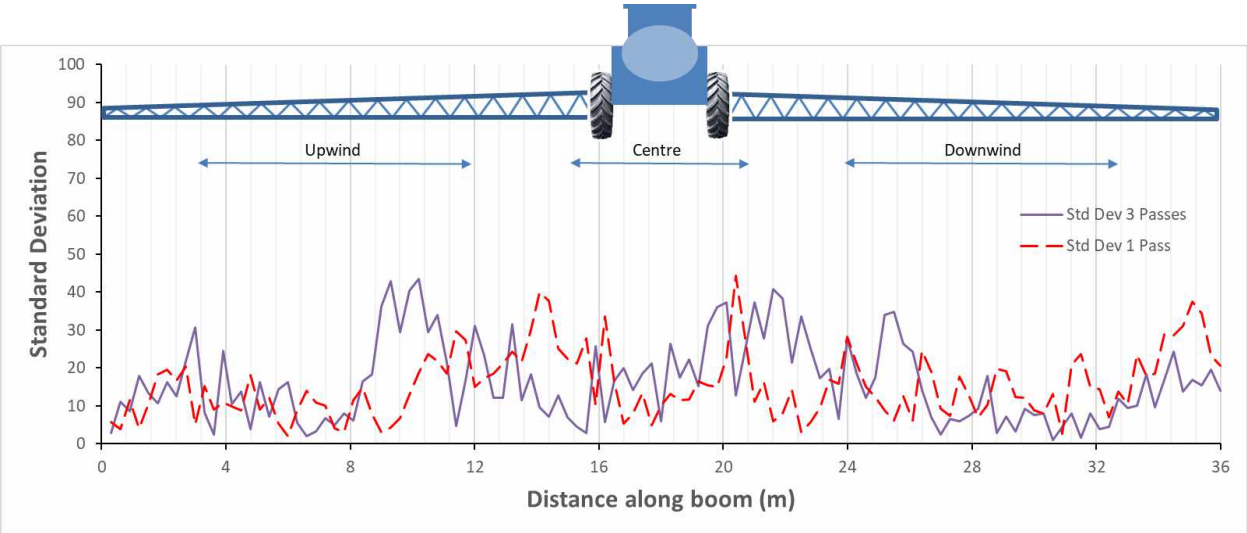

Figure 21: Standard Deviation of deposits of three strings having been sprayed in one or three passes.

Deposit Features by Boom Region

On examining the deposit profiles for 2017, 2019, and 2020, there were often apparent differences in deposit amount and uniformity on the upwind and downwind boom, as well as behind the tractor unit.

The deposit CV was calculated for three regions of each trial. For the 36 m booms, the region under the upwind boom extended from 3 m to 12 m from the outer edge of the upwind side of the boom. The same section of the downwind boom was sampled. The central region comprised the central 6 m, 3 m out on either side from the centre of the sprayer. For the 30 m boom (2020), the outer wings sections extended from 3 m to 9 m and the centre was again 6 m wide.

Results were depicted separately for 2017, 2019, and 2020 trials. 2017 was the year when overall deposit CVs were somewhat lower than in subsequent years of study. This could be due to the use of coarser sprays that were less prone to displacement. Possibly as a result of that, the upwind and

central region of the deposits had similar CVs, 22 and 23% respectively (Figure 22). The mean deposit amount was also similar for both regions (Table 10).

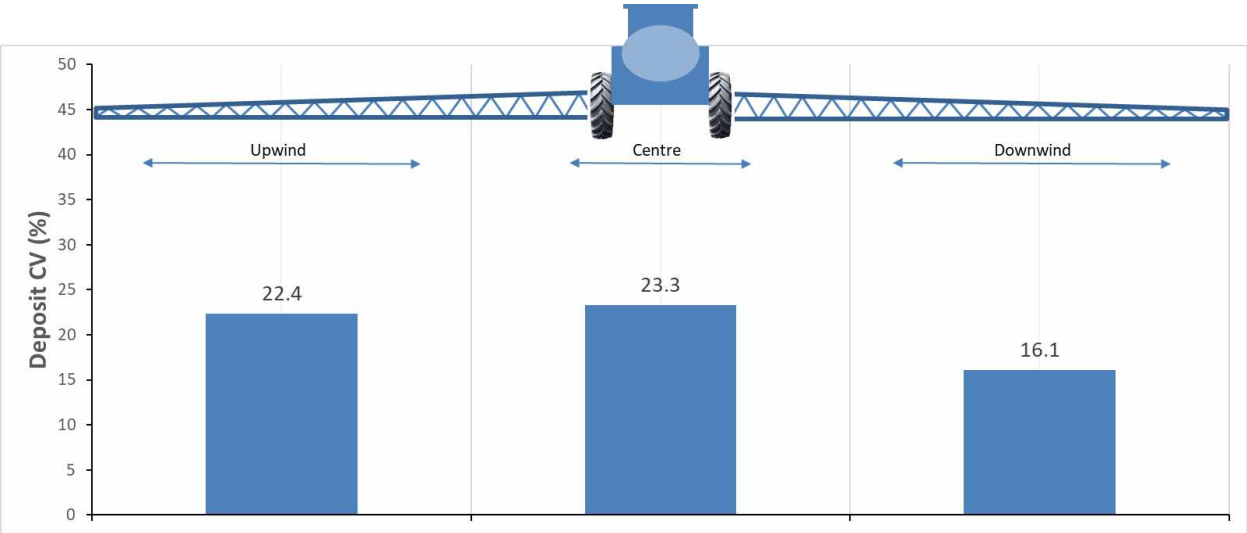

Figure 22: Deposit CVs for three regions of sprayer booms, averaged over 15 trials conducted in 2017

Table 10: Mean deposit amounts (% of average recovered) and CV for three boom regions over three years.

Location	Parameter	2017 n=15	2019 n=12	2020 n=4
Up wind	**Mean**	104.9	112.9	96.9
	CV%	22.4	17.5	17.8
Centre	**Mean**	96.9	66.5	117.3
	CV%	23.3	46.0	32.5
Downwind	**Mean**	105.3	113.8	94.8
	CV%	16.1	16.9	17.8

For both 2019 and 2020 trials, there was a strong association with boom region and CV. In both years, the upwind and downwind regions had lower CVs than the central region, about 17-18% (Table 10, Figure 23,Figure 24). The central regions had CVs of 46 and 33% in 2019 and 2020, respectively. Again, the higher CVs, and the susceptibility to greater effects of the tractor unit may have been due to the finer overall spray quality used in those years, Medium and Coarse compared to Coarse and Extremely Coarse in 2017.

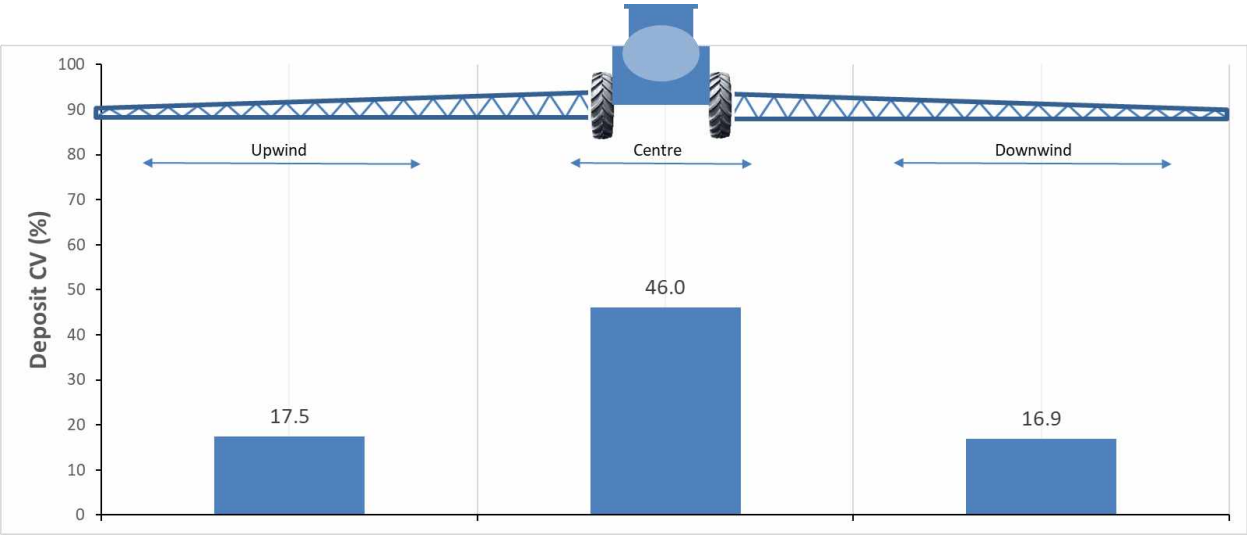

Figure 23: Deposit CVs for three regions of sprayer booms, averaged over 12 trials conducted in 2019

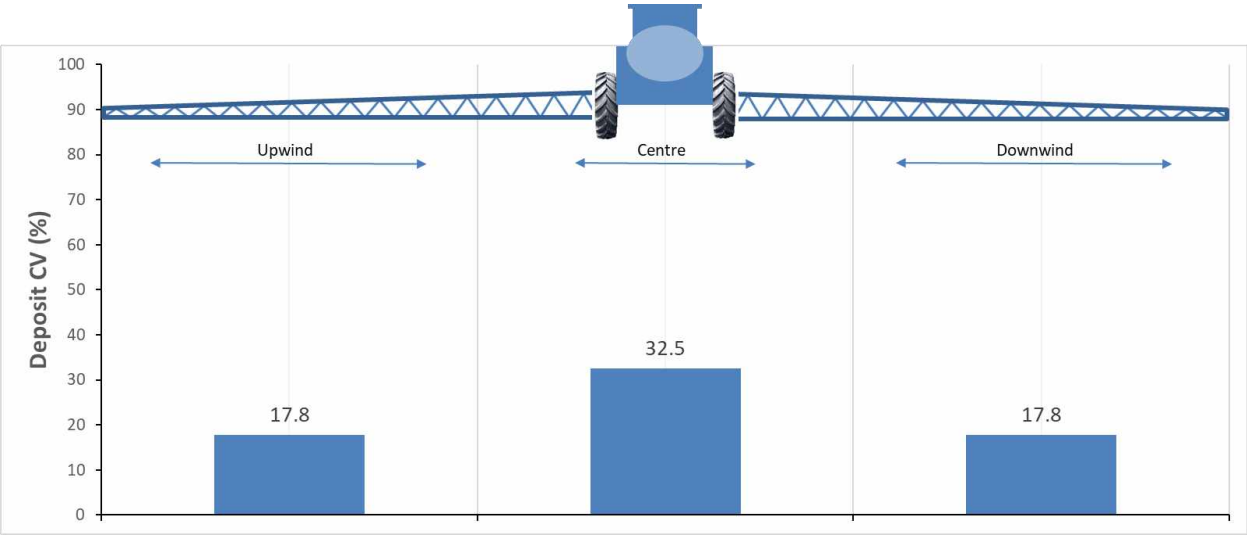

Figure 24: Deposit CVs for three regions of sprayer booms, averaged over 4 trials conducted in 2020

Effect of Sampling Resolution

The effort of sampling the spray deposit at 30 cm resolution of 36 m is significant, and time can be saved by combining a longer distance of sampling string in each fluorimetry cuvette. But the overall sensitivity to deposit variability would need to be retained for this to be viable. To identify opportunities for reduced sampling intensity, adjacent samples were averaged to simulate merging of these string sections. Distances of 60 cm, 90 cm, 120 cm, 150 cm up to 900 cm were evaluated for their effect on CV, and compared to the original sampling resolution of 30 cm.

Results are depicted for one such trial in 2019 (Figure 25). When sampling the entire boom, there was a small but significant relationship with lower sampling resolution and measured deposit CV. CVs were reduced from 26 at the highest resolution to 18 at the 12 m resolution.

The central boom section was very sensitive to measurement resolution. The 2019 trials were noted for the strong impact of the sprayer wheels, with noticeable reductions in spray deposits at each wheel

location. These reductions manifested themselves over short distances, with deposits falling sharply on reaching the wheels, then rising again between the wheels, and the pattern repeating at the other wheel. Capturing this variability required high sampling resolution. The outer wings, both upwind and downwind, were less sensitive to changes in resolution. Deposit CVs remained relatively constant at intermediate values of about 15% throughout.

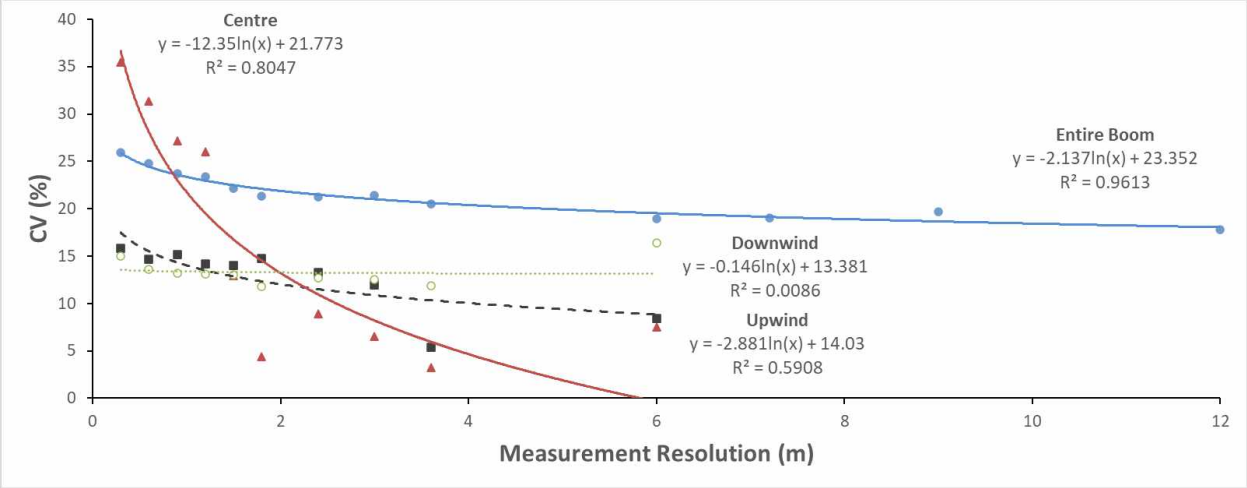

Figure 25: Effect of sampling resolution on measured deposit variability (Trial 19-05 L2)

Potential for Subsampling

Having shown that measurement resolution of 30 cm was required to capture the variability of turbulent regions behind the boom, there remains another opportunity to decrease the analytical effort and still capture the inherent deposit CV accurately. For 17 deposit distributions at 30 cm resolution, one, two, three, four, or five values were randomly selected from each of the three previously identified boom regions. This resulted in three, six, nine, twelve, or fifteen values describing the boom deposit from which a CV was calculated, and compared to the actual deposit CV using linear regression. This exercise was repeated 100 times, and the p-value for the regression coefficient was noted each time. The frequency of significant R-square values was then calculated. The results showed that subsampling may be an effective tool depending on the standard for R-squared values that need to be upheld. For example, at R-square p=0.7, 82% of random subsamples of fifteen values met that standard (Table 11).

Table 11: Percentage of significant R-squares at three p-levels when correlating CVs developed from random subsampling of spray deposition datasets at various sampling intensities to the actual deposit CV.

	Percentage of significant r^2 at subsampling frequency				
p level	**15**	**12**	**9**	**6**	**3**
0.8	40	30	12	6	2
0.7	82	68	36	30	7
0.6	94	87	70	51	25

Impact of Spray Quality

The larger droplets produced by coarser sprays are known to resist displacement in moving air. In the 2017 trials, a Coarse spray produced by a John Deere LDX11004 was compared to an Extremely Coarse spray produced by a John Deere ULD11004 nozzle. As shown earlier, the deposits from each sprayer run differed enough to make it impossible to detect repeated patterns with the exception of the wheel tracks in some instances. However, when the three replicate runs were averaged, some different characteristics could be seen. The finer spray had lower low deposits and higher high deposits than the coarser spray, as shown by the 10th and 90th percentile values (Table 12). The average deposit CV was higher for the Coarse spray, at 26% compared to 23% for the Extremely Coarse spray.

Table 12: Spray deposit variability across the spray swath of two spray qualities, LDX11004 (Coarse) and ULD11004 (Extremely Coarse). Applications made at 15 mph with 35" boom height

	LDX11004			ULD11004		
	Rep 1	**Rep 2**	**Rep 3**	**Rep 1**	**Rep 2**	**Rep 3**
Mean Deposit	102	105	105	103	105	104
CV%	20.5	28.3	29.6	19.7	27.4	20.8
10th Percentile	75	71	71	80	68	77
50th Percentile	99	98	99	101	106	102
90th Percentile	130	148	148	125	143	133
Span	0.55	0.78	0.78	0.45	0.7	0.55
Mean 10th		72.3			75.0	
Mean 50th		98.7			103.0	
Mean 90th		142.0			133.7	
Mean Span		0.70			0.57	
Mean CV		26.1			22.6	

Impact of Boom Height

The trial comparing boom height were conducted in 2019, with a slightly finer spray than had been used in 2017, and under somewhat windier conditions. As a result, variability was generally greater in these trials. These trials also showed the wheel track effect more than other years although the same sprayer and wheel sized were used as in 2017.

The lower boom had slightly higher 10th percentile and lower 90th percentile values, indicating that the range of values in the distribution were narrower (Table 13). This was shown with the lower span value Table 13of 0.92 for the 24" height compared to 1.07 for the higher height. The resulting CV value was relatively high for both boom heights, at 34 and 39%, but 5% lower for the 24" boom height.

Table 13: Effect of boom height on deposit parameters, 2019

	24" Boom Height			40" Boom Height		
	Rep 1	**Rep 2**	**Rep 3**	**Rep 1**	**Rep 2**	**Rep 3**
Mean Deposit	100	100	100	99	99	101.1
CV%	31.9	38.0	33.2	41.9	40.5	35.8
10th Percentile	50	38	43	36	35	33.8
50th Percentile	105	109	104	105	96	110.5
90th Percentile	136	144	143	148	150	140.0
Span	0.82	0.98	0.97	1.06	1.20	0.96
Mean 10th		43.7			35.1	
Mean 50th		106.1			103.8	
Mean 90th		141.5			146.0	
Mean Span		0.92			1.07	
Mean CV		34.4			39.4	

Impact of Travel Speed

Travel speed could be evaluated in two separate years, 2017 and 2019. In 2017, the LDX11004 was operated at 60 psi, creating a Coarse spray at both 15 and 7.5 mph at a 25" boom height. In 2019, the same sprayer model and nozzles were used, but the spray pressure was increased to 80 psi to generate a Medium spray that would be more likely to displace and therefore show turbulent effects.

Table 14: Effect of travel speed on deposit parameters, 2017.

	15 mph			7.5 mph		
	Rep 1	**Rep 2**	**Rep 3**	**Rep 1**	**Rep 2**	**Rep 3**
Mean Deposit	104	103	103	103	102	103
CV%	42.5	24.0	19.8	25.6	25.2	18.5
10th Percentile	52	69	77	70	72	81
50th Percentile	87	105	102	101	98	101
90th Percentile	163	134	127	133	138	129
Span	1.27	0.63	0.48	0.62	0.67	0.48
Mean 10th		66.0			74.3	
Mean 50th		98.3			100.0	
Mean 90th		141.5			133.3	
Mean Span		0.79			0.59	
Mean CV		28.8			23.1	

As before, individual runs differed significantly in 2017 but when looking at averages some trends were apparent. The faster travel speed had more variable deposits overall, which was evident by the lower 10th percentile and higher 90th percentile numbers (Table 14). The disadvantage in CV was 5% for the faster speed, with a CV of 28% compared to 23% for the 7.5 mph speed.

Table 15: Effect of travel speed on deposit parameters, 24" boom height, 2019.

	17 mph			7.3 mph		
	Rep 1	**Rep 2**	**Rep 3**	**Rep 1**	**Rep 2**	**Rep 3**
Mean Deposit	100	100	100	103	103	101
CV%	31.9	38.0	33.2	27.6	41.4	28.5
10th Percentile	50	38	43	68	42	61
50th Percentile	105	109	104	102	103	102
90th Percentile	136	144	143	147	165	134
Span	0.82	0.98	0.97	0.78	1.19	0.71
Mean 10th		43.7			57.0	
Mean 50th		106.1			102.2	
Mean 90th		141.5			148.4	
Mean Span		0.92			0.89	
Mean CV		34.4			32.5	

Table 16: Effect of travel speed on deposit parameters, 40" boom height, 2019.

	17 mph			7.3 mph		
	Rep 1	**Rep 2**	**Rep 3**	**Rep 1**	**Rep 2**	**Rep 3**
Mean Deposit	99	99	101	100	99	103
CV%	41.9	40.5	35.8	27.0	26.4	23.8
10th Percentile	36	35	34	65	68	75
50th Percentile	105	96	110	103	102	106
90th Percentile	148	150	140	133	130	130
Span	1.06	1.20	0.96	0.65	0.61	0.52
Mean 10th		35.1			69.5	
Mean 50th		103.8			103.5	
Mean 90th		146.0			131.0	
Mean Span		1.07			0.60	
Mean CV		39.4			25.7	

In 2019, faster travel speed did not seem to create much of a disadvantage when the boom was low, but that may have been partly due to an unusually high CV for one of the considered strings (Table 15). At the higher boom height, the behaviour was more uniform across replicates and the advantage of the slower travel speed was a 13% reduction in deposit CV (Table 16).

Comparing Best and Worst Case

Based on the results for boom height and travel speed, it was possible to assemble two cases that would be expected to illustrate the best and worst cases, for comparison. A low boom and slow travel speed ("Low & Slow"), and a high boom and fast travel speed ("High & Fast") could be compared.

In 2017, a Coarse spray was operated at boom height of 35" and at a travel speed of 15 mph three times, and the same nozzle was also operated at a 25" height and 7.5 mph. Differences in deposit properties were relatively small, with both application methods averaging deposit CVs in the mid 20%, with a small 3% advantage to the low and slow configuration (Table 17).

Table 17: Comparison of deposit parameters for a low boom and slow speed with a high boom and fast speed, 2017.

	High & Fast			Low & Slow		
	Rep 1	**Rep 2**	**Rep 3**	**Rep 1**	**Rep 2**	**Rep 3**
Mean Deposit	102	105	105	103	102	103
CV%	20.5	28.3	29.6	25.6	25.2	18.5
10th Percentile	75	71	71	70	72	81
50th Percentile	99	98	99	101	98	101
90th Percentile	130	148	148	133	138	129
Span	0.55	0.78	0.78	0.62	0.67	0.48
Mean 10th		72.4			74.3	
Mean 50th		98.8			100.0	
Mean 90th		141.9			133.3	
Mean Span		0.70			0.59	
Mean CV		26.1			23.1	

In 2019, a Medium spray quality was operated at a 40" boom height and a speed of 18 mph. The same nozzle was also operated at a 24" height and a speed of 7.3 mph. In these trials, the "High & fast" configuration had a CV of 39% compared to a CV of 33% for the "Low & Slow" configuration (Table 18). Most parameters showed an advantage for the "Low & Slow", although the variability between reps of the same treatment added some doubt as to the consistency with which these results could be obtained.

Table 18: Comparison of deposit parameters for a low boom and slow speed with a high boom and fast speed, 2019.

	High & Fast			Low & Slow		
	Rep 1	**Rep 2**	**Rep 3**	**Rep 1**	**Rep 2**	**Rep 3**
Mean Deposit	99	99	101	103	103	101
CV%	41.9	40.5	35.8	27.6	41.4	28.5
10th Percentile	36	35	34	68	42	61
50th Percentile	105	96	110	102	103	102
90th Percentile	148	150	140	147	165	134
Span	1.06	1.20	0.96	0.78	1.19	0.71
Mean 10th		35.1			57.0	
Mean 50th		103.8			102.2	
Mean 90th		146.0			148.4	
Mean Span		1.07			0.89	
Mean CV		39.4			32.5	

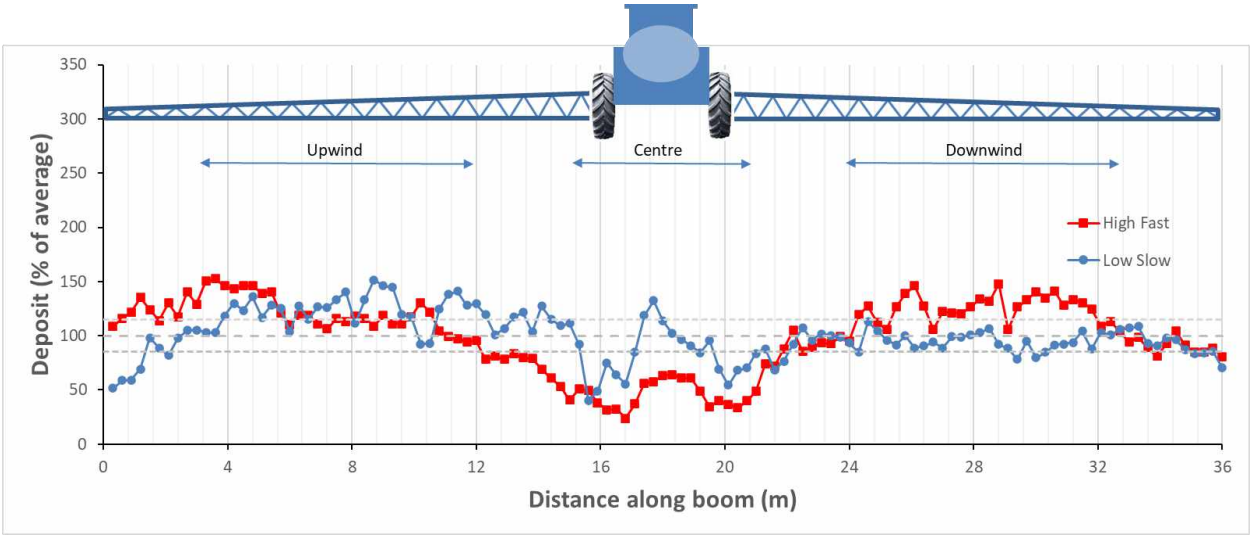

Figure 26: Average of replicate lines for "High & Fast" and "Low & Slow", 2019

A smaller treatment list was available in 2020, with only two replicate strings being available for the tested configurations (the remaining strings broke during the trial and could not be used). In these trials, the “Low and Slow” had a larger advantage than in the other trials. Both replicates were in agreement, with a much tighter span and a 15% lower CV compared to the “High & Fast” treatment (Table 19).

Table 19: Comparison of deposit parameters for low boom and slow speed with high boom and fast speed, 2020.

	High & Fast		Low & Slow	
	Rep 1	**Rep 2**	**Rep 1**	**Rep 2**
Mean Deposit	107	103	104	102
CV%	44.8	28.7	22.5	20.8
10th Percentile	56.9	76.3	79.3	80.7
50th Percentile	95.8	98.1	100.0	101.4
90th Percentile	187.5	133.3	133.7	122.8
Span	1.36	0.58	0.54	0.41
Mean 10th	66.6		80.0	
Mean 50th	97.0		100.7	
Mean 90th	160.4		128.2	
Mean Span	0.97		0.48	
Mean CV	36.7		21.7	

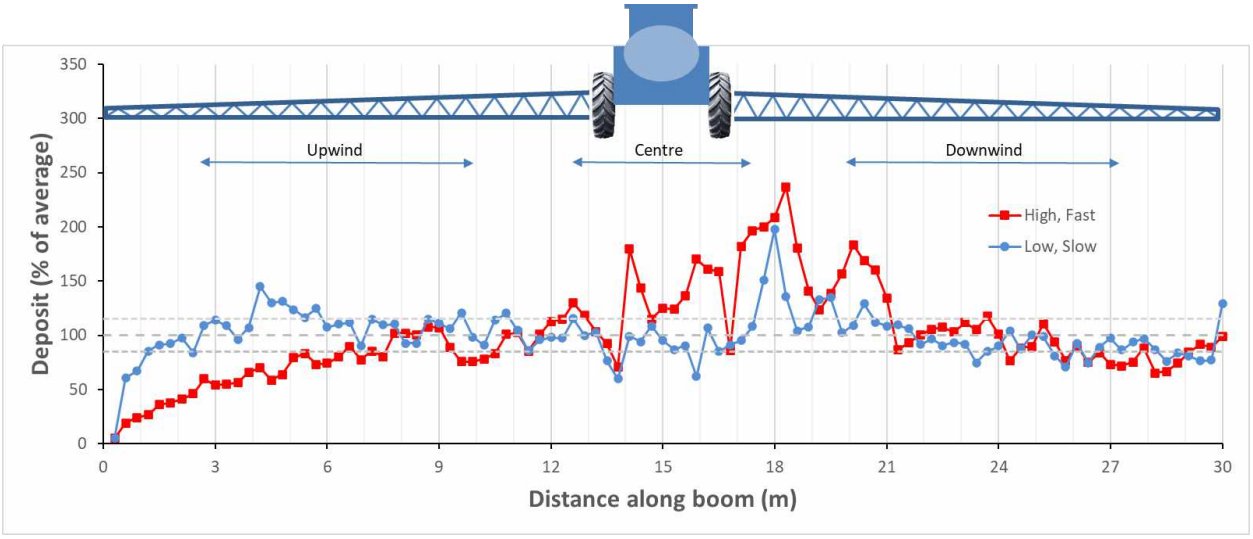

Figure 27: Average of 2 lines for 20-01 and 20-02 (LDA120035, "High & Fast" vs "Low & Slow")

Impact of Sampling Along Direction of Travel

Sampling along the direction of travel showed that even when sprayer-induced aerodynamic regions were held at a constant distance, other variable such as atmospheric turbulence, contributed to deposit variability. Each of the lanes selected for sampling exhibited its own inherent level of deposition, with the upwind side of the left wheel depositing more than the downwind side of the right wheel (Table 20). The regions near the wheels also exhibited lower variability than those in open air. Overall spray deposit variability along the direction of travel was lower, overall, than across the spray swath.

Examples of the deposits can be seen in Figure 28 to Figure 32, and again in Appendix A. The summary table of more detailed deposition statistics for all ten strings is shown in Appendix A Table 26.

Table 20: Spray deposit variability along the spray swath of LDX11004 (Coarse) spray. Applications made at 15 mph with 35" boom height

	Upwind-1	Upwind-2	Left Wheel	Centre	Right Wheel	Mean
Min	131	129	125	95	92	**92**
Max	338	291	207	195	162	**338**
Mean	229	186	155	143	124	**167**
Std Dev	46	39	19	22	15	**28**
CV	20	21	12	15	12	**16**

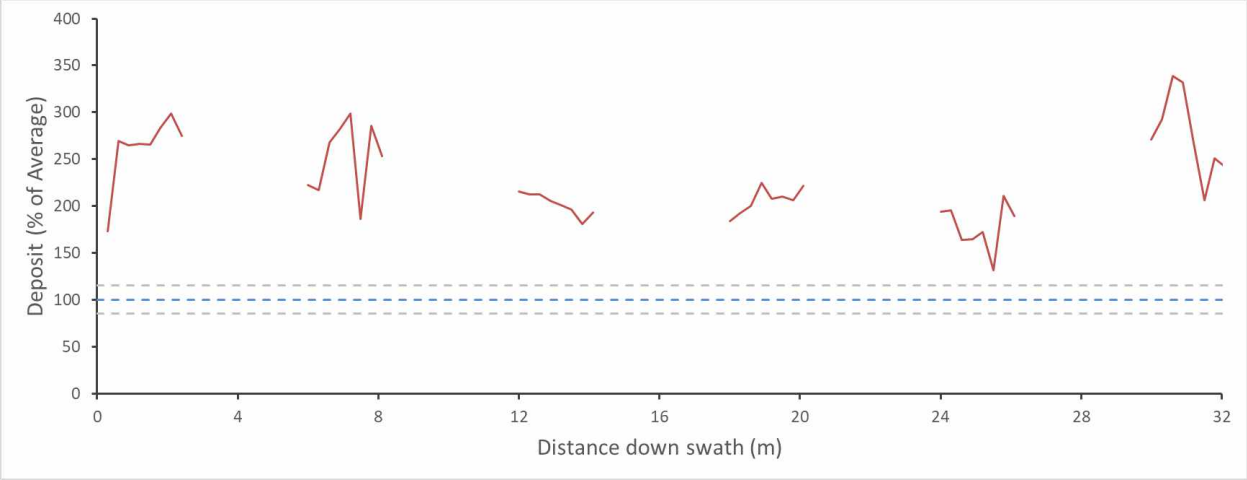

Figure 28: Spray deposits of Coarse spray in direction of travel, 4 m downwind from upwind edge of spray boom.

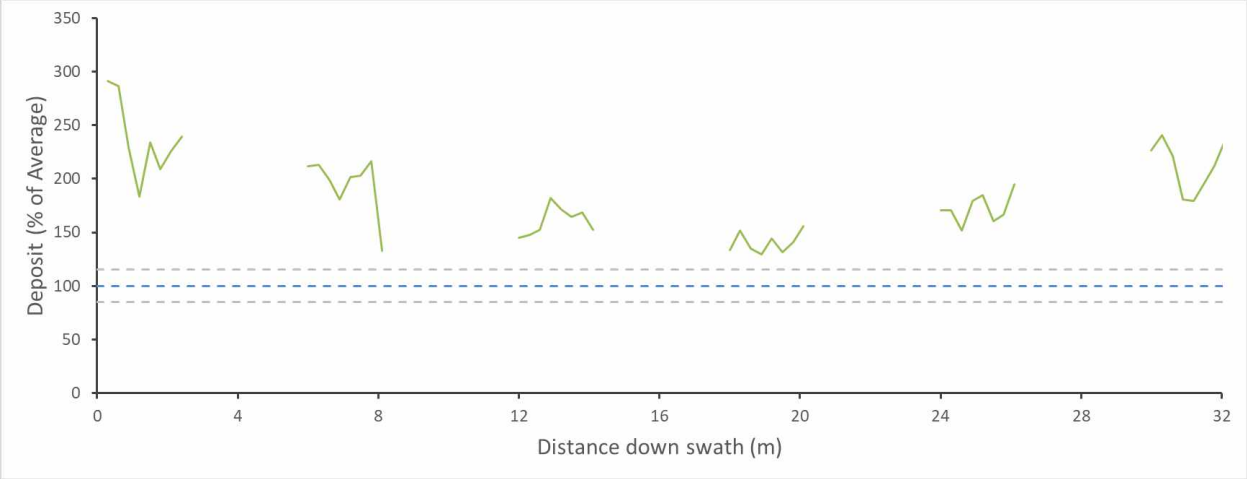

Figure 29: Spray deposits of Coarse spray in direction of travel, 11 m downwind from upwind edge of spray boom.

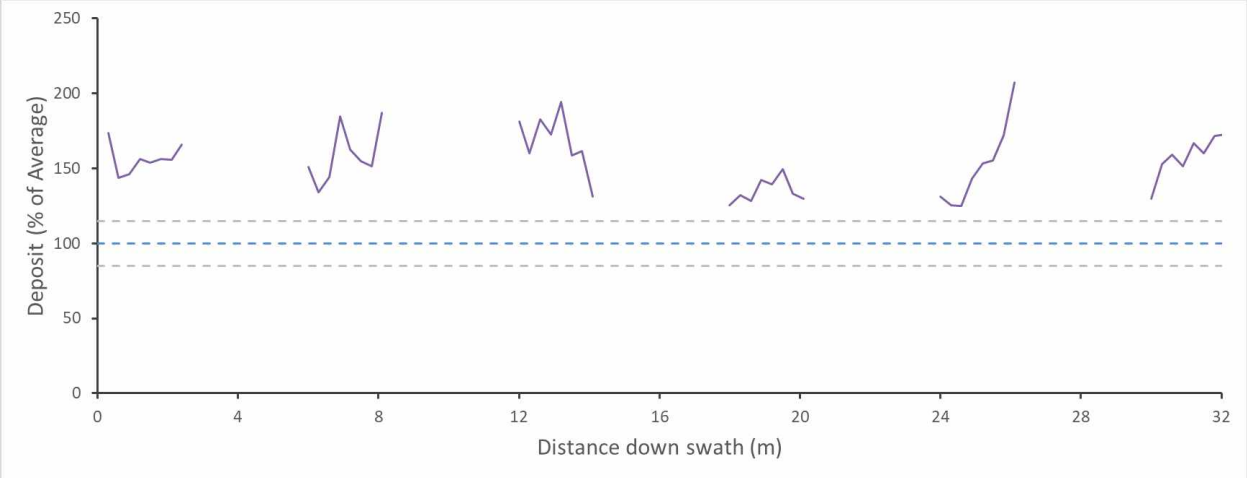

Figure 30: Spray deposits of Coarse spray in direction of travel, 15.5 m downwind from upwind edge of spray boom (0.5 m upwind of left wheel).

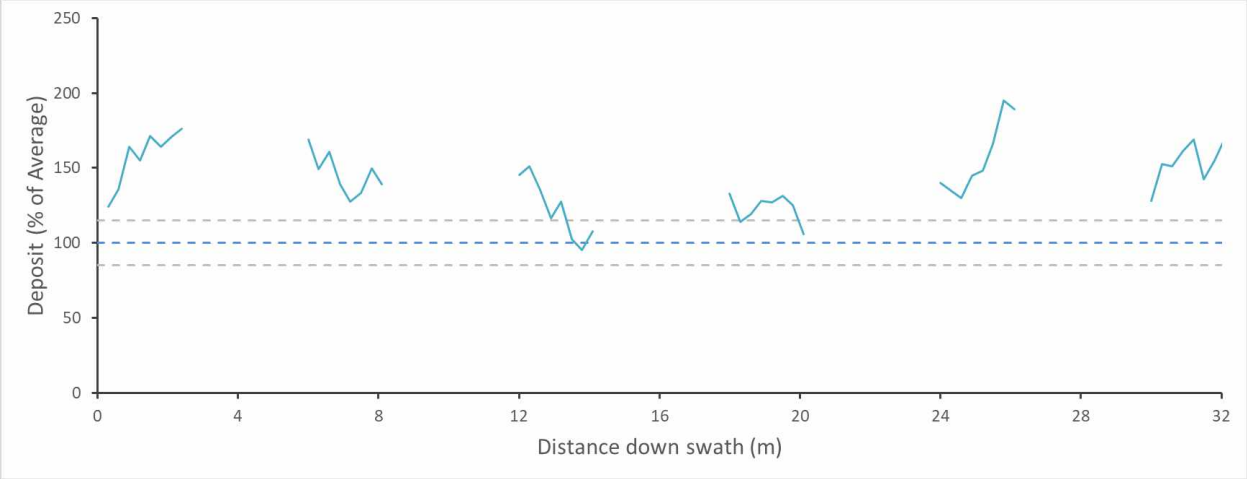

Figure 31: Spray deposits of Coarse spray in direction of travel, 18 m downwind from upwind edge of spray boom (centre of sprayer).

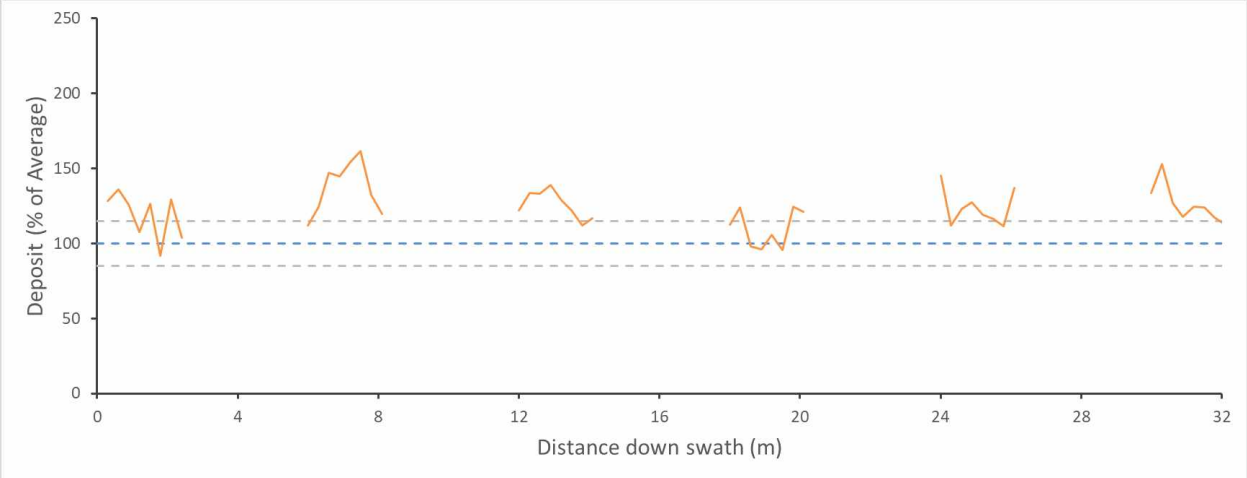

Figure 32: Spray deposits of Coarse spray in direction of travel, 20.5 m downwind from upwind edge of spray boom (0.5 m downwind of right wheel).

Table 21: Spray deposit variability along the spray swath of ULD11004 (Extremely Coarse) spray. Applications made at 15 mph with 35" boom height

	Upwind-1	Upwind-2	Left Wheel	Centre	Right Wheel	Mean
Min	71	67	62	56	66	**56**
Max	186	161	145	173	139	**186**
Mean	139	113	107	118	101	**115**
Std Dev	23	24	19	21	17	**21**
CV	17	21	18	18	17	**18**

The Extremely Coarse spray had similar deposition characteristics to the Coarse spray in the direction of travel. Again, the upwind portions of the sprayer had somewhat greater deposits than the regions near the wheels. However, the centre of the sprayer had high deposition (Table 21).

String Grid

Using the 4 x 4 grid of string, where each of the four strings was sampled at 15 cm increments, it was possible to create a surface that illustrated the variability of the spray in two directions (Figure 33). Furthermore, it was possible to characterize the relative variability of the spray in each of the two dimensions simultaneously, as the entire grid could be traversed in 1.5 s at the slowest speed (9.1 mph) and about 0.5 s at the fastest speed (20 mph).

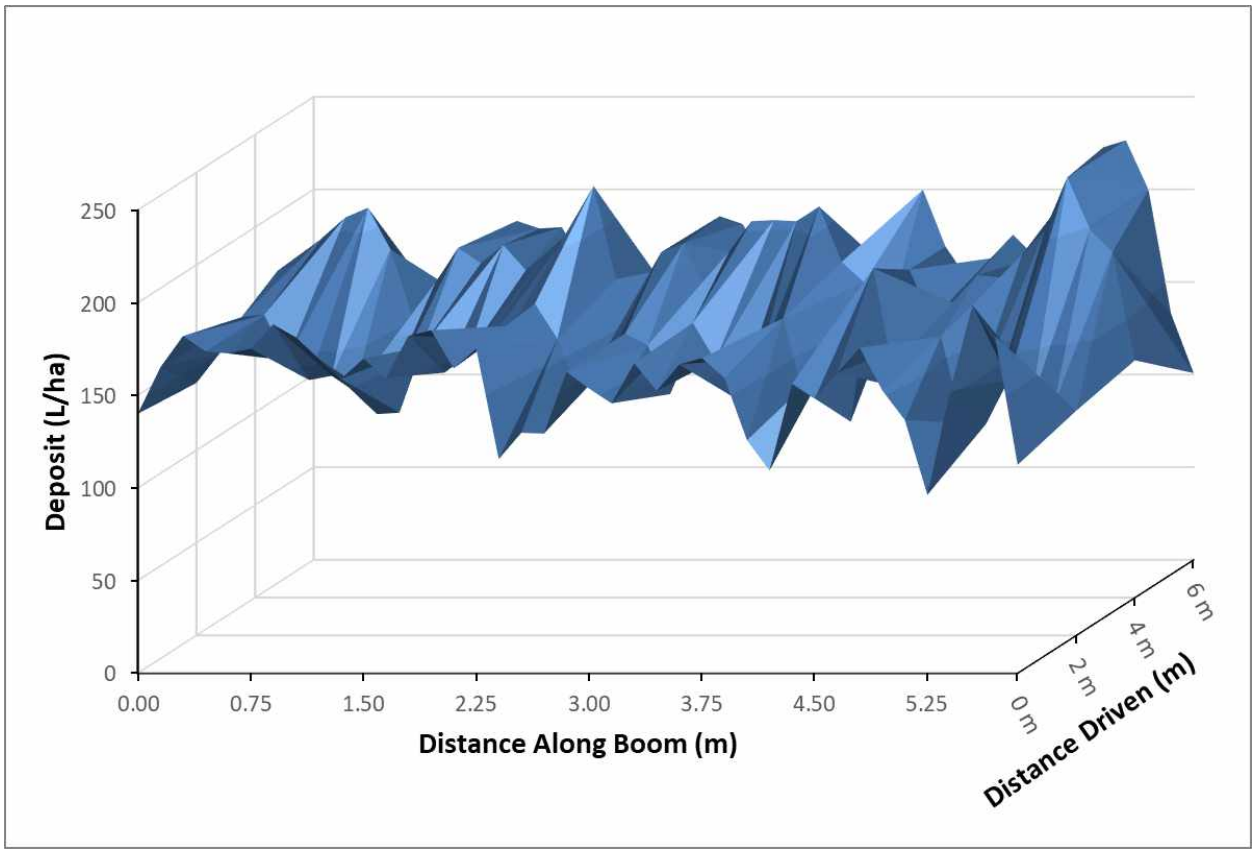

Figure 33: Appearance of a 6 m x 6 m grid of deposit, measured at a resolution of 15 cm along the boom and 2 m along the direction of travel (4 lines). Boom height 28:, Travel speed 9.1 mph, CV 16.3%

Evaluation of the effects of boom height and travel speed confirmed that the deposition variability differed depending on the direction of travel. Variability along the width of the boom in the X-direction was greater than along the direction of travel in the Y-direction (Table 22). In the direction of travel, CV values were between 12% and 16% for all treatments. Along the boom, CVs ranged from 14% to 42%, with the two highest values (39% and 42%) at the fastest travel speed.

Table 22: Variability of deposit samples among in the X- (boom) and Y- (travel) direction. CV values were calculated from 160 values (four lines and 40 samples per line).

Travel Speed (mph)	Boom Height (in)	Line Direction	Deposit (L/ha) Line 1	Line 2	Line 3	Line 4	Mean	CV (%)
9.1	28	X	157.6	145.3	182.6	161.0	161.6	16.3
9.1	28	Y	119.7	123.3	127.7	124.2	123.7	11.5
9.1	45	X	208.7	209.8	197.4	107.7	180.9	25.7
9.1	45	Y	100.1	94.9	91.0	96.6	95.6	16.0
13.4	28	X	115.1	123.9	120.4	122.5	120.5	14.4
13.4	28	Y	69.7	62.6	62.6	73.8	67.2	11.8
13.4	45	X	115.2	117.5	118.7	119.4	117.7	26.2
13.4	45	Y	58.3	59.8	62.6	69.2	62.5	15.6
20.0	28	X	24.7	22.5	19.6	18.7	21.4	39.3
20.0	28	Y	43.3	54.6	49.4	57.1	51.1	14.2
20.0	45	X	52.9	49.2	49.1	52.3	50.9	42.4
20.0	45	Y	58.1	48.3	48.5	54.4	52.3	14.7

Samplers along the boom had CVs that were about 5 to 10% higher for the 45” boom height compared to the 28” boom height. A travel speed od 20 mph significantly increased variability for both boom heights (Figure 34).

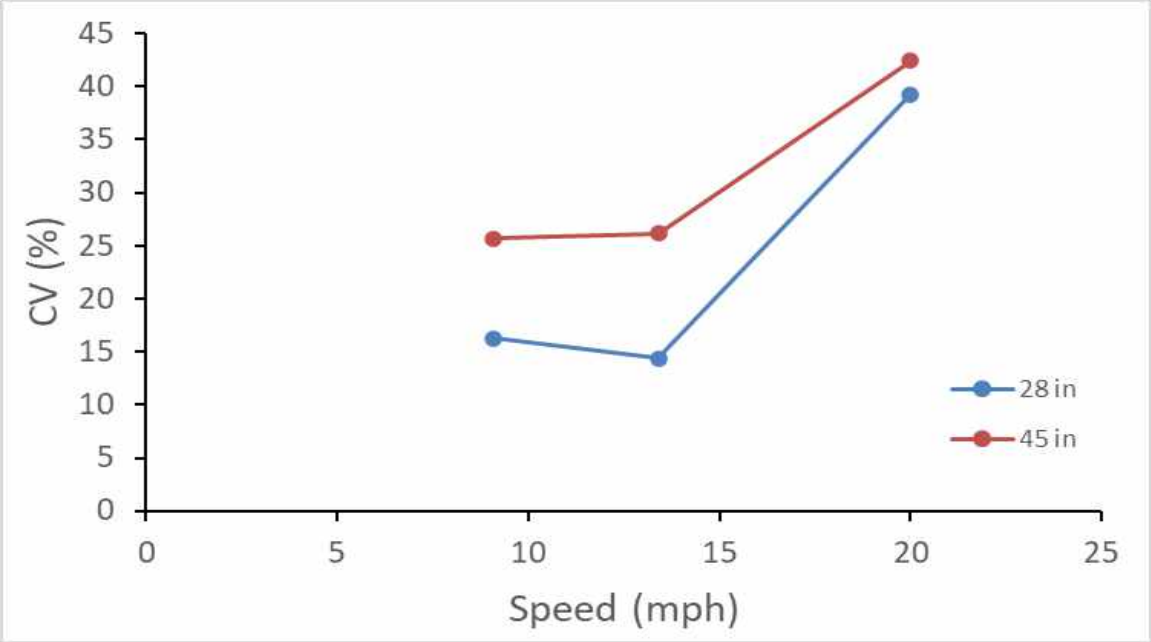

Figure 34: Effect of travel speed on deposit CV along the boom for 6 m in 15 cm increments, at two boom heights (28” and 45”)

In the direction of travel, overall VCs were lower and were not influenced by either travel speed. The greater boom height did increase deposit CV values, but these were not affected by travel speed (Figure 35).

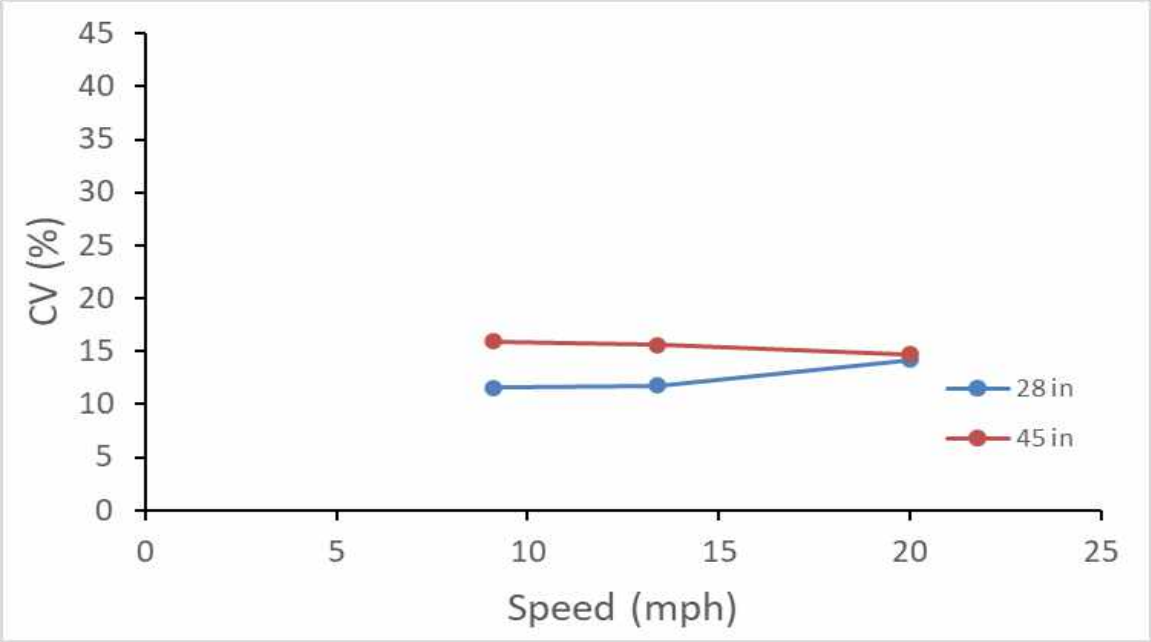

Figure 35: Effect of travel speed on deposit CV along the direction of travel for 6 m in 15 cm increments, at two boom heights (28" and 45")

Multiple Regression

This study was able to evaluate the effects of various sprayer configurations on spray deposit patterns and overall uniformity. To determine what the ranking of these variables, including wind speed, was on deposit CV for all 36 string trials, a multiple regression analysis was done. The independent variables were spray quality, boom height, travel speed, and wind speed. The stepwise regression found that only travel speed and spray quality contributed to a predictive model (Table 23). The binary nature of the tested variables (low and high booms and slow and fast travel speed) limited the power of this test. However, it is instructive to see that the deposit CVs were influenced by travel speed more than any other variable.

Table 23: Coefficients for a simple stepwise multiple regression model evaluating the effects of travel speed, spray quality, boom height, and wind speed on deposit CV

N=36 F(2,33)=5.0514 p<0.012	R= 0.484 R^2= 0.234 Adjusted R^2= 0.188					
	b*	**Std. Err.**	**b**	**Std. Err.**	**t(33)**	**p-value**
Intercept			22.111	5.589	3.956	0.000
Speed	0.474	0.155	1.060	0.346	3.065	0.004
Spray Quality	-0.209	0.155	-1.693	1.249	-1.355	0.185

Project No. A20134P

Date: October 8, 2021

Revised: October 26, 2021

Humboldt, Saskatchewan

Final Report

Applying Computational Fluid Dynamics to Understand Factors that Influence Spray Drift

Justin Gerspacher,

Project Engineer

Ian Paulson, P.Eng., M.Sc.

Technical Services Lead

Bryan Lung, P.Eng., M.Sc.

Director, Project Management

Executive Summary (CFD)

Pesticide application using high-clearance sprayers is an important activity in modern agriculture. Minimizing off-target spray application (spray drift) is an important consideration that must be balanced with productivity demands. Air flow patterns created by a sprayer body and boom while in operation are known to be an important cause of spray drift. The flow of air around a sprayer while it travels creates disturbances in the flow field that spray droplets must pass through, which can cause the droplets to be directed off target. Therefore, understanding how the wake of a sprayer is influenced by operational parameters of the sprayer is important in the study of minimizing spray drift.

To investigate the air flow patterns induced by a sprayer during operation, a computational fluid dynamics (CFD) model based on a John Deere 4045 sprayer was created. A low sprayer travel speed (3.35 m/s) and a low boom height (0.635 m) was compared to a configuration with a high travel speed (6.71 m/s) and a high boom height (0.889 m). A sprayer model with wide tires (size: 800/55 R46) was compared to one with narrow tires (size: 380/105 R50). The velocity flow field and turbulence production in the wake of the sprayer was analyzed for each configuration to compare the potential for spray drift.

A high travel speed resulted in larger disturbances in the flow field compared to a low travel speed. The relationship between the upward and lateral components of air velocity and travel speed was approximately linear in regions behind the sprayer body and tires, which increased the potential for spray droplets to be directed off target. More turbulence was produced at the higher travel speed. The high boom height demonstrated a more chaotic flow at important locations beneath the boom when compared to the lower boom height.

Including wider tires on the sprayer resulted in a greater disturbance in the flow field when compared to the narrower tires. The width of the wake behind the sprayer tractor extended several tire widths beyond the width of the machine, and greater turbulence in the wake of the wide tires was observed.

Operational parameters of a sprayer were shown to influence the characteristics of the sprayer wake that cause spray drift. Higher travel speed, higher boom height, and/or wider tires increased the disturbance in the air flow field (both turbulence and detrimental flow direction) and therefore increased the amount of potential for off-target deposition.

Introduction

The timely, accurate, and efficient application of pesticides is an important activity in modern crop production methods. Increased productivity continues to be demanded by the market; however, minimizing the environmental impact of pesticide application due to spray drift remains paramount to sustainable and responsible agricultural activities. Understanding the factors that affect the behavior of spray droplets upon release from a high-clearance sprayer is a critical building block to reducing the drift of pesticide.

Simulating spray droplets continues to be an active area of research. After droplets are released, a primary influence on the droplet trajectory is the flow field through which droplets travel. The wake that results from the flow of air around a bluff vehicle, like a modern high-clearance sprayer, can create a significant disturbance in the flow field where droplets pass through. Therefore, understanding how sprayer wakes are influenced by the operating variables remains critical to the problem of spray drift.

Computer simulations using computational fluid dynamics (CFD) are a viable method to estimate the flow patterns around modern high-clearance sprayers much more efficiently than field experiments. Field experiments provide means to quantify the movement of droplets by measuring the total accumulation of droplets at a particular location. However, as sampling points typically remain stationary, the evolution of the flow field as the sprayer passes over a sampling point cannot be determined. CFD provides a data-rich solution to support a deeper interpretation of field measurements, as many points can be sampled simultaneously.

To support field drift measurements conducted as part of a larger body of research by Agrimetrix Research & Training, a CFD model based on a John Deere R4045 sprayer was developed by the Prairie Agricultural Machinery Institute (PAMI) to investigate the change in flow patterns around the machine as boom height, travel speed, and tire size were modified.

Details of the development of the CFD model are given. Results from a model configuration with a low travel speed and a low boom height were compared to a configuration with an increased travel speed and higher boom. This “high and fast” simulation was then compared to a similar model in which wide tires were simulated.

Model Description

Modeling efforts in this project built upon the work published in Landry and Wolf (2019) where a very basic John Deere R4045 sprayer was simulated. In the current work, improvements were made to the geometry of the sprayer to more realistically represent the top of the cab, operator platform, and tank shape, as well as the center section of the boom and the linkages between it and sprayer tractor. Past work highlighted the importance of the region between the rear tire and boom, so this distance was verified during the modeling process.

Three configurations of the sprayer were created in SolidWorks, and the geometry was exported for further set-up of the actual CFD model in Star-CCM+ (Siemens PLM Software, 2019). Two different boom heights were modeled: 0.635 m and 0.889 m, as measured from the ground to the location of the nozzle tips. Two sprayer travel speeds were simulated: 3.35 m/s and 6.71 m/s. For maximum contrast, the low speed (3.35 m/s) and low boom height (0.635 m), and high speed (6.71 m/s) and high boom height (0.889 m), were grouped to create two configurations: 1) low and slow, and 2) high and fast. Narrow tires of size 380/105 R50 were modeled for both the low and slow and high and fast configurations. A third configuration with wide tires (size: 800/55 R46) was also simulated using a high speed (6.71 m/s) and high boom height (0.889 m). Model configurations are summarized in Table 24.

Table 24: Geometries used in CFD simulations.

Model Configuration	Boom Height (m)	Tire Size	Travel Speed (m/s)
Low and Slow	0.635	380/105 R50	3.35
High and Fast	0.889	380/105 R50	6.71
High and Fast with Wide Tires	0.889	800/55 R46	6.71

The geometry of the sprayer with narrow tires is shown in **Error! Reference source not found.** (in low boom configuration). The wide-tire configuration (with high boom height) is shown in Figure 37. A close-up view of the boom is shown in Figure 38. Note how the geometry has been simplified and the nozzles themselves are not included in the model.

(a)

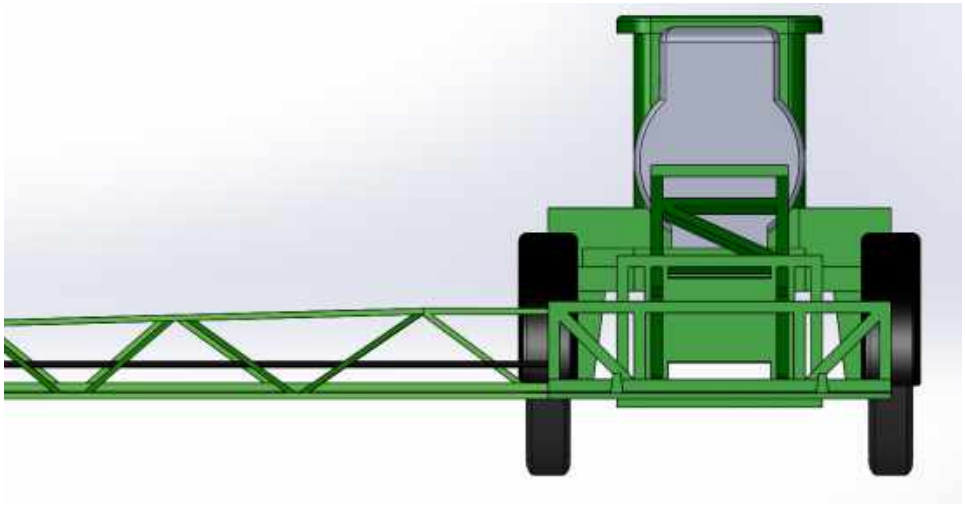

(b)

Figure 36: Geometry of the sprayer model with narrow tires and low boom configuration). Isometric view (a) and rear view (b).

(a)

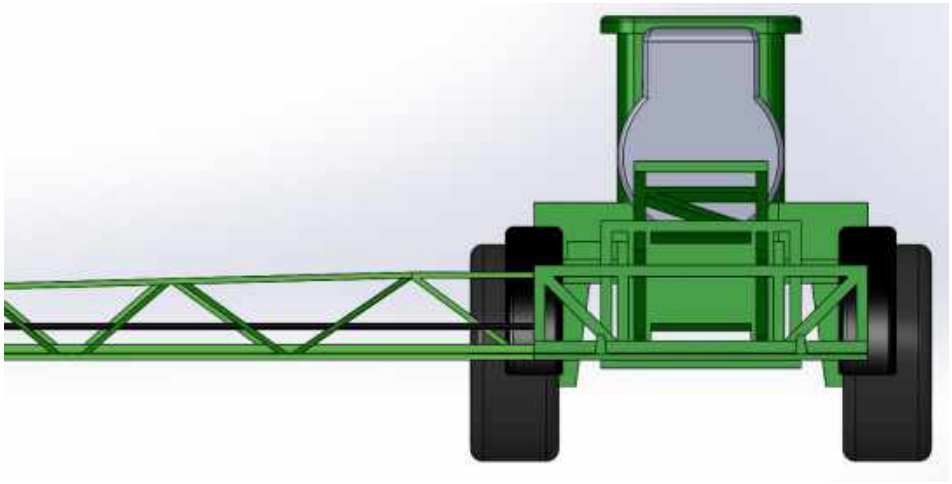

(b)

Figure 37: Geometry of the sprayer model with flotation tires and high boom configuration. Isometric view (a) and rear view (b).

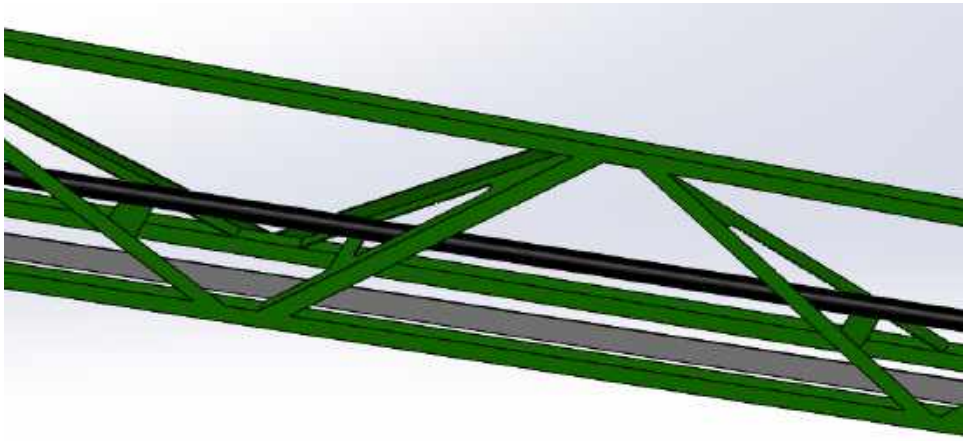

Figure 38: Close-up view of the boom. The wet boom tube and nozzles were not included in the model but would be mounted on the backside of the vertical flat bar that was included and shown here in grey. The black tube is representative of the hose that carries fluid to the outer boom.

The theoretical nozzle location relative to the ground plane and the sprayer's rear axle are shown in Figure 39 for both the low boom (a) and high boom (b) positions.

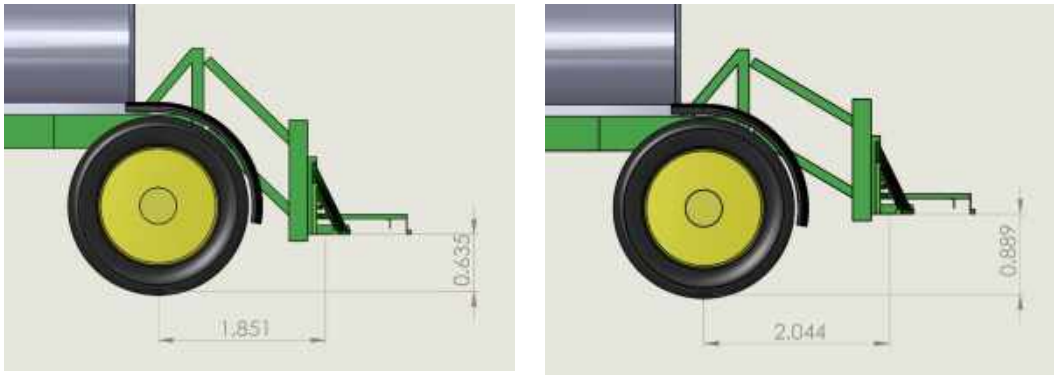

(a) (b)

Figure 39: Theoretical nozzle location relative to ground plane and rear axle in low-boom (a) and high-boom (b) positions.

The John Deere R4045 sprayer is available with up to a 36 m wide boom. However, only the center sections, out to a width of 22 m, were included in the model. This was done in the interest of managing calculation times. Flow patterns at the ends of the boom are expected to be relatively consistent, as these areas are outside of the wake of the tractor. Therefore, modeling the far ends of the boom was of low interest.

In this application, relative motion between the sprayer and air was simulated in a manner similar to aerodynamic experiments in a wind tunnel. In the simulation, the sprayer was stationary with the air entering the wind tunnel and flowing over the sprayer at the desired speed of travel to simulate the

motion. To maintain the appropriate relative motion to the sprayer, the ground plane of the simulation domain was set to move at the same velocity as the inlet air velocity. To minimize wall effects, a significant volume of air around the sprayer was also included in the simulation. The goal in sizing this volume was to maintain freestream conditions far away from the sprayer itself. A virtual wind tunnel with dimensions of 14 m wide x 80 m long x 20 m height was used. The front of the sprayer was 14 m from the inlet.

To maintain a manageable calculation time, symmetry along the center plane of the sprayer was exploited to cut the computational domain in half. While this imposes a symmetrical requirement on the results, it is a common simplification in CFD modeling when the object of interest is symmetrical. This prohibits the introduction of a crosswind component in the simulation.

The rotational speed of the tire surface was included in the boundary conditions of the model. A deliberate choice was made to omit the tread geometry of the tire and to model the tire face as a smooth surface. Due to the chosen model type, the tire is modeled as being stationary. To simulate the tire's rotation, the outer surfaces of the tire have a tangential velocity boundary condition applied that is equivalent to the speed that the surface travels as the tire rotates. However, this boundary condition can only apply a velocity tangential to the surface, so it is only representative on the surfaces of the tire that are tangent to the rotation (outer face of tread and the sides of tire). A normal velocity component cannot be applied to surfaces that are normal to the rotation (lugs of the tread). If this was attempted, it would create an inaccurate representation of the air velocity on the tire surface (Hobeika and Sebben, 2018). For this reason, the tire geometry was modeled as being smooth without treads. A numerical surface roughness factor was applied to the smooth surface to approximate the impact of the tire tread. Multiple iterations of tire representation were considered during the development of the full-vehicle model.

Relevant meshing parameters used to discretize the fluid domain are given in Table 25.

Table 25: Relevant meshing and model parameters.

Mesh Parameter	Value
Mesh type	Trimmed cell (hexagons)
Target Surface size - Tractor (m)	0.020
Target Surface size - Boom (m)	0.010
Far field size (m)	0.320
Number of cells	39.0 - 40.6 million
Model type	Reynolds-averaged Navier-Stokes (RANS)
Turbulence model	Shear-stress transport **Invalid source specified.**

Steady state simulations were run utilizing a Reynolds-averaged Navier-Stokes (RANS) model. Each configuration required approximately 67 hours to complete the calculations using a four-core Intel ®

Xeon ® E5-2660 2.20 GHz processor. Approximately 3,000 iterations were required during each configuration to achieve convergence of the numerical solution.

The results of a RANS simulation show the time-averaged values of the flow field. The transient fluctuations in the velocity magnitude and direction are not able to be captured with this model. The time-average flow field is expected to give a good indication of the effect of the vehicle-induced air flow patterns on spray deposition and drift. However, the large-scale transients that were not captured likely also affect spray deposition and induce drift.

Although fluctuations in velocity with time are not captured, the average representation of the variations are included in the model as turbulence. The time-varying component of velocity is related to the turbulence of the air flow. A time-varying velocity u(t) can be defined as the sum of a time-average component $\bar{u}$ and a time-varying component $u(t)'$ as

$$u(t) = \bar{u} + u(t)'. \qquad (1)$$

Turbulent kinetic energy (TKE) is a scalar measure of turbulence. It is defined by

$$TKE = 0.5\left(\overline{u'^2} + \overline{v'^2} + \overline{w'^2}\right), \qquad (2)$$

where $\overline{u'^2}$, $\overline{v'^2}$, and $\overline{w'^2}$ are the variances of the air velocity in the x, y, and z directions.

Based on this definition, TKE is a scalar measure of variation in velocity. In the context of spray drift, increased TKE is associated with enhanced mixing between the air flow and the spray droplets. However, the effect of TKE magnitude on droplet trajectory must be interpreted in concert with the direction of mean air flow.

Results and Discussion

In the context of spray drift in general, and the field data sets more specifically related to this research, two comparisons of air flow patterns are presented:

(a) Low and slow compared to high and fast.

(b) High and fast compared to high and fast with wide tires.

The goal of these comparisons was to highlight the effect of a) real-time operator choices during pesticide application, and b) tire selection choices during equipment preparation.

The simulation of droplet trajectories in turbulent flow conditions is a complex and active area of research. While many mechanisms will contribute to the accurate prediction of spray droplet movement, the velocity and turbulence of the flow field through which the droplets pass were the two main considerations investigated in this work given the demonstrated presence of disturbed air flow following modern high clearance sprayers.

Travel Speed and Boom Height Effects

Results of the simulation are shown as velocity streamlines over select locations of the sprayer for the low and slow configuration in Figure 40. Some interesting characteristics in the flow field are evident in this image. Incoming flow was accelerated around the hood and cab of the sprayer. Behind the tank, the air flowed inward and was subsequently decelerated to fill the void created by the sprayer body. The flow in this region was turbulent, as evidenced by the chaotic directions of the streamlines. The mudguard on the front tire directed the air flow downward behind it, and with chaotic flow evolving

around the rear tire. The streamlines over the boom outside of the tractor show the distortion created by the boom geometry. Air was accelerated both over and under the boom, but the streamlines converged back together behind the boom.

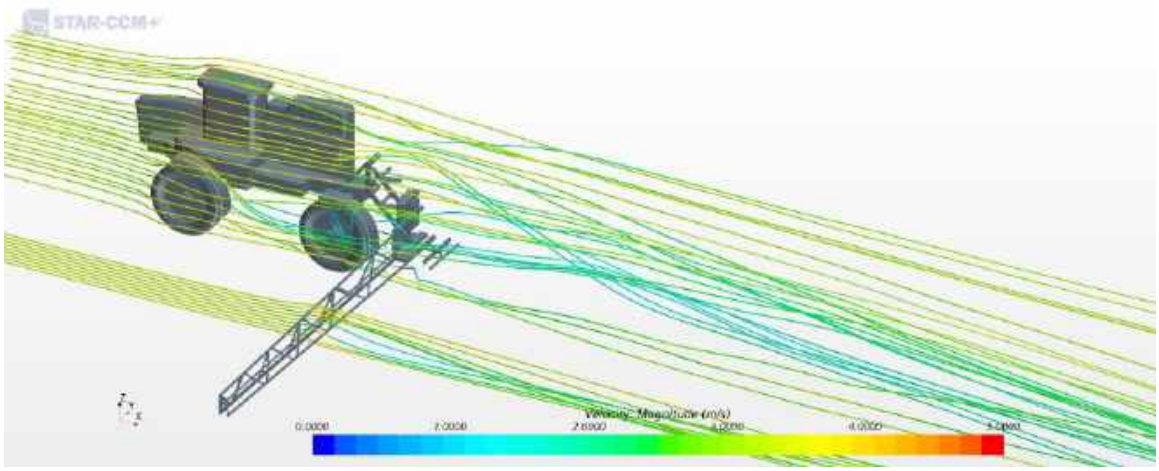

Figure 40: Velocity streamlines for the low and slow configuration.

Based on some of the distinct features highlighted by the streamlines in Figure 40, velocity vector plots on 2D planes of interest were used to further investigate the flow field. In the following vector plots, the arrows indicate the velocity direction while the color indicates the velocity magnitude. Only the components of velocity that are tangential to the display plane are shown; components normal to the plane are omitted. For each plane section, the low and slow configuration is compared to the high and fast configuration.

Regions where the velocity magnitude was either above or below the freestream value (3.35 m/s low and slow and 6.71m/s for high and fast) were of interest. Magnitudes below these values indicated areas where the spray droplets may be pulled along with the sprayer. Magnitudes above these values indicated areas where the spray droplets may be propelled backwards away from the sprayer. An upward component of velocity was also of interest, as it is likely to cause the spray droplets to be suspended in the air for longer periods of time, increasing the ability of ambient winds to carry them off target. A lateral component of velocity is likely to direct the spray droplets off target. Areas where the velocity field appears to swirl indicate vortex structures and areas where spray droplets are likely to become entrained in the air and carried off target.

A series of velocity vector plots showing a side view on vertical planes, parallel to the freestream flow direction of the sprayer are shown in Figure 41 to Figure 44. The series of plots starts at a plane on the centerline of the sprayer and progress out toward the end of the boom.

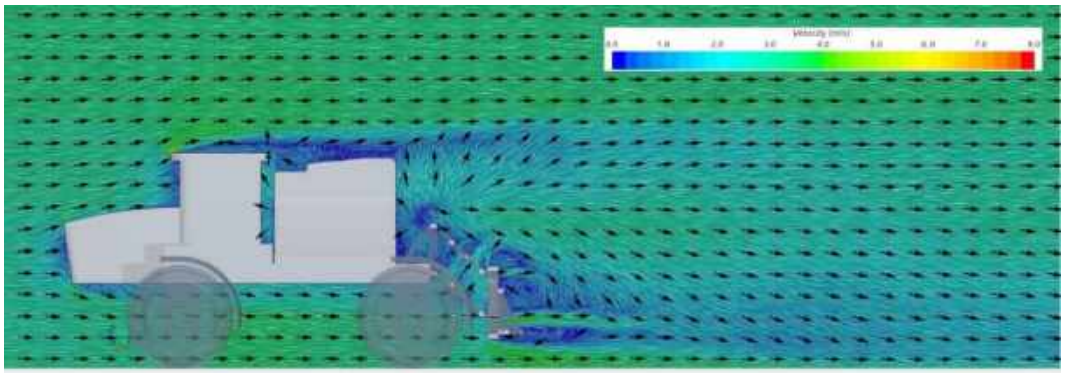

(a)

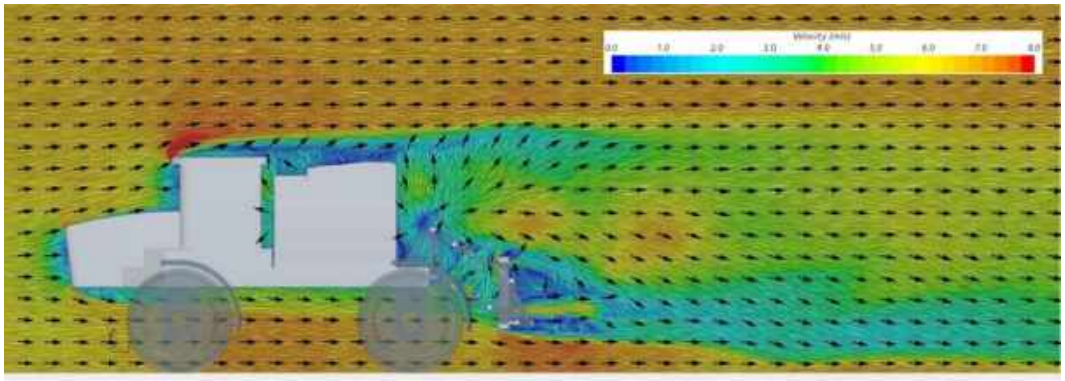

(b)

Figure 41: Velocity vector plots on a vertical plane through the tractor centerline. Low and slow configuration (a), and high and fast configuration (b).

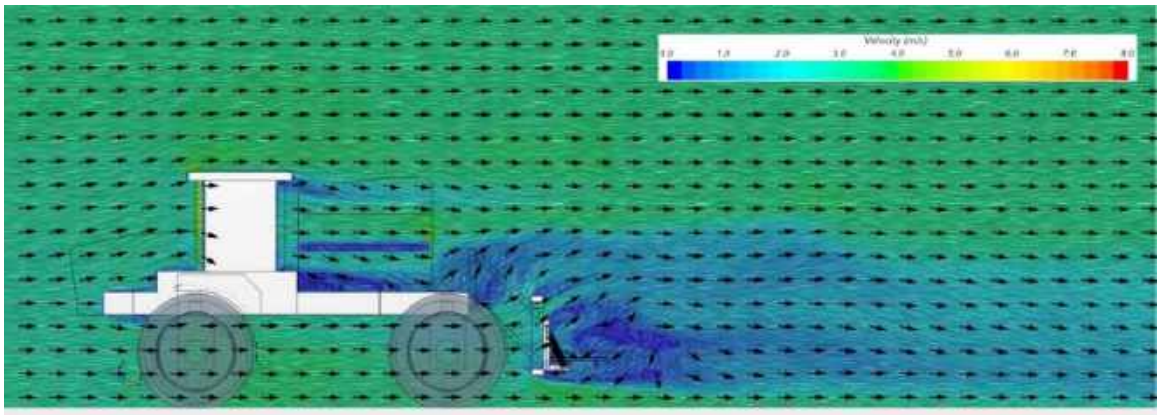

(a)

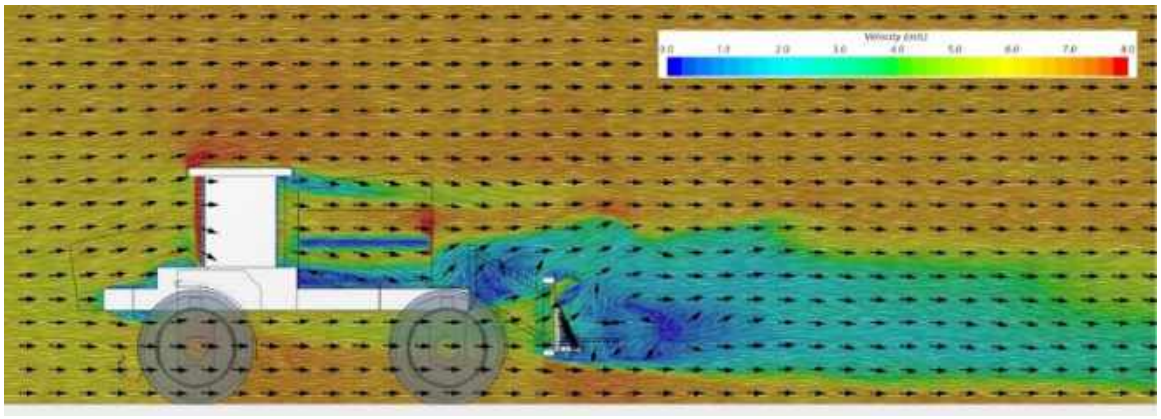

(b)

Figure 42: Velocity vector plots on a vertical plane between the center plane and the tires (0.762 m from centerline). Low and slow configuration (a), and high and fast configuration (b).

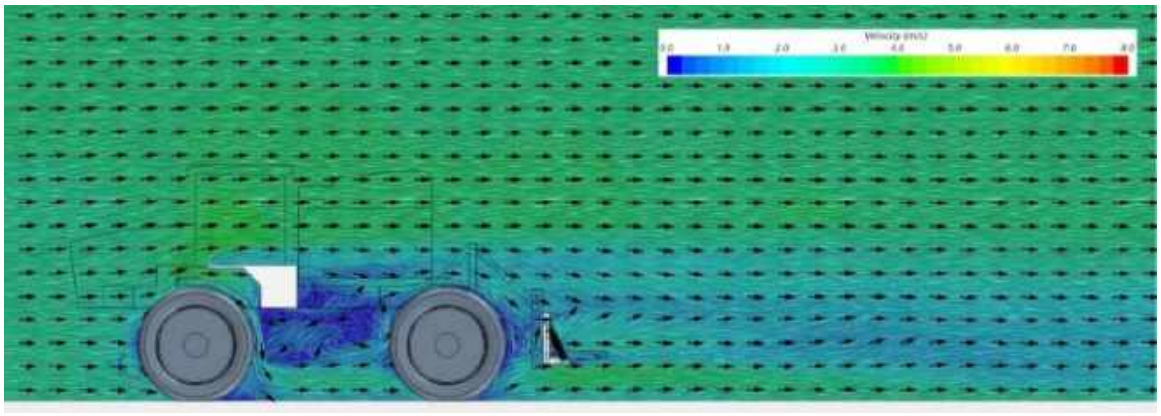

(a)

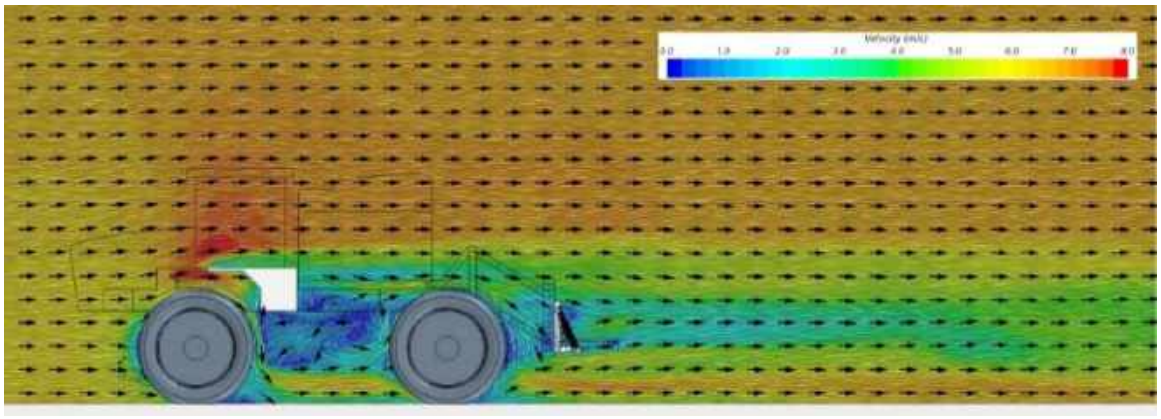

(b)

Figure 43: Velocity vector plots on a vertical plane through the center of the tires (1.524 m from centerline). Low and slow configuration (a), and high and fast configuration (b).

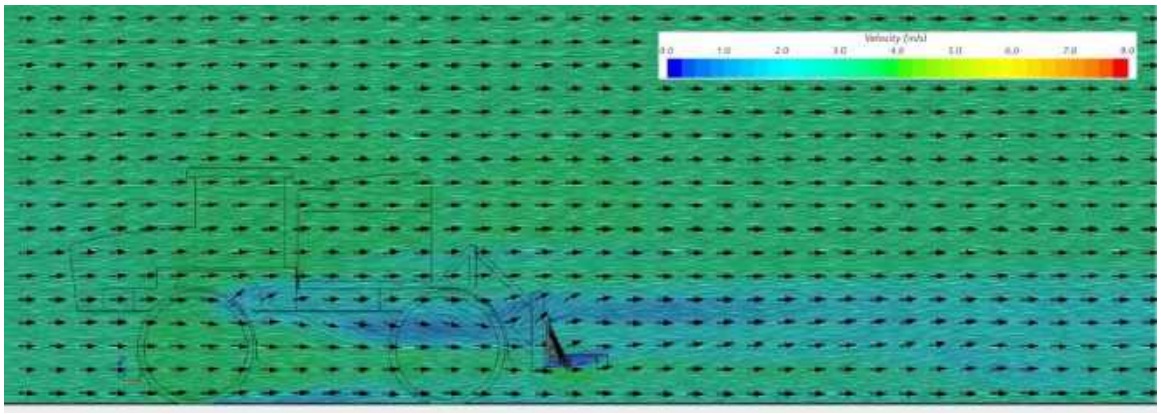

(a)

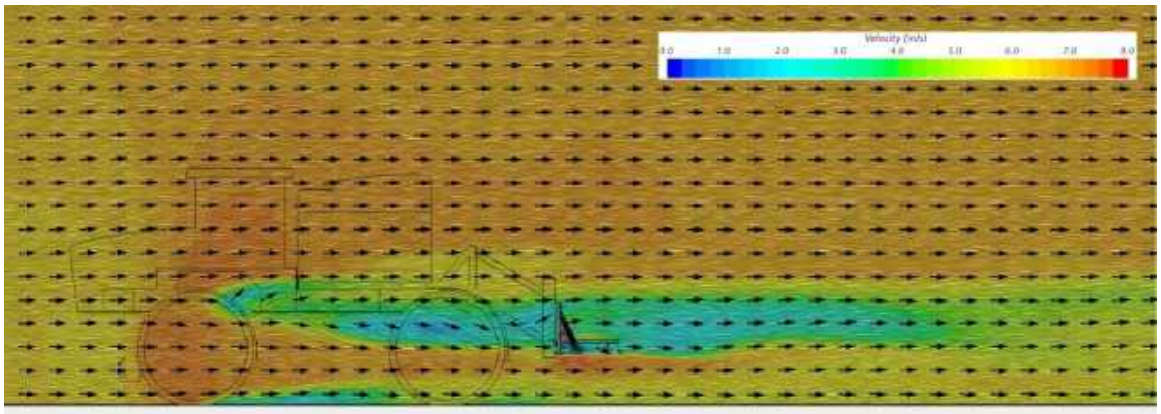

(b)

Figure 44: Velocity vector plots on a vertical plane outside of tires (2 m from centerline). Low and slow configuration (a), and high and fast configuration (b).

Some interesting observations were made from these plots. In general, the region behind the sprayer tractor had a reduced velocity and increased turbulence. Along the centerline of the machine, reversed flow (streamwise component) was observed immediately behind the tank. Outside of the centerline, there tended to be an upward component to the velocity in the region behind the tractor; at 0.762 m from the centerline, the upward component of velocity exceeded 1.0 m/s behind and above the boom.

The front tire and mud guard directed flow downward and a turbulent, low-velocity zone was created between the front and rear tire. Behind the rear tire, the air had an upward component as it flowed towards the boom.

As the flow encountered the boom, it was directed both up and over as well as down and under the boom. In the area below the boom where the spray is injected, a velocity magnitude higher than the free stream value was present in throughout much of the boom except behind the rear tire.

Outside of 2 m from the centerline, the effects of the tractor on the flow diminish and the disturbance created by the boom itself was of most concern. The boom geometry created different flow patterns at different locations along the boom. The flow at two different cross sections of the boom was studied.

Figure 45 shows a section where the angled braces meet the bottom boom members (6 m from centerline). Figure 46 shows an open section where there is no obstruction from the angled braces (6.65 m from centerline).

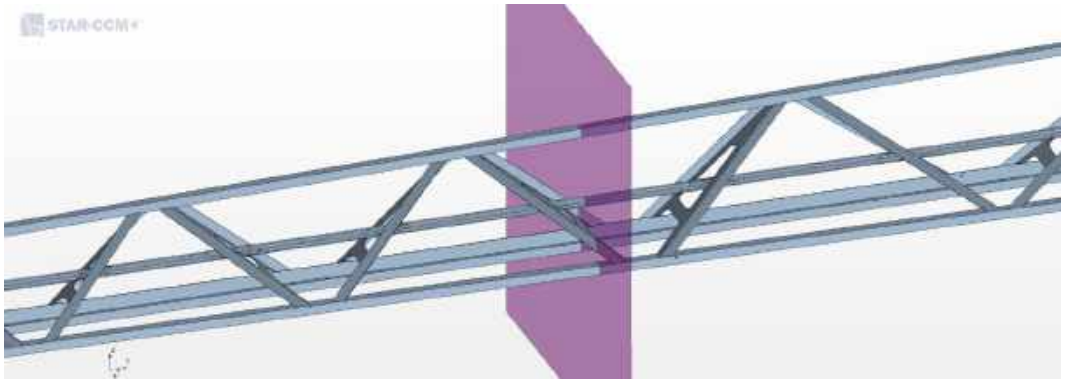

(a)

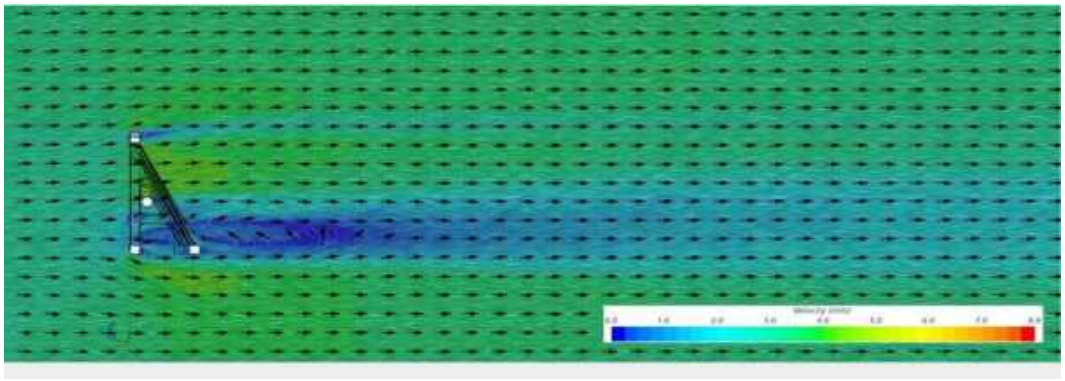

(b)

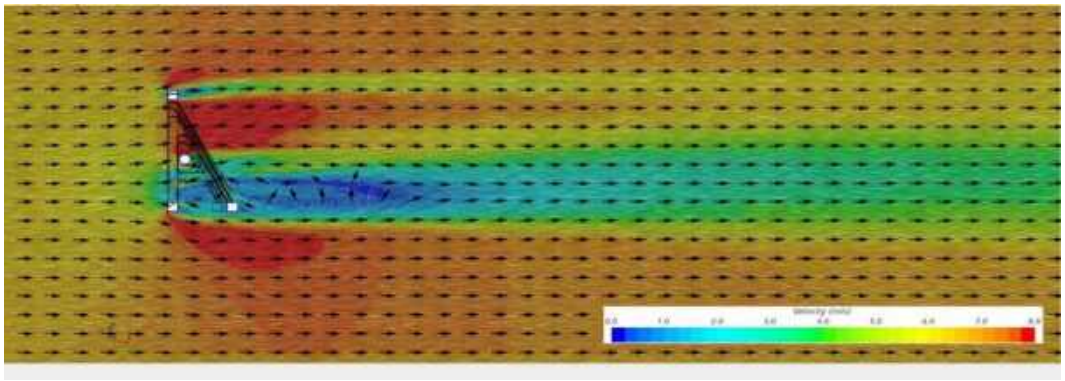

(c)

Figure 45: Velocity vector plots on a vertical plane through an obstructed section of the boom (6 m from centerline); a) section location, b) low and slow configuration, c) high and fast configuration.

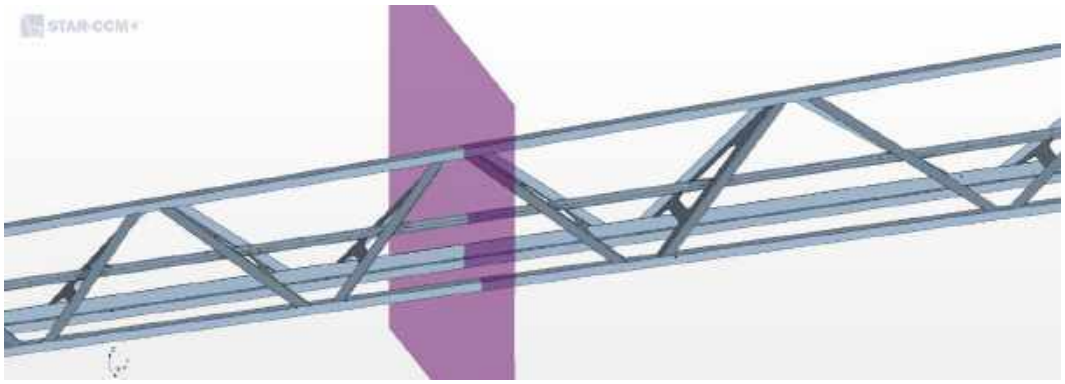

(a)

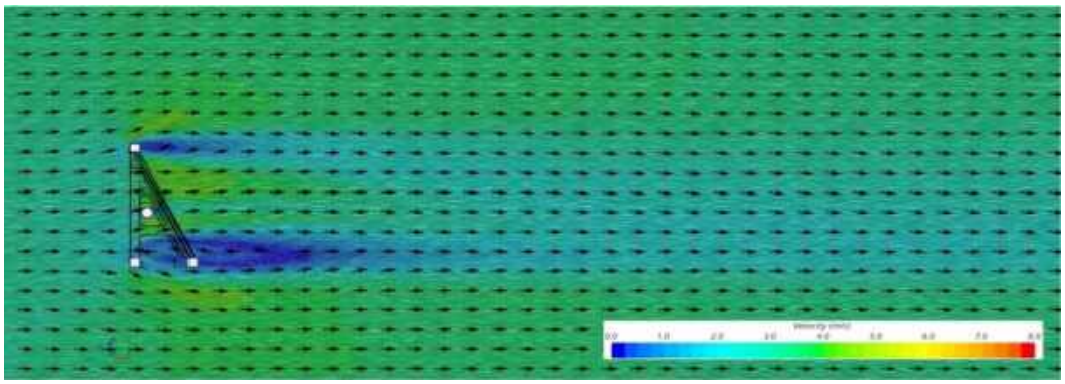

(b)

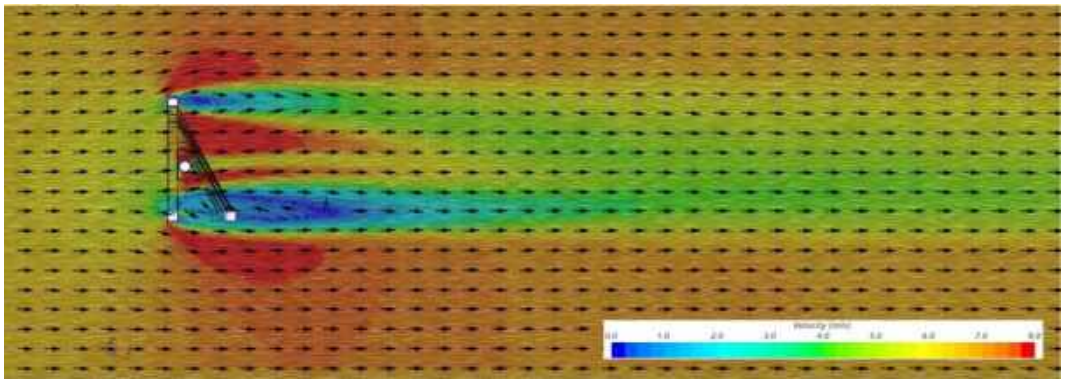

(c)

Figure 46: Velocity vector plots on a vertical plane through an open section of the boom (6.65 m from centerline); a) section location, b) low and slow configuration, c) high and fast configuration.

In the first section, the more obstructive geometry created a taller zone of reduced velocity and back flow. A greater upward component of velocity behind the boom was also evident in the obstructed section versus the open section.

The flow field was also studied on a series of velocity vector plots showing a top view of horizontal planes. The plot in Figure 47 shows a plane at the height of the nozzle location (0.635 m for low and slow and 0.889 m for high and fast). In these plots, the disturbance in the flow field created by the tractor as well as the boom was evident. In general, the area at and behind the boom showed reduced velocity. However, the geometry of the boom created bands where the velocity reduction was more pronounced and extended further behind the boom.

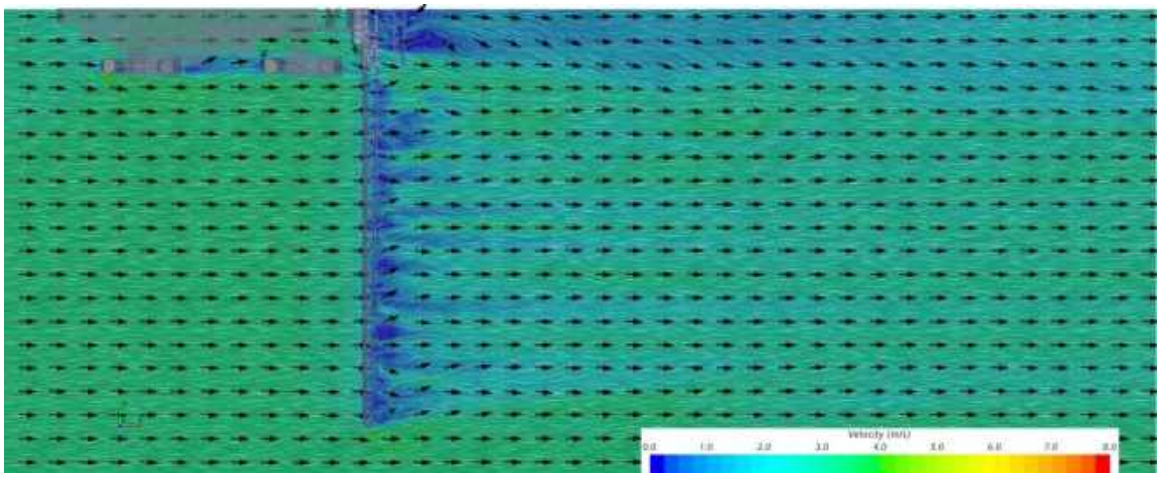

(a)

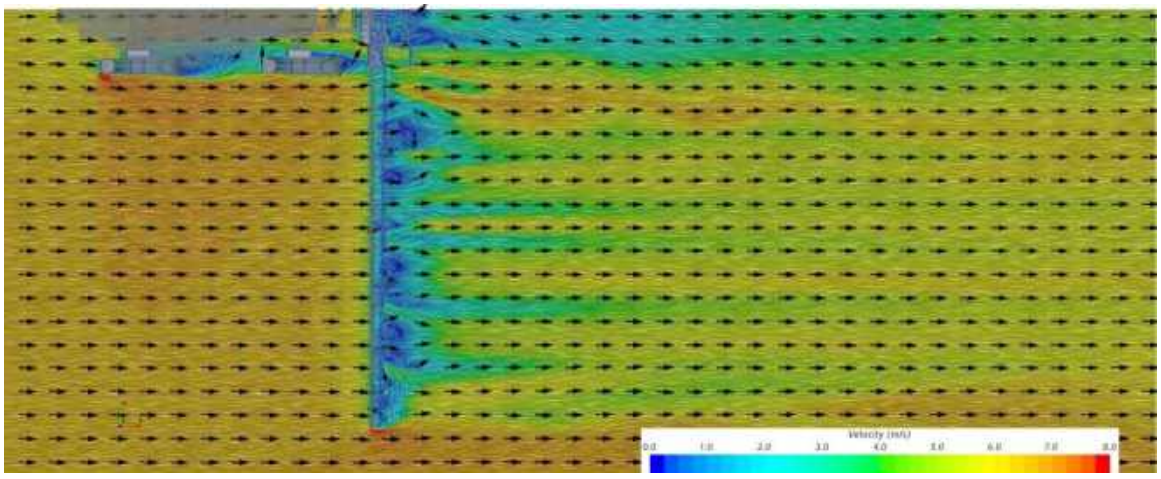

(b)

Figure 47: Velocity vector plots on a horizontal plane at the height where the nozzles would be located: 0.635 m above the ground for low and slow and 0.889 m above ground for high and fast. Low and slow configuration (a), and high and fast configuration (b).

Figure 48 shows a plane 0.318 m below the nozzle location (0.318 m above the ground for low and slow and 0.571 m above the ground for high and fast). It was observed that the flow underneath the boom was accelerated in some regions by up to 0.8 m/s in the high and fast configuration, and 0.46 m/s in the low and slow configuration. The exception to this was in the area immediately behind the tire where

the velocity is reduced (especially for the high and fast configuration). The streamwise component of velocity 0.318 m immediately below the nozzle location along the length of the whole boom for both configurations is plotted in Figure 49.

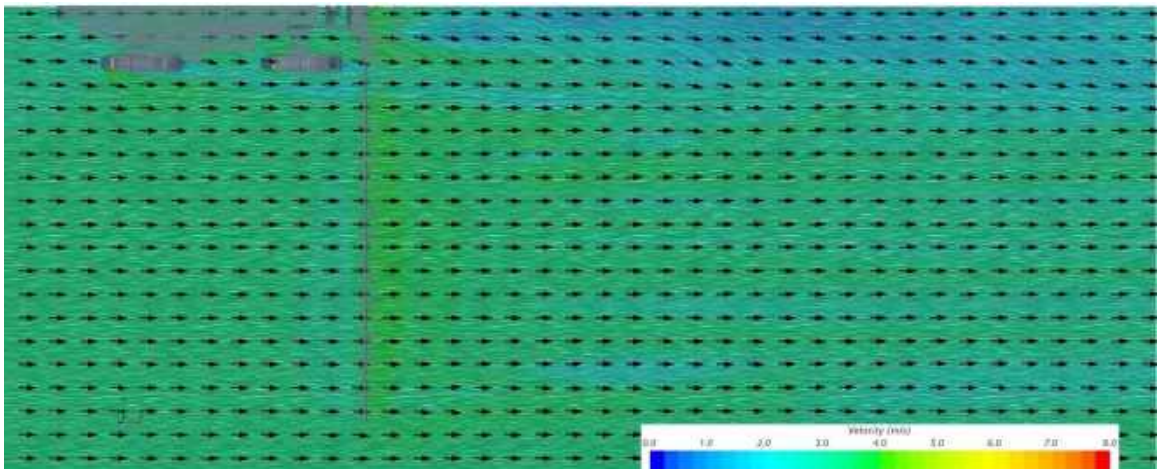

(a)

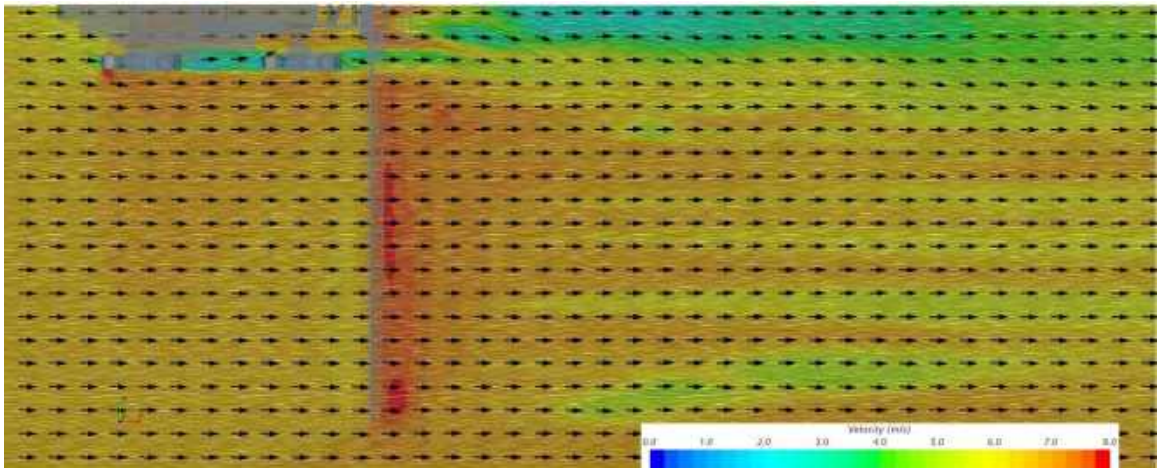

(b)

Figure 48: Velocity vector plots on a horizontal plane 0.318 m below where the nozzles would be located: 0.318 m above the ground for low and slow and 0.571 m above ground for high and fast. Low and slow configuration (a), and high and fast configuration (b).

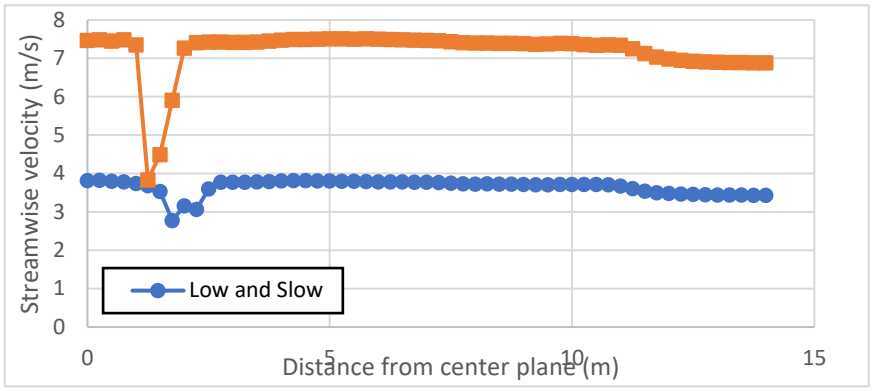

Figure 49: Streamwise velocity component 0.318 m below the nozzle across the width of the boom.

Figure 50 shows a plane 0.889 m above the nozzle location (1.524 m above the ground for low and slow and 1.778 m above the ground for high and fast). This plane is just above the top of the boom structure. At this height, the area behind the tractor showed more turbulent flow as the velocity was reduced to near 0 m/s and the direction of flow reversed in some regions. The velocity tended to have a lateral component directed towards the sprayer centerline in this area. Outside of the tractor, the flow accelerated over the boom.

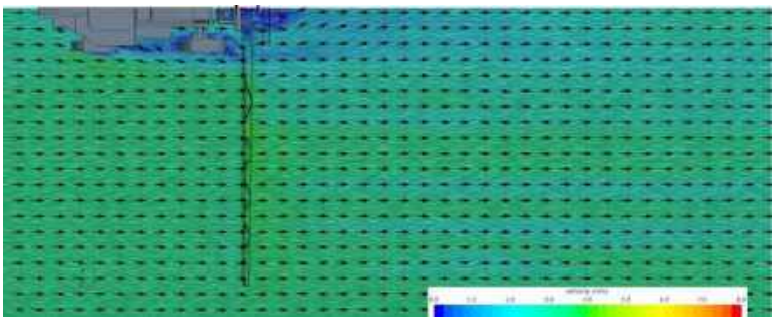

(a)

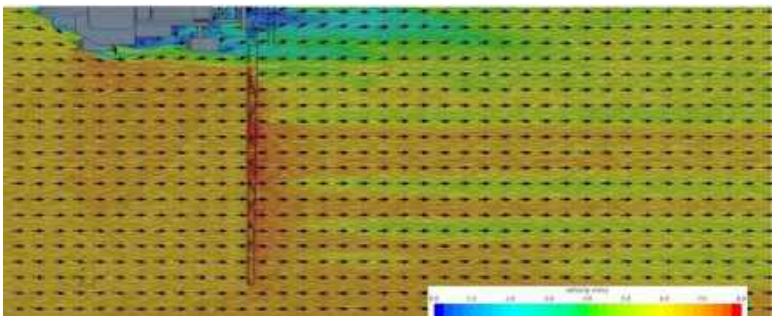

(b)

Figure 50: Velocity vector plots on a horizontal plane 0.889 m above nozzle location: 1.524 m above ground for low & slow (a) and 1.778 m above ground for high & fast (b). Low and slow configuration (a).

Lastly, the flow field was studied on vertical planes normal to the freestream flow. Figure 51 shows velocity vector plots on a vertical plane through the theoretical location of the nozzles. The view is from behind the sprayer, looking forwards. From these plots, it was again seen that the flow behind the tractor was chaotic. The flow behind the tractor and underneath the boom was directed outwards away from the centerline. In the high and fast configuration, a vortex was observed directly behind the tire and below the boom. This vortex was not present in the low and slow configuration. This resulted in lateral velocities of greater than 2 m/s in the high and fast configuration compared to a lateral velocity magnitude of approximately 1 m/s in the low and slow configuration. Under the rest of the boom, the flow was directed downwards. Above the boom in the area outside of the tractor, the flow was directed upwards.

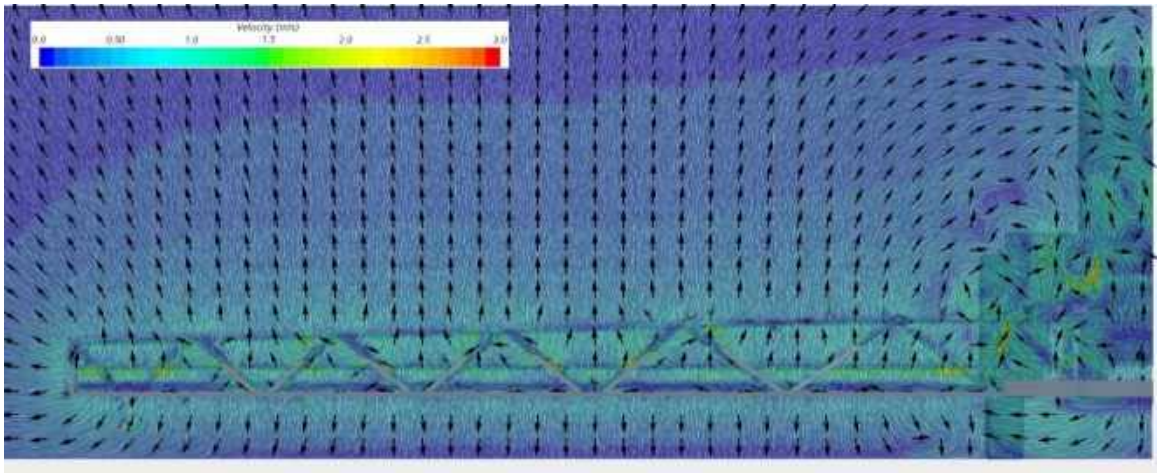

(a)

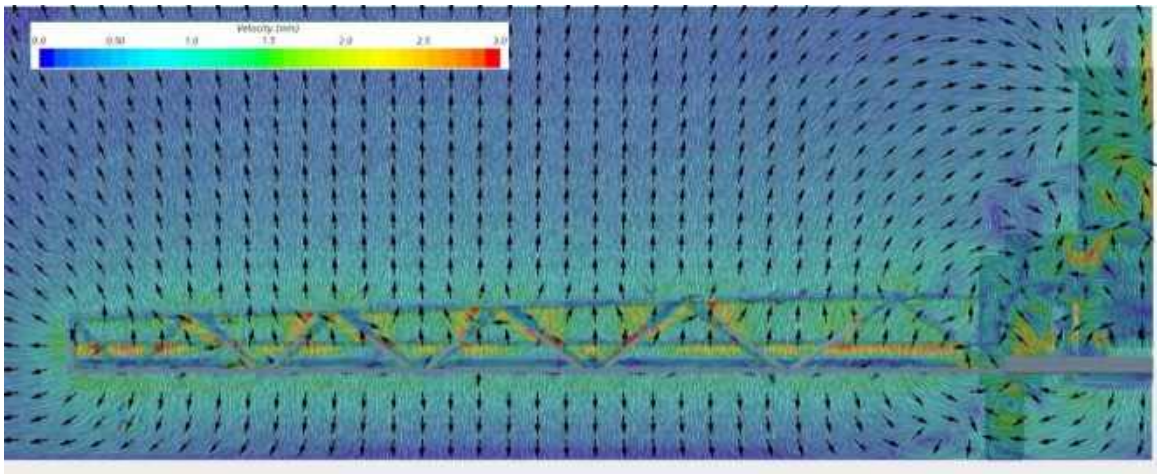

(b)

Figure 51: Velocity vector plots on a vertical plane through the location of the nozzles. View is from behind the sprayer looking forwards. Low and slow configuration (a), and high and fast configuration (b).

Figure 52 and Figure 53 show velocity vector plots on a vertical plane 1 m and 3 m behind the nozzle location, respectively. The flow behind the tractor at these distances was still turbulent. Above the boom on the right side of the images, the air flowed in towards the centerline. At the centerline, the air flowed downward. Below the boom, there was an outward component to the flow in the area behind the tractor; the vortex identified behind the tire in Figure 51 (b) was still present 1 m behind the boom (Figure 52 (b)) but dissipated by 3 m behind the boom (Figure 53 (b)) . Outside of the tractor, flow below the boom had an upward velocity component close to 1 m/s at 1 m behind the nozzle location at the higher speed. At 3 m behind the nozzle location, swirling patterns were present; the magnitude of the velocity scaled was approximately linear with travel speed.

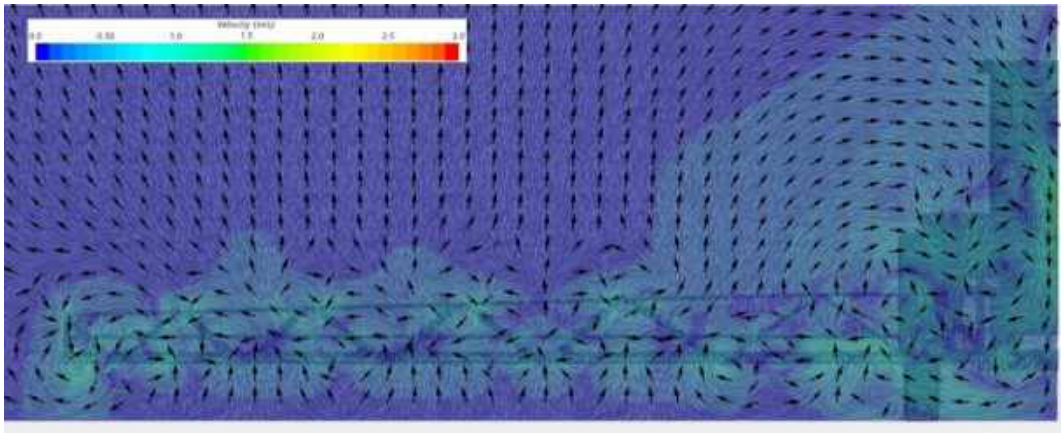

(a)

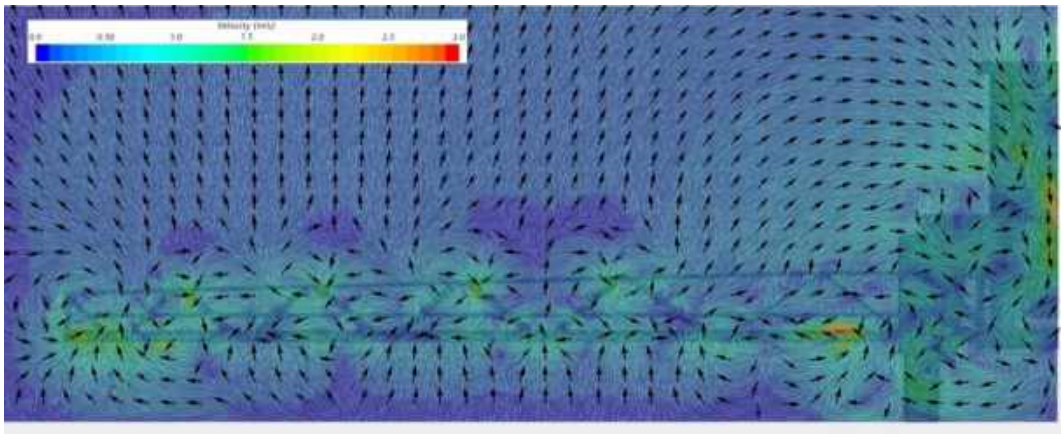

(b)

Figure 52: Velocity vector plots on a vertical plane 1 m behind the theoretical nozzle location. View is from behind the sprayer looking forwards. Low and slow configuration (a), and high and fast configuration (b).

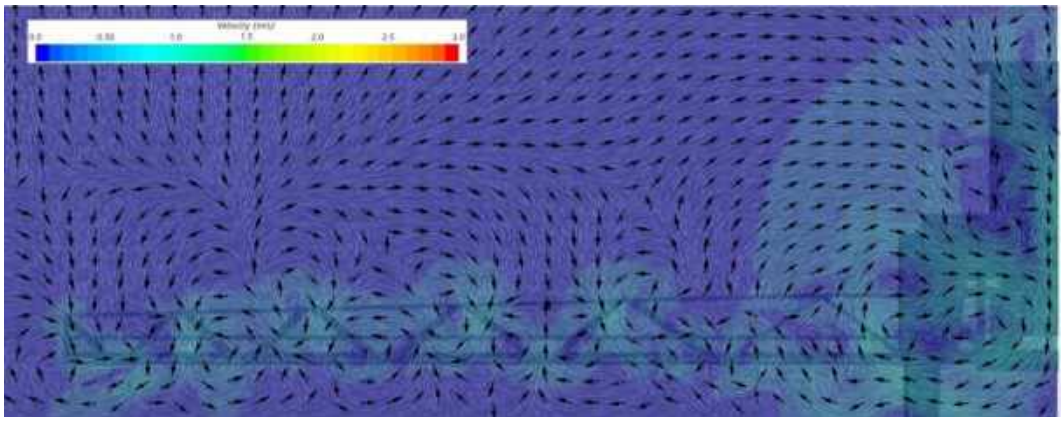

(a)

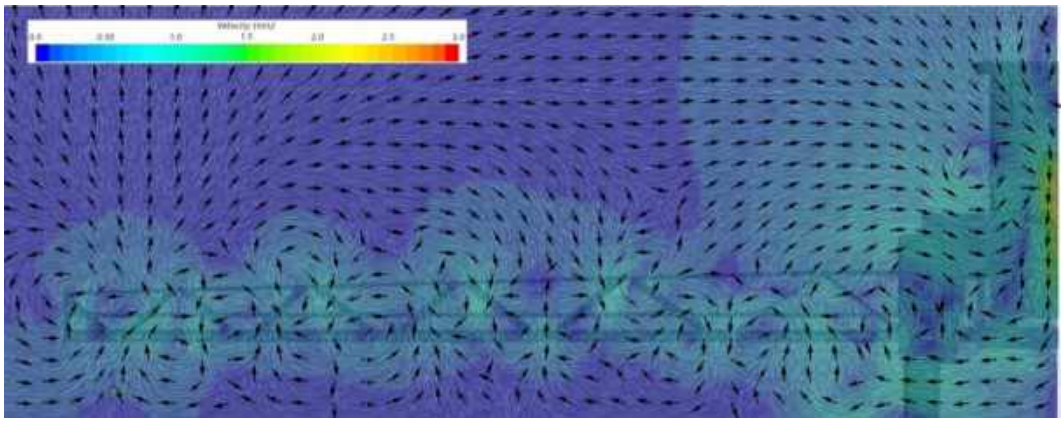

(b)

Figure 53: Velocity vector plots on a vertical plane 3 m behind the theoretical nozzle location. View is from behind the sprayer looking forwards. Low and slow configuration (a), and high and fast configuration (b).

From the series of velocity vector plots, some comparisons can be made between the low and slow and high and fast configurations. Generally, the direction of the flow was similar throughout the flow field for the two configurations. However, the magnitude of velocity in all directions was typically increased by a factor of two for the high and fast configuration compared to the low and slow configuration. Due to the increased magnitude, in areas where the velocity has an upward or lateral component, the potential for spray drift is greater at the higher travel speed. The higher boom height also showed increased potential for spray drift. Under the boom, greater vorticity was seen in locations behind the tractor body and tires for the high and fast configuration compared to the low and slow. This is in addition to the increased distance the spray droplets must travel to reach the ground with a higher boom, which would also increase the potential for the air flow field to direct them off target.

The turbulence of the flow field was also considered as an indication of spray drift potential. Regions of elevated turbulence, as measured by the scalar TKE value, were of concern due to the occurrence of increased mixing of the spray droplets and the air. Images showing the value of TKE in the areas around and behind the sprayer are shown in Figure 54. Note that a cut-off technique was used such that regions developing TKE values below 0.25 J/kg are not colored.

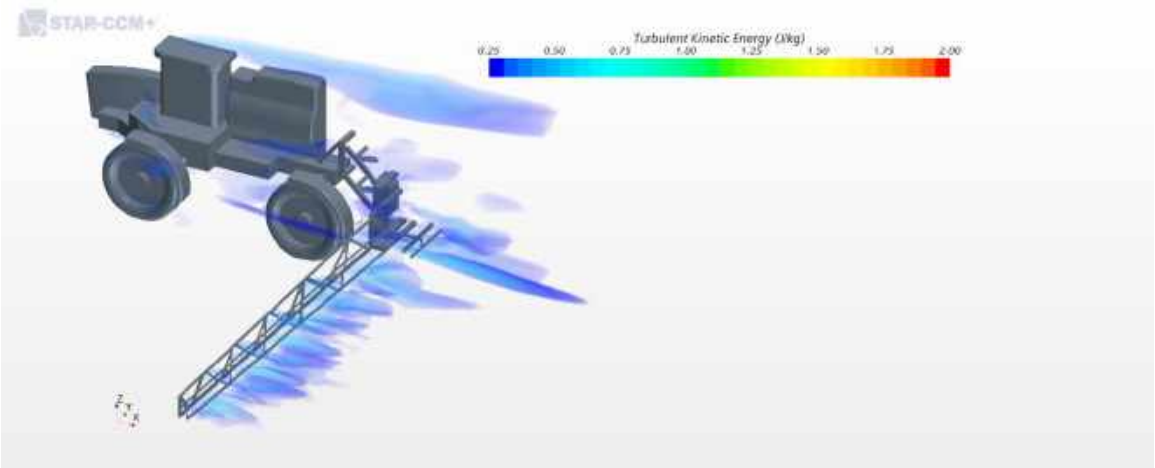

(a)

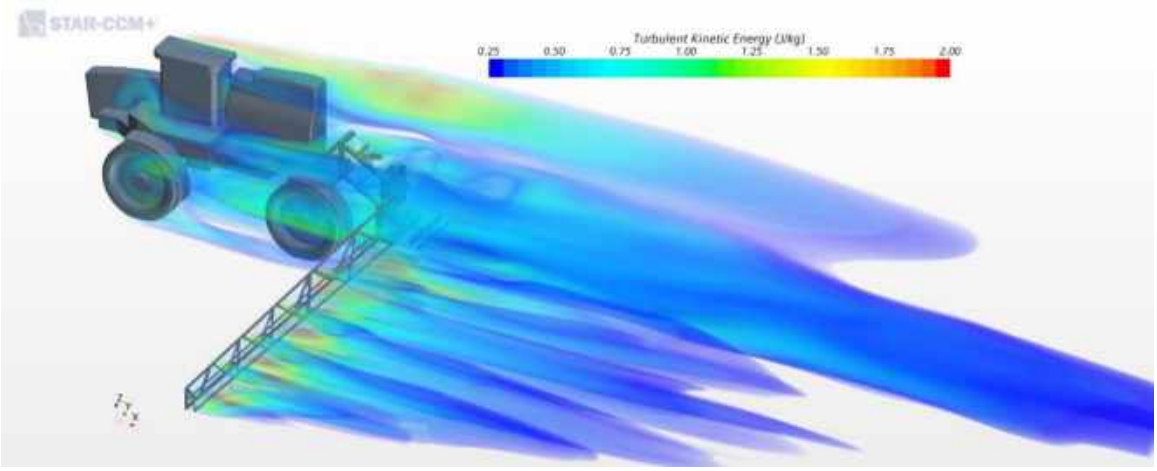

(b)

Figure 54: TKE values around and behind the sprayer. Only regions where TKE exceeds 0.25 J/kg are shown. Low and slow configuration (a), and high and fast configuration (b).

A stark contrast was seen in the production of TKE between the low and slow and the high and fast configurations. The higher travel speed resulted in much higher values of TKE around and behind the sprayer; peak TKE values in close proximity behind the center boom section (approximately 0.75 J/kg) were identified in the wake more than one vehicle length behind the sprayer at the higher travel speed. The areas of greatest TKE for both configurations included above and behind the cab and tank, around and behind the rear tire, and behind the boom structure.

Plots of TKE values on a 2D horizontal plane at the height of the nozzles is shown in Figure 55. TKE values were elevated in regions behind the tractor and behind the boom.

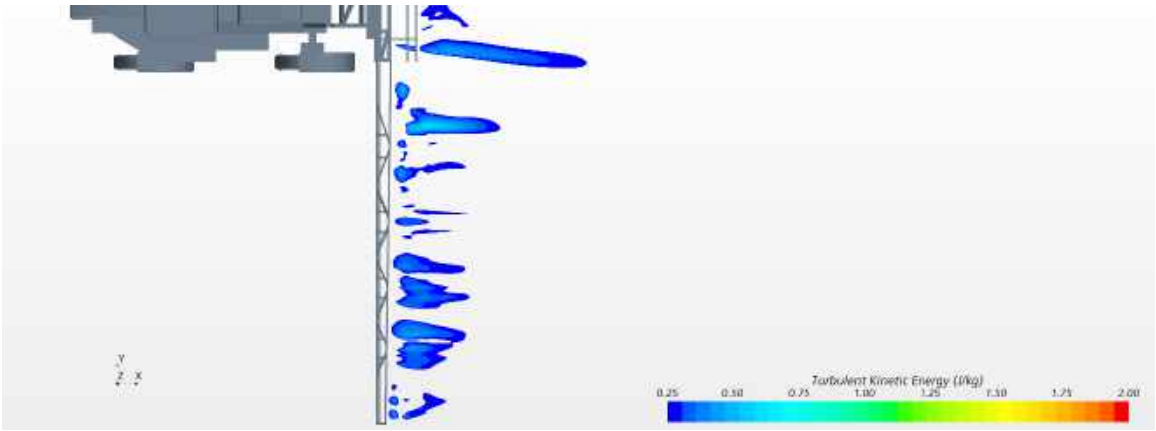

(a)

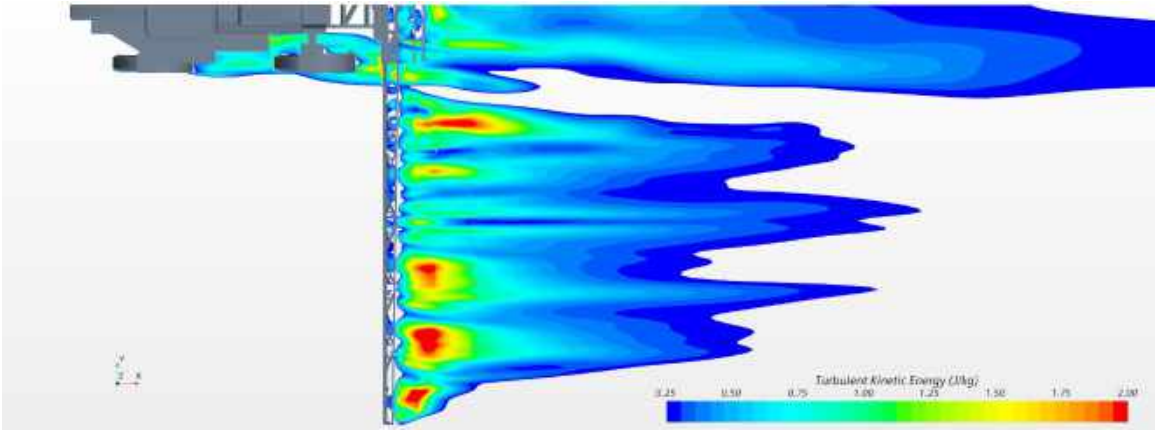

(b)

Figure 55: TKE contour plot on a horizontal plane through the theoretical nozzle location (0.635 m above ground for low & slow, (a) and 0.889 m for high & fast, (b)). Only regions where TKE exceeds 0.25 J/kg shown.

Again, the high and fast configuration showed much higher values of TKE compared to the low and slow. With the doubling of the travel speed and increase in boom height, small zones of weak turbulence behind the boom away from the tractor that were almost negligible at the lower speed (approximately 0.5 J/kg) coalesced into larger and much stronger turbulence zones (in excess of 2.0 J/kg and at least 0.5 m wide). A non-linear increase in TKE with travel speed was expected; however, the degree of the relationship between droplet drift and turbulence was not addressed in the literature.

Spray droplets that enter regions of elevated TKE will be subject to increased mixing with the air. This leaves the droplets more susceptible to being carried off target by lateral velocity components. In the wake of the sprayer where a velocity reduction in the direction of travel was observed, droplets entrained in the air are likely to be carried along with the sprayer and eventually expelled from this wake in an unpredictable location.

Effect of Tire Size

To investigate the effects of installing wider tires on the sprayer, two configurations were compared: narrow tires and wide tires. Both configurations used the high boom height (0.889 m) and fast travel speed (6.71 m/s). The narrow tire configuration was the same as the high and fast configuration above. The narrow tire size is 380/105 R50 while the wide tires are a much wider size 800/55 R46.

Velocity vector plots were again used to compare the two configurations. Figure 56 shows the plots on a horizontal plane at the height of the theoretical nozzle location (0.889 m above the ground). It was observed that the wide tires created a wake behind the tractor that extended beyond the tires when compared to the narrow tires; the wake of the narrow tire was nominally contained to track width.

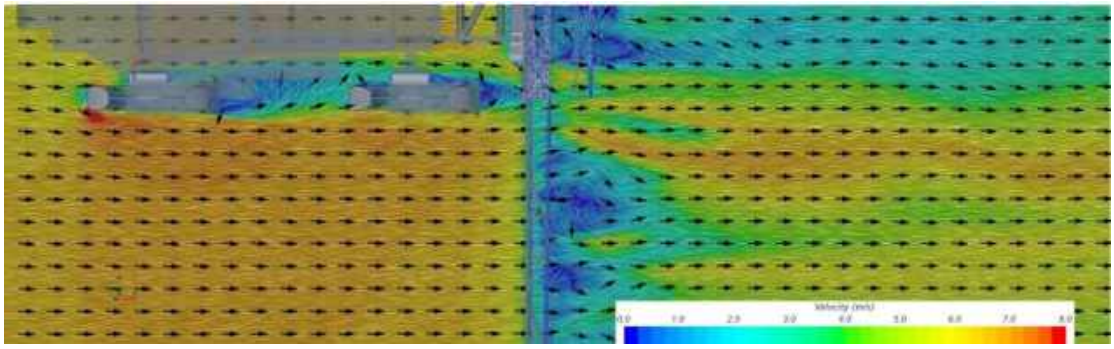

(a)

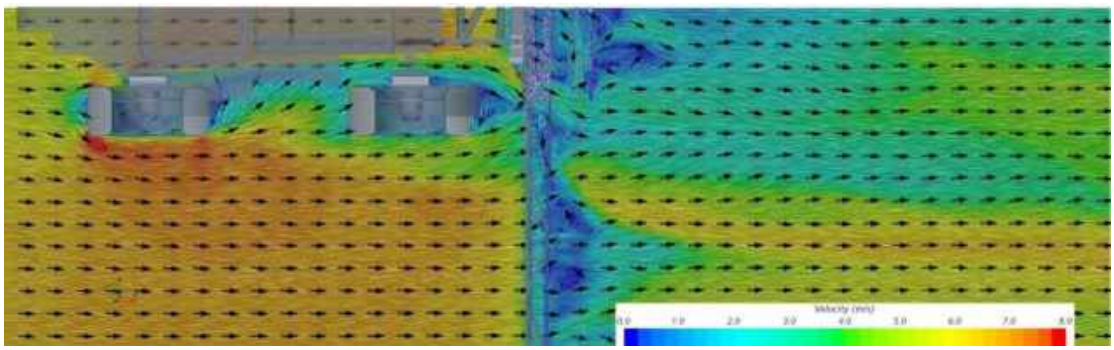

(b)

Figure 56: Velocity vector plots on horizontal plane at the height of the nozzles (0.889 m above ground). Narrow tires configuration (a) and wide tires configuration (b).

Figure 57 shows the vector plots on a horizontal plane 0.318 m below the nozzle location (0.571 m above the ground). At this height the trend in wake width was similar to the height of 0.889 m. The wide tires created a wide and distinct wake between the front and rear tires where flow reversal was observed. Beside and behind the rear tires, the reduction in velocity was nearly as severe (2.0 m/s or less) as that found in the wake directly behind the tank. This wide wake extended far behind the sprayer. The magnitude of the lateral velocity component was greater with wide tires.

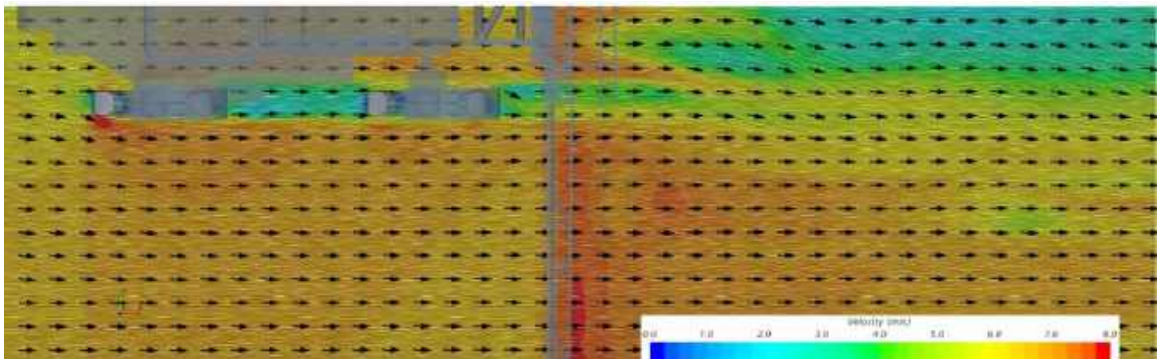

(a)

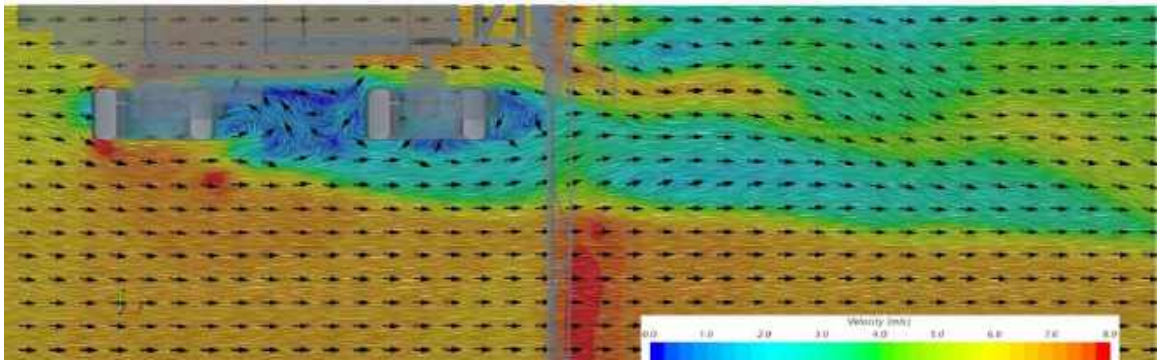

(b)

Figure 57: Vector plots on a horizontal plane 0.318 m below the nozzle location (0.571 m above the ground). Narrow tires configuration (a) and wide tires configuration (b).

Figure 58 shows the vector plots on a horizontal plane 0.889 m above the location of the nozzles (1.778 m above the ground). At this height, the wake around the tires was similar in both configurations. Immediately behind the rear tire, the flow was directed inward towards the sprayer centerline. This occurred in both configurations but appeared more pronounced with the wide tires.

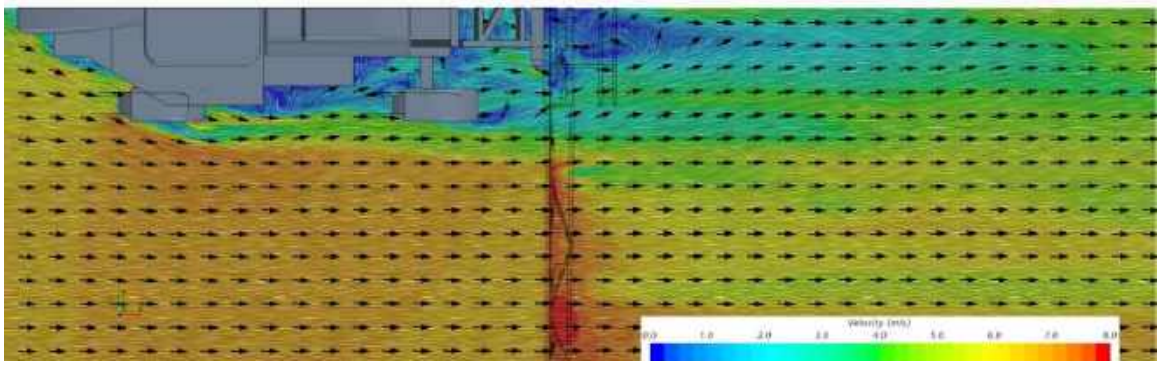

(a)

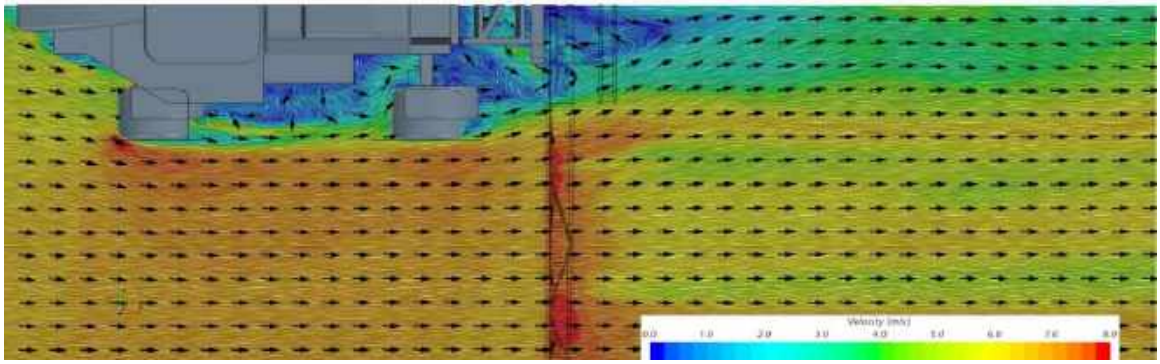

(b)

Figure 58: Vector plots on a horizontal plane 0.889 m above location of the nozzles (1.778 m above the ground). Narrow tires configuration (a) and wide tires configuration (b).

Figure 59 shows velocity vector plots on a vertical plane normal to the flow, in the plane of the nozzles. The wide tire configuration showed a stronger downward and outward component of the air flow below the boom and inside of the rear tire. Flow was oriented in almost a completely horizontal fashion in this region with an increase in magnitude of at least 2.5 m/s compared to the narrow tire. Below the boom, the velocity magnitude was approximately double that of the narrow tire (2.25 m/s compared to about 1.0 m/s) for about 1.5 m immediately beyond the wide tire.

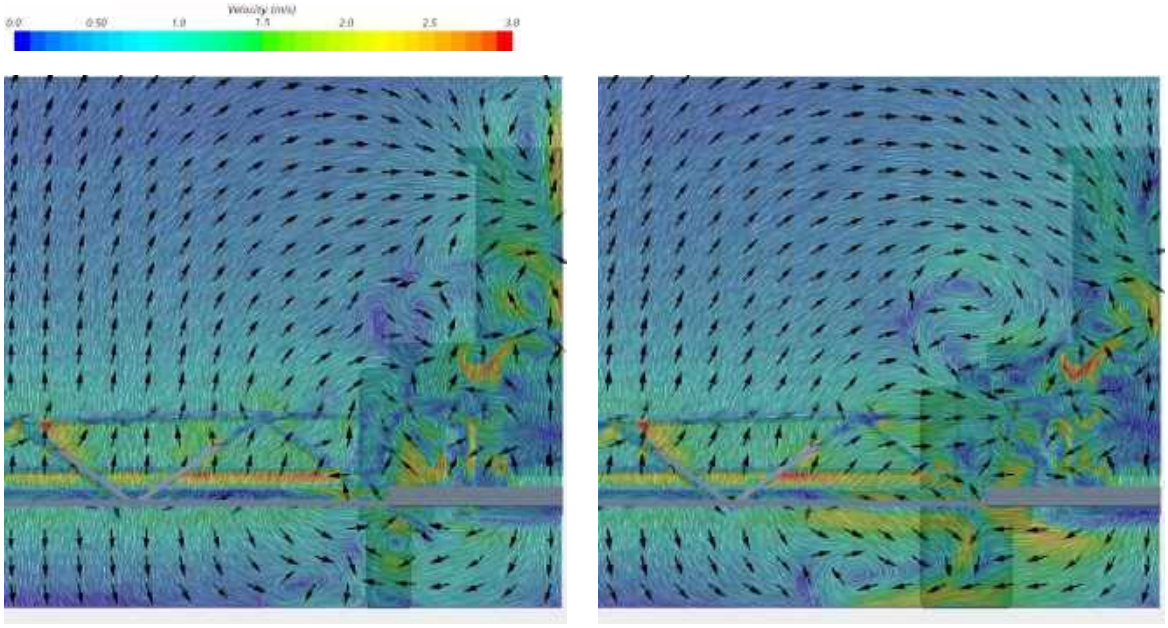

(a) (b)

Figure 59: Velocity vector plots on vertical plane through theoretical nozzle location. View is from behind the sprayer looking forwards. Narrow tires configuration (a) and wide tires configuration (b).

Further behind the sprayer (not shown), the wider tires continued to create a stronger outward air flow over a wider area below the boom.

TKE production around the tires was also studied to compare the two configurations. Figure 60 shows TKE values in a 3D image for each configuration. Higher values of TKE were present for the wide tire configuration. This was most evident at the area in front of the rear tire.

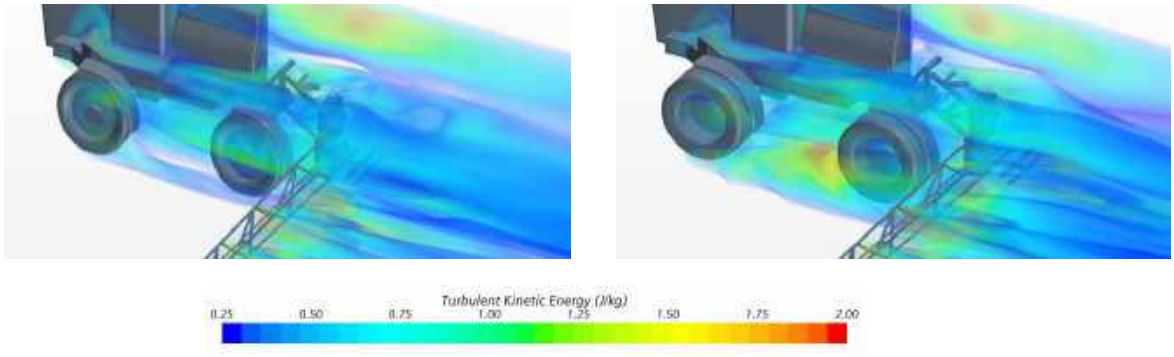

Figure 60: TKE values around sprayer tires. Only regions where TKE exceeds 0.25 J/kg are shown. Narrow tires configuration (a) and wide tires configuration (b).

Plots of TKE values on a 2D horizontal plane 0.318 m below the location of the nozzles (0.571 m above the ground) are shown in Figure 61. The wide tires created a much larger zone of high TKE in the area between the front and rear tire and beside the rear tire. This region of turbulence immediately spread outward from the machine and extended behind the tire, below the boom, and behind the boom. As a result, the turbulent wake spread outward at least two tire widths beyond the track width of the machine. The turbulent wake with the narrow tires was confined to the nominal track width of the sprayer at the same distance behind the boom. When spray is injected into this region of elevated TKE, increased mixing of the spray droplets and the air is likely to occur, increasing the potential for drift.

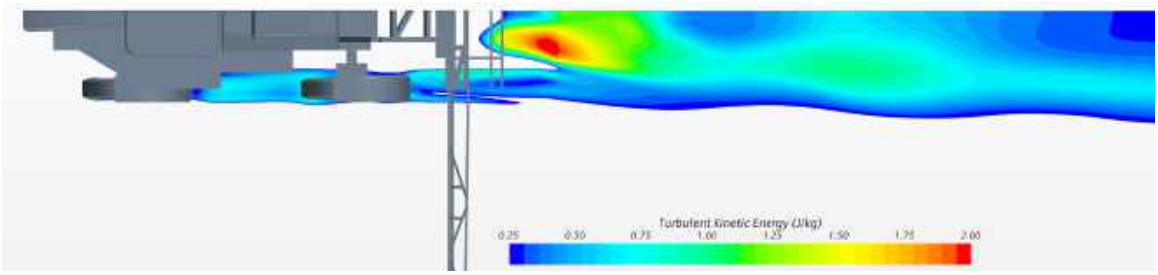

(a)

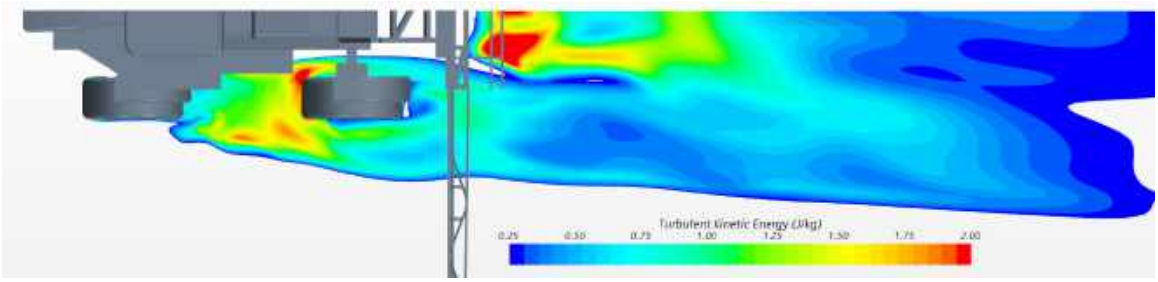

(b)

Figure 61: TKE contour plot on a horizontal plane 0.318 m below the boom (0.571 m above the ground). Only regions where TKE exceeds 0.25 J/kg are shown. Narrow tire (a) and wide tire configurations (b).

Conclusions (CFD)

The results of the CFD model of the John Deere R4045 sprayer showed significant disturbances in the air flow field around and behind the sprayer tractor and boom that have the potential to cause spray drift.

The high and fast configuration showed an increase in disturbances in the flow field compared to the low and slow configuration. The higher travel speed increased the magnitude of upward and lateral components of velocity, most notably in the areas behind the tractor body and tires. The reduction in air velocity behind the tractor body and the boom structure coupled with the acceleration of the air under the boom was more pronounced with the higher travel speed when compared to the low and slow simulation. The amount of turbulence produced increased non-linearly with travel speed; however, this effect was confounded with a change in boom height in this numerical study. A higher boom height and travel speed resulted in a more turbulent air flow under the boom in the area behind the rear tires. These larger disturbances in the velocity field and more chaotic flow indicated an increased potential for spray drift with a higher travel speed and/or higher boom height.

The wide-tire configuration showed an increase in the size of the wake behind the tractor compared to the narrow tire configuration. The wider tire size resulted in a wider area of reduced velocity and chaotic flow behind the sprayer that extended wider than the tires themselves. In particular, the presence of wider tires nominally doubled the magnitude of the lateral velocity component of air flow behind the tires. Turbulence behind the larger tires was higher in a wider area behind the tractor compared to the narrow tires. These results showed an increased potential for spray drift when wider tires are installed on a sprayer.

Increasing travel speed, boom height, and/or tire size increased the disturbances in the air flow around the sprayer, which increases the potential for spray drift. By studying the air flow patterns behind modern high-clearance sprayers, specific influences on wake characteristics can be explored. Additionally, it is anticipated that patterns in physical measurements of spray droplet deposition can be better understood and potentially connected to specific features of sprayer wakes.

Recommendations for Future Work (CFD)

Several opportunities for future work were identified during this project regarding both improvements to the CFD models developed and the aerodynamic performance of the high clearance sprayer itself.

1. Injection of fluid droplets: due to the complexity (both in set-up and computational cost) associated with modeling the injection of liquid droplets into the air flowing around a sprayer, air-only simulations were conducted in this work. However, it is the behaviour of these droplets that ultimately define spray drift. PAMI is currently involved in ongoing research work involving methodology development related to injecting liquid droplets into sprayer simulations. Although computationally costly (computations increase by at least two to three times compared to runtimes quoted in this work), the effect of sprayer wake features on the severity of droplet drift can be assessed more directly when droplets are included in the simulations.
2. Simplified tire geometry: the tire treads were intentionally omitted and were replaced with smooth geometry. Numerical surface roughness was then introduced into the CFD calculations to represent some of the momentum transfer that would occur due to treaded geometry. Introducing tread geometry involves some numerical error because only tread faces that are tangential to the local flow field transfer momentum. Methods to improve the accuracy of the

flow between tread blocks were identified late in the course of this work (Hobeika and Sebben, 2018); however, suitability to the application of large agricultural tires should be investigated further. Given the distinct disturbance caused by the sprayer tires found in the work herein, improvements to the accuracy of their representation would benefit future predictions of the flow field near the tires.

3. Boom aerodynamic signature: the boom wake contains distinct features that are detrimental to spray drift performance. The results of this work indicated regions of increased turbulence behind the boom, and evidence of lateral and upward mean air velocity components that extended at least 3 m behind the boom. While only one representation of a sprayer boom was investigated within this project, general features of the wake are likely common across most modern high-clearance sprayer boom designs given the similarity of commercial designs. These detrimental characteristics highlight that aerodynamic improvements, through changes in component and system packaging, would serve to only reduce the risk of spray drift.
4. Sprayer tire wake reduction: the results of the project herein indicated detrimental wake features due to the presence of the tires that worsened with increased tire width. Further research into ways (possibly through design changes or additional components) to reduce the severity of the tire wakes would likely yield tangible and immediate recommendations on further means to reduce spray drift.

Overall Discussion and Conclusions

This study demonstrated that the uniformity of spray deposits from modern self-propelled sprayers is lower than predicted in existing lab and field studies. The observed variability, as measured by CV, exceeded 20% in nearly all cases and reached as high as 50% despite the use of nozzles with little wear, proper boom height, uniform driving speed, and relatively smooth, level terrain.

In Study 1, the larger samplers tended to report lower variability than the string samplers in Study 2 despite travelling at similarly fast speeds. Poor variability was more the result of suboptimal boom heights resulting in insufficient overlap. The boom heights used in Study 2 were sufficient for good pattern overlap, and poor variability was caused by spray displacement.

Some of the variability may have been an artifact of the measurement technique. Although 2 mm string is an internationally accepted spray collector, its collection efficiency favours smaller droplets and these are the portion of the spray that is most susceptible to turbulent displacement in the wake of a sprayer. This was no accident – we were interested in the movement of the smaller droplets because from a biological perspective, they are very important. Small droplets are better able to target smaller objects such as insects or small leaves and are thus instrumental in developing acceptable pest control. Small droplets are present in all sprays, although their relative abundance has been diminished by the widespread adoption of low-drift sprays. In that context, their importance may even have increased, as the coverage they provide is essential in making sprays more robust under a variety of conditions. The increased use of fungicides, for which coverage is important, as well as contact herbicides, which require small droplets for activity, requires applicators to pay attention to their movement.

It was surprising that the CV of the sprays was not only high, but also fairly stubbornly so. The use of coarser sprays, lower booms, and slower travel speeds did in small measure improve deposition uniformity. But the overall degree to which the situation could be improved was disappointingly small. An aspect of these studies that may have contributed to the persistent poor deposition uniformity is the use of side winds in almost all the trials. Calmer conditions may, in hindsight, have lowered the CVs, or perhaps winds that were oriented in the direction of travel rather than oblique, would have made the trials more repeatable.

However, it again was no accident that we chose to use side winds, as these are recommended for spraying. Side winds are preferred because the alternative, headwinds, create dramatically different aerodynamic environments depending on whether one heads into them or drives with them. A 10 mph driving speed into a 15 mph headwind creates an effective 25 mph aerodynamic situation. On turning in the opposite direction, it results in a 5 mph tailwind, completely altering the conditions in which the spray is atomized and encounters shear forces and vortices.

The role of structural components that affect spray deposition must focus on the tractor unit of the sprayer itself. If anything was consistent, it was poor deposition in the wheel tracks, and erratic deposition amounts in their vicinity. The sheer size and velocity of these structures had a strong negative impact in these studies, and this is corroborated by the CFD studies conducted by PAMI. The re-direction of airflows due to the circular motion of the wheels, the funnelling of oncoming air into mudguards, the displacement and re-direction of air in their wake, these are all issues that require attention. Even the tractor unit itself showed strong evidence of highly turbulent wakes that can generate vortices, as shown by the CFD work.

Recommendations

It is recommended that:

1. Sprayer manufacturers take into consideration the possible aerodynamic consequences of certain sprayer design features and make an effort to study and address these prior to bringing a new design to market. Although this study was not able to pinpoint specific requirements, an effort in the design phase of a new sprayer may be able to minimize certain negative effects before they cause problems for applicators.

2. Specifically the impact of wheels needs to be studied, and ways to mitigate their effects need to be developed. Sprayers will have wheels, and these are getting larger. Understanding how to minimize their turbulent wakes will improve the quality of the spray operation.

3. Methods for the more efficient evaluation of dynamic spray patterns be acquired. The CAAA (Canadian Aerial Applicators Association) has conducted patternation studies as part of their required certification of aircraft for decades. If their efficient approaches can make their way into ground application the work to improve deposit uniformity can grow.

4. Although the overall effect of slower speeds and lower booms were not as large as hoped, they nonetheless represent the single best tool available to applicators at this time. Studies on the productivity of the spray operation are needed, so that slower speeds can still offer a fast, timely and effective spray operation. Rather than use travel speed to increase productivity, it is worth exploring the time accounting of a spray day and directing efforts at maximizing the proportion of that day that the sprayer is treating a field.

5. Field surveys be conducted to examine the role of sprayer wheel tracks in creating niches for the establishment of weeds and perhaps, through repeated under-dosing of that specific region, the development of herbicide resistance. Although tram lines are not in use in western Canada, some fields will repeatedly, or in alternate years, see the same tracks be used due to the geometry of fields.

6. CFD studies be funded so that other conditions can be evaluated. In the present study, winds were taken to be head-on, sprays were not emitted from the boom, and the tractor wheels did not have realistic lugs on them. Additional work needs to be done so that CFD models can better simulate the types of wind conditions experienced in the field.

Citations

1. Carlton, J.B., Bouse, L.F., Stermer, R.A., Kirk, I.W. 1990. Aerial spray deposit analysis I: cylindrical collector drop size effects. Trans ASAE 33(6): 1795-1800.
2. Carpenter, T. G., Reichard, D. L., Ozkan, H. E., Holmes, R. G., and Thornton, E. 1988. Computerized weighing system for analyses of nozzle spray distribution. Trans ASAE 31(2):375-379.
3. Farooq, M., Balachandar, R., Wolf, T. 2001. Assessment of an agricultural spray in a non–uniform cross–flow. Trans ASAE 44(6): 1455–1460.
4. Furness, G.O., Wearne, M.M., Hastings, J.J., Barton, P.S. and Frensham, A.B. 2001. A wedge shaped bluff plate air-assisted sprayer: I. Spray deposits on artificial targets. Plant Protection Quarterly Vol.16(2): 75-83.
5. Grover, R., Caldwell, B.C., Maybank, J, and Wolf, T.M. 1997. Airborne off-target losses and ground deposition characteristics from a Spra-Coupe using “low drift” nozzle tips. Can. J. Plant Sci. 77:493-500.
6. Hobeika, T., & Sebben, S. (2018). CFD investigation on wheel rotation modelling. Journal of Wind Engineering and Industrial Aerodynamics, 174, 241-251.
7. Jeon, H. Y., Womac, A. R., Gunn, J. 2004. Sprayer boom dynamic effects on application uniformity. Trans ASAE 47(3): 647−658.
8. Krishnan, P., Kemble, L. J., Gal, I. 2005. Dynamic spray pattern displacement of extended range fan nozzles. Applied Engineering in Agriculture 21(5): 751−753.
9. Landry, H., and T.M. Wolf. 2019. An investigation of airflow patterns created by high-clearance sprayers during field operations. Canadian Biosystems Engineering/Le genie des biosystemes au Canada 61: 2.01-2.12.
10. Lardoux, Y., Sinfort, C., Enfalt, P., and Sevila, F. 2007. Test Method for Boom Suspension Influence on Spray Distribution, Part I: Experimental Study of Pesticide Application under a Moving Boom. Biosystems Engineering 96 (1): 29-39.
11. Menter, F. (1994). Two-equation eddy-viscosity turbulence models for engineering applications. AIAA Journal, 32(8), 1598-1605.
12. Sayinci, B and Bastaban, S. 2011. Spray distribution uniformity of different types of nozzles and its spray deposition in potato plant. African Journal of Agricultural Research Vol. 6(2):352-362.
13. Sidahmed M.M.; Awadalla H.H.; Haidar M.A. 2004. Symmetrical multi-foil shields for reducing spray drift. Biosystems Engineering 88 (3):305–312.
14. Siemens PLM Software. (2019). Simcenter STAR-CCM+ 2019.3 User Guide. Plano, Texas, USA: Siemens PLM Software.
15. Smith, D. B. 1992. Uniformity and recovery of broadcast sprays using fan nozzles. Trans ASAE 35(1): 39-44.
16. Teske, M. E., Thistle, H. W., Lawton, T. C. R., Petersen, R. L. 2016. Evaluation of the flow downwind of an agricultural ground sprayer boom. Trans ASABE 59(3): 839-846.
17. Teske, M.E., Thistle, H.W., Gross, G.M., Lawton, T.C.R., Petersen, R.L. and Funseth, T.G.. 2015. Evaluation of the Wake of an Agricultural Ground Sprayer. Trans ASABE 58(3): 621-628.
18. Thistle, H.W., Teske, M.E., Richardson, B. 2004. Spray droplet trajectory length in ambient vortices. Proceedings of the 2004 ASAE/CSAE Annual International Meeting, Ottawa, Ontario, Canada 1 - 4 August pp 9-13.

19. Tsay, J., Ozkan, H. E., Fox, R. D., Brazee, R. D. 2002. CFD simulation of mechanical spray shields. Trans ASAE 45(5): 1271–1280.
20. Whitney, R. W. and Roth, L. O. 1985. String collectors for spray pattern analysis. Trans ASAE 28(6):1749-1753.
21. Wolf, T.M., Liu, S.H., Caldwell, B.C., and Hsiao, A.I. 1997. Calibration of greenhouse spray chambers - the importance of dynamic nozzle patternation. Weed Technol. 11:428-435.
22. Wolf, T.M., Grover, R., Wallace, K., Shewchuk, S.R., and Maybank, J. 1993. Effect of protective shields on drift and deposition characteristics of field sprayers. Can. J. Plant Sci. 73:1261-1273.
23. Womac, A.R., Etheridge, R., Seibert, A., Hogan, D. Ray, S. Sprayer speed and venturi–nozzle effects on broadcast application uniformity. Trans ASAE 44(6):1437–1444.
24. Yates, W.E. 1962. Spray pattern analysis and evaluation of deposits from agricultural aircraft. 1962. Trans ASAE 5:69-53.
25. Young, B. W. 1990. Droplet dynamics in hydraulic nozzle spray clouds. In Proc. Pesticide Formulation and Applic. Systems, 10th vol. ASTM STP 1078: 142–155. L. E. Bode, J. L. Hazen, and D. G. Chasin, eds. Philadelphia, Pa.: ASTM.

Acknowledgements

This work spanned four years and involved assistance from many individuals and organizations.

Brian Caldwell prepared all the samplers, conducted their extraction and analysis, provided the initial data reduction and valuable insights. This work would not have been possible without his hard work and initiative.

Study 1 was done jointly with PAMI and Norac. The assistance of Adam Wilkinson, Roy Maki, and Mitchel Drayton is appreciated.

Study 2 was assisted by Shane Moore, Henry Wolf, Paul Caldwell, CJ Shepard, Justin Gerspacher, Katelyn Blechinger, Ben Gagnon and Mohammad Giahi.

Computational Fluid Dynamics work was conducted by Justin Gerspacher and Ian Paulson (replacing Hubert Landry).

Land for trials and spray equipment was made available by Ben Vanderkooi, Martin Prince, Cervus Equipment, and Pattison Agriculture.

Funding was provided by the Canola Agronomic Research Program and their member commissions in Manitoba, Saskatchewan, and Alberta. Their ongoing support for original research is much appreciated.

Appendix A

Figure 62: Spray drift tests included measurement of on swath deposit variability

Figure 63: On swath deposit collected on 15 cm petri plates

Figure 64: AAFC Track Room for dynamic spray pattern testing.

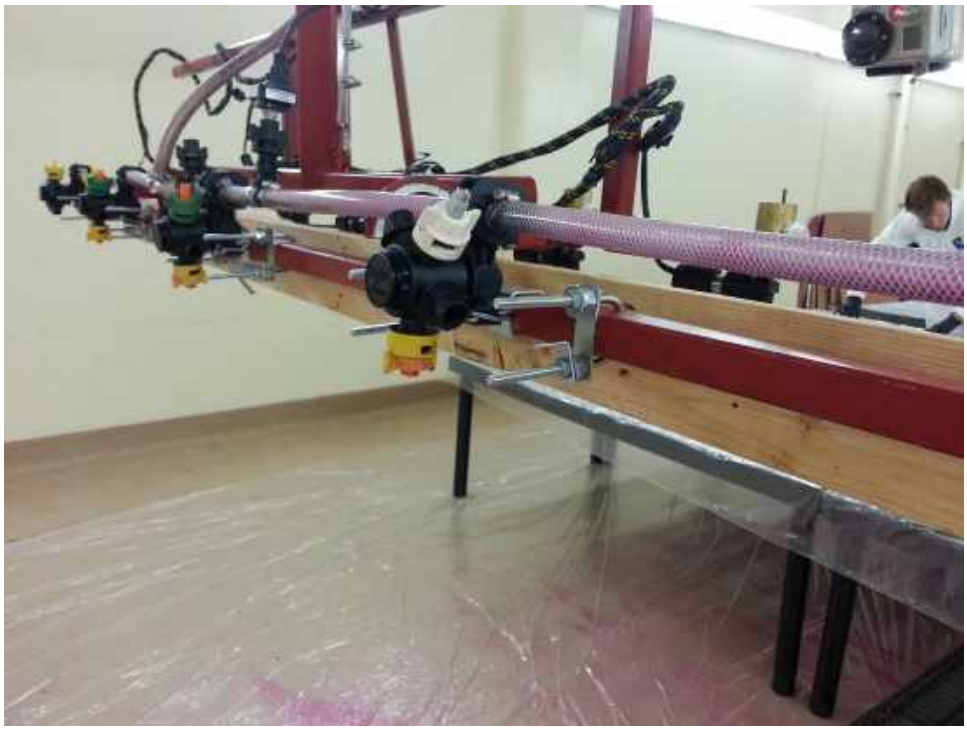

Figure 65: Spray boom without any aerodynamic modifications

Figure 66: Spray boom fitted with aerodynamic foil

Figure 67: Spray boom fitted with splitter.

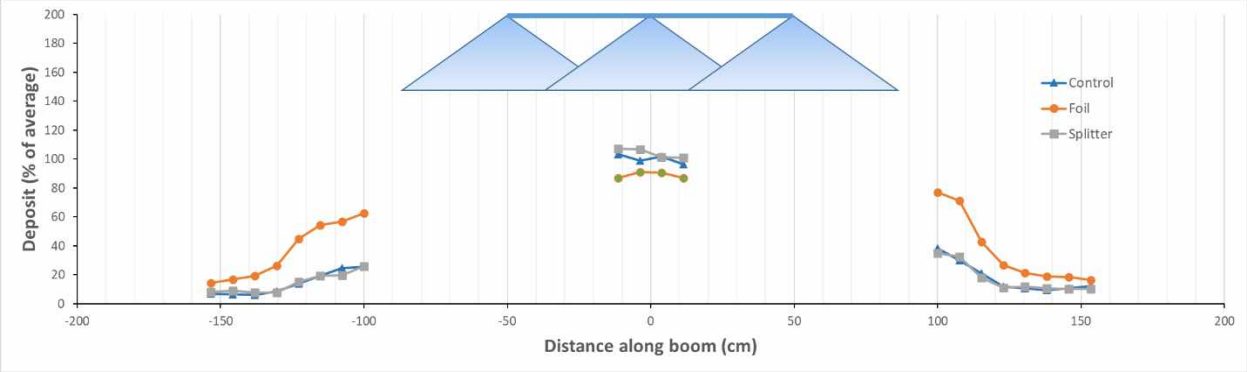

Figure 68: Displacement of spray cloud from centre to periphery due to aerodynamic foil

Figure 69: Placement of plastic drinking straw samplers onto sampling pole

Figure 70: Borosilicate tubes to hold exposed samplers and extract dye using solvent

Figure 71: Exposed samplers showing spray deposits

Figure 72: Sampling line dispensed from reel

Figure 73: String collector placement adjacent to sprayer wheel

Figure 74: A number of strings arranged in the direction of sprayer travel

Figure 75: Conducting a spray application

Figure 76: Installing sampling line, 2020

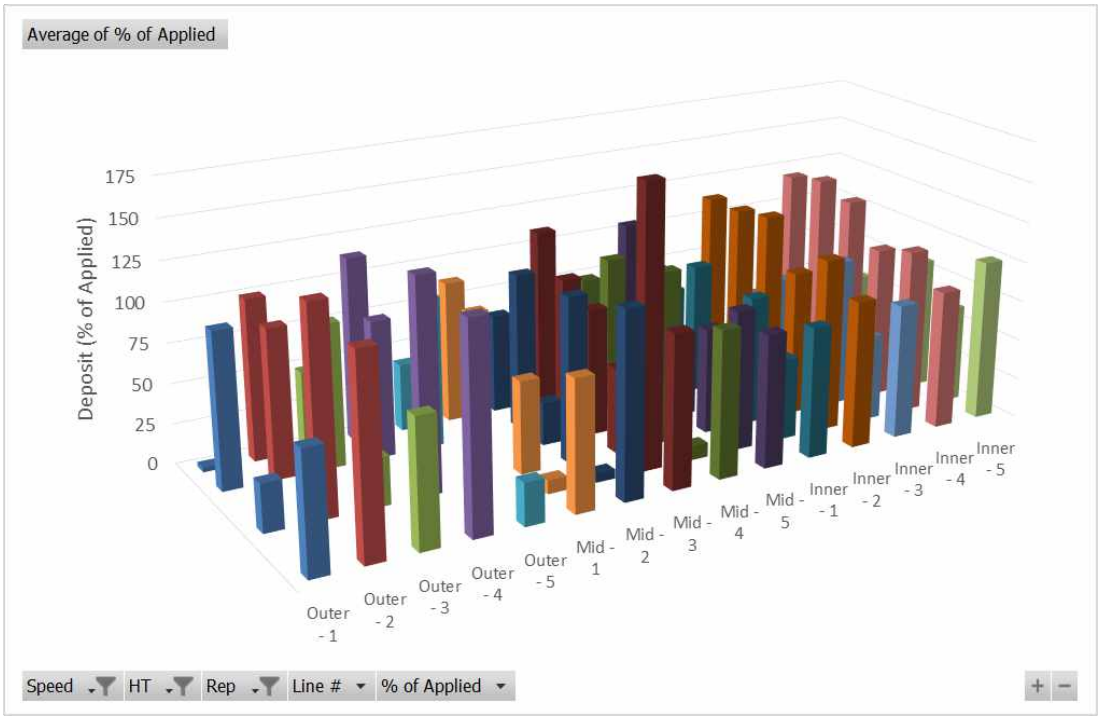

Figure 77: Spray deposit at 8 mph travel speed, boom height set 8" above target. From left, three sampling towers located under outer, mid, and inner section of left boom. Rows represent two sampling lines, replicated three or four times.

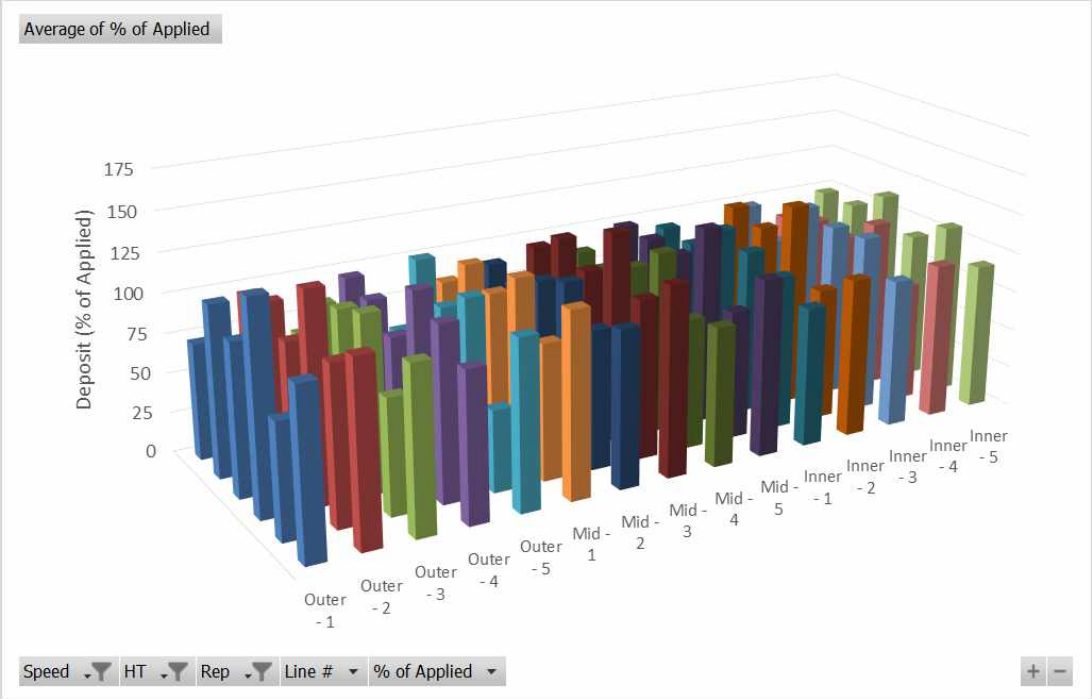

Figure 78: 8 mph, 16" boom height

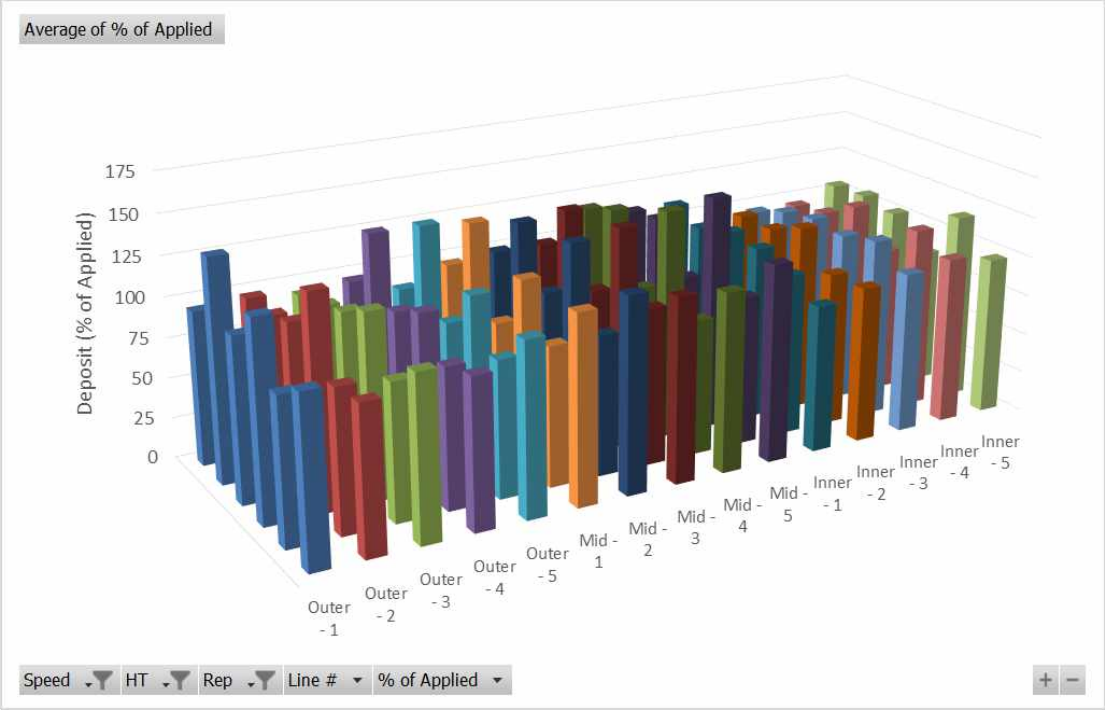

Figure 79: 8 mph, 32" boom height

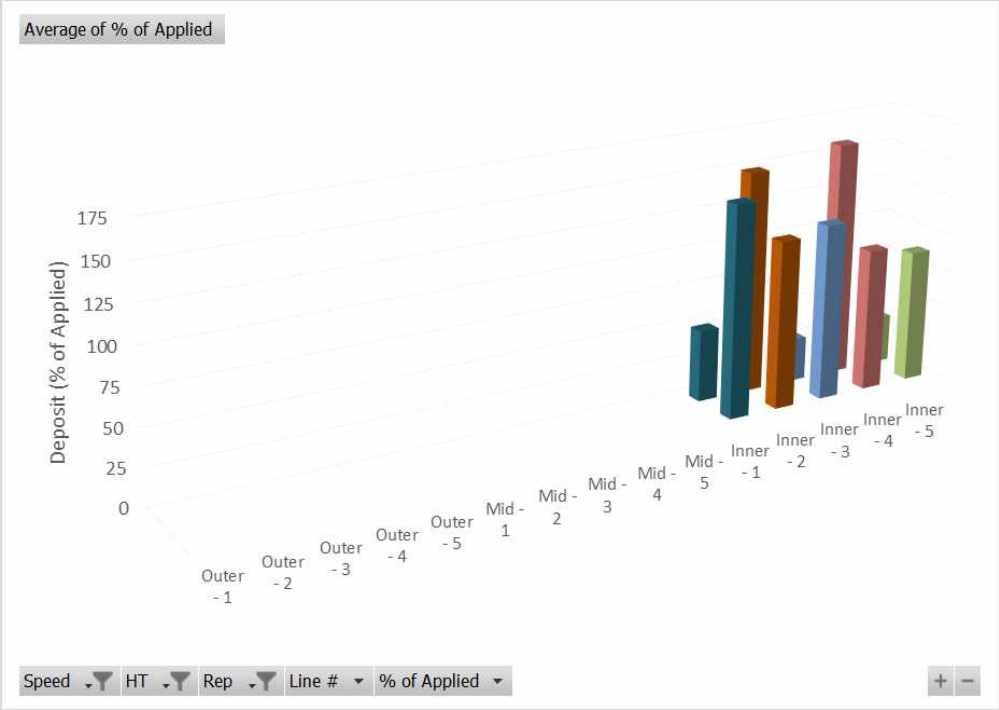

Figure 80: 14 mph, 8" boom height (outer samplers knocked over by boom), remaining replicates not conducted.

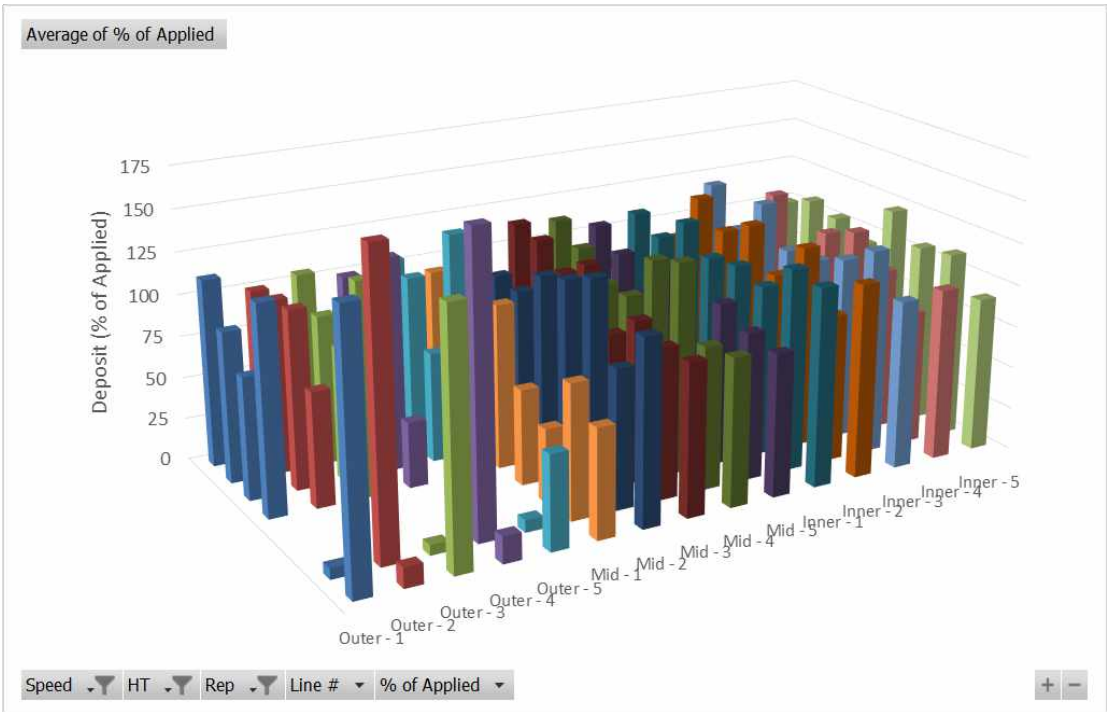

Figure 81: 14 mph, 16" above target

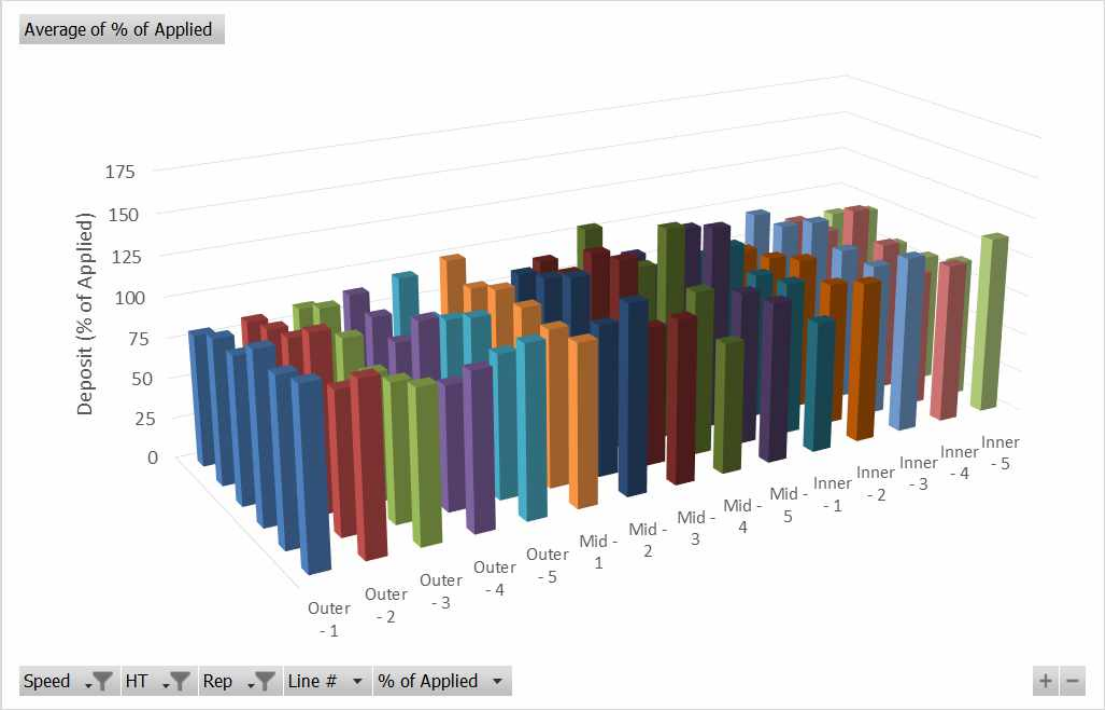

Figure 82: 14 mph, 32" above target

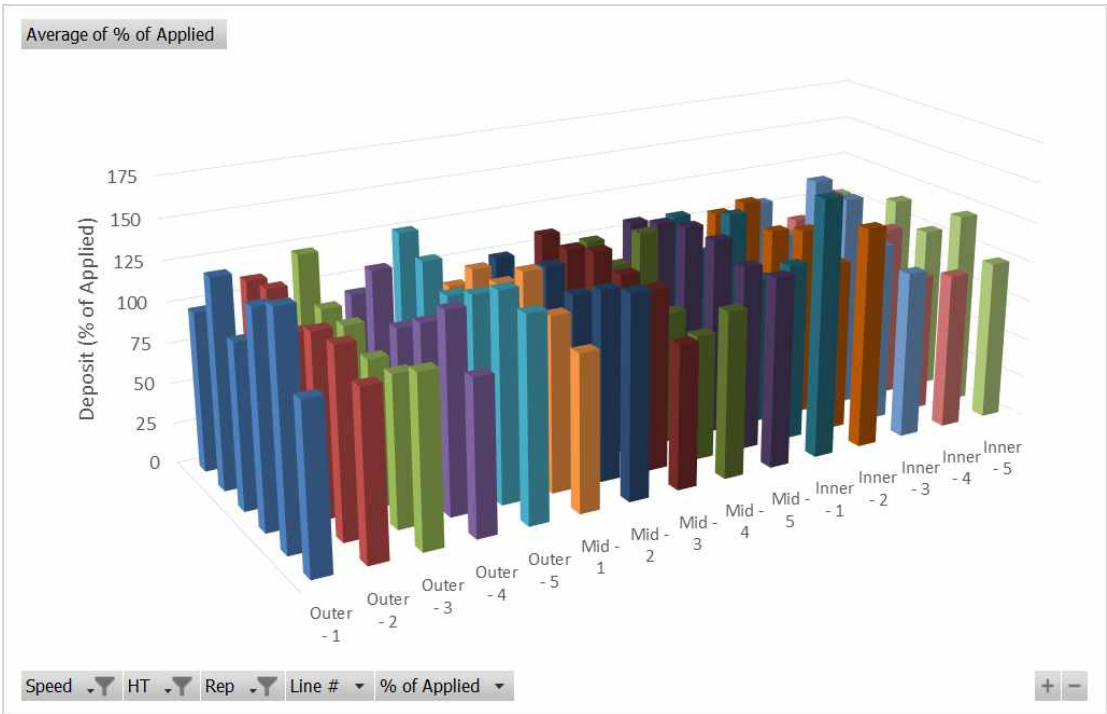

Figure 83: 20 mph, 16" above target

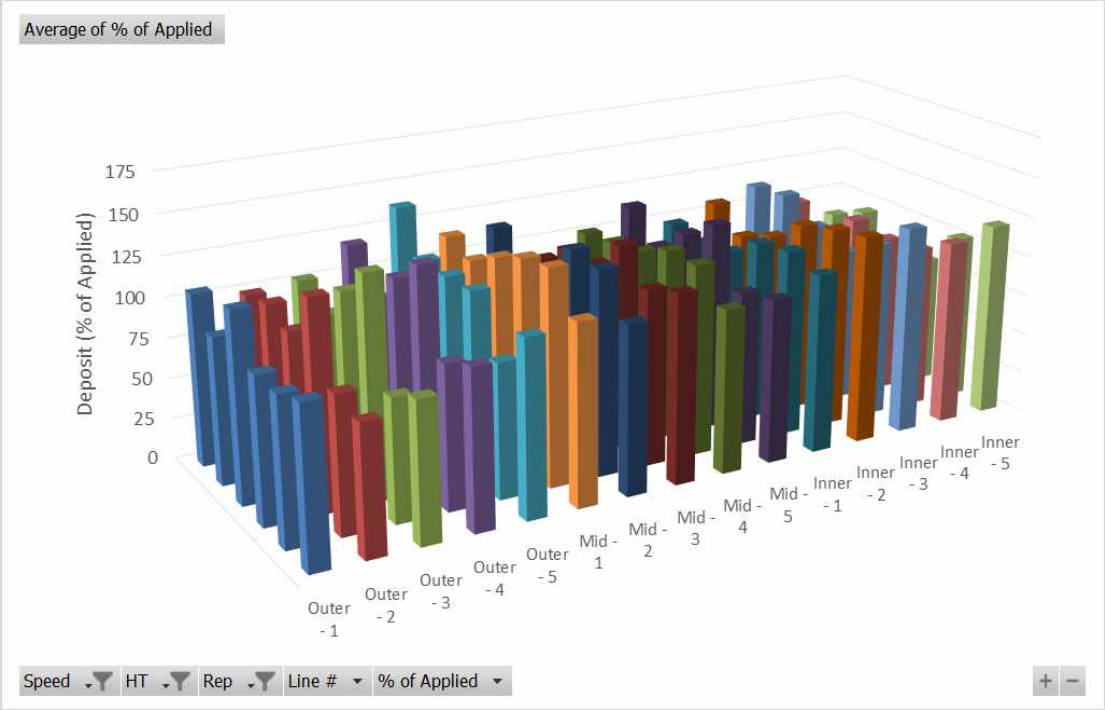

Figure 84: 20 mph, 32" above target

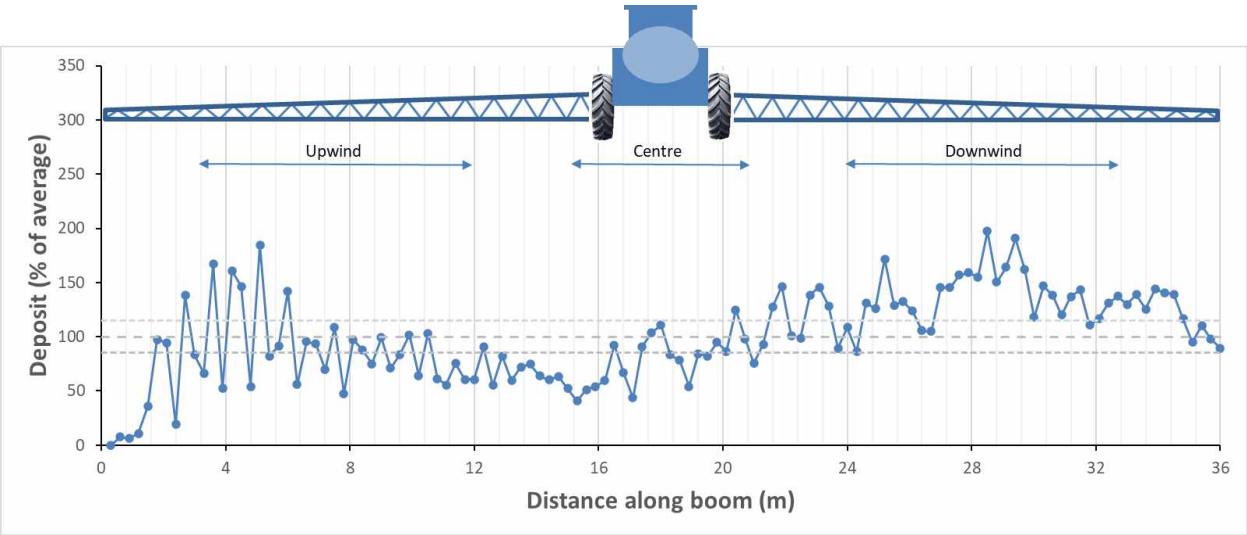

Figure 85: String 7 (ULD11004, 25" 15 mph)

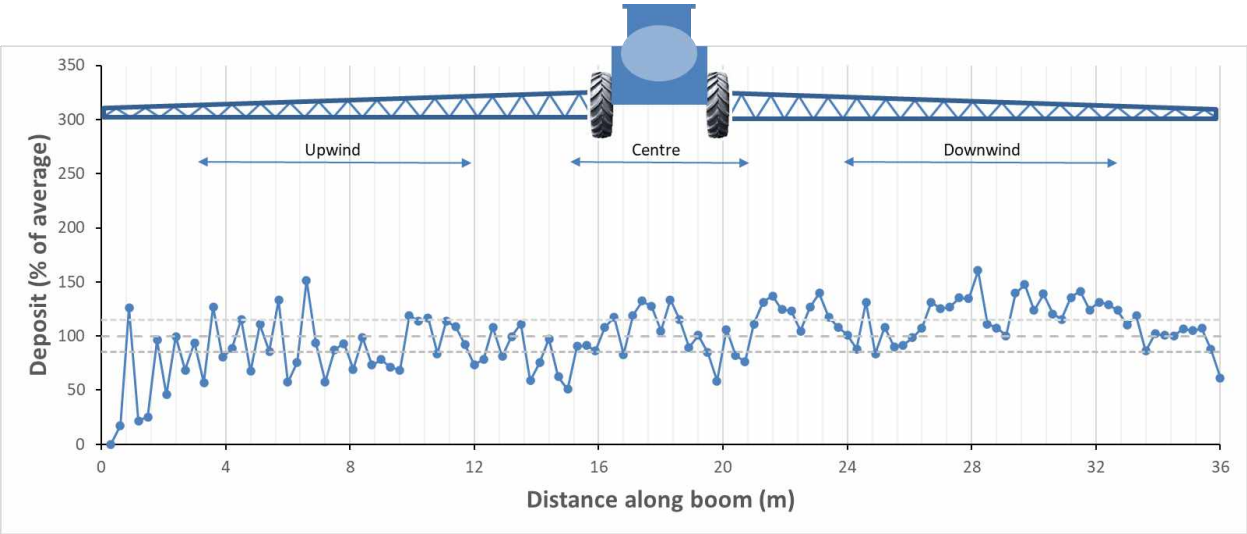

Figure 86: String 8 (LDX11004, 25" 15 mph)

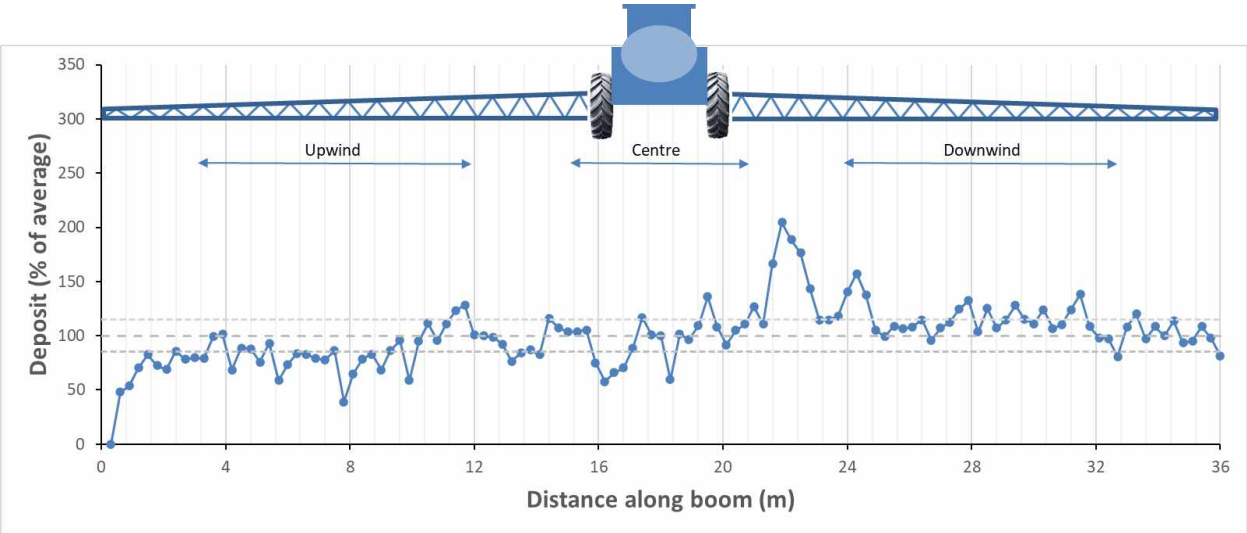

Figure 87: String M (LDX11004, 25" 7.5 mph)

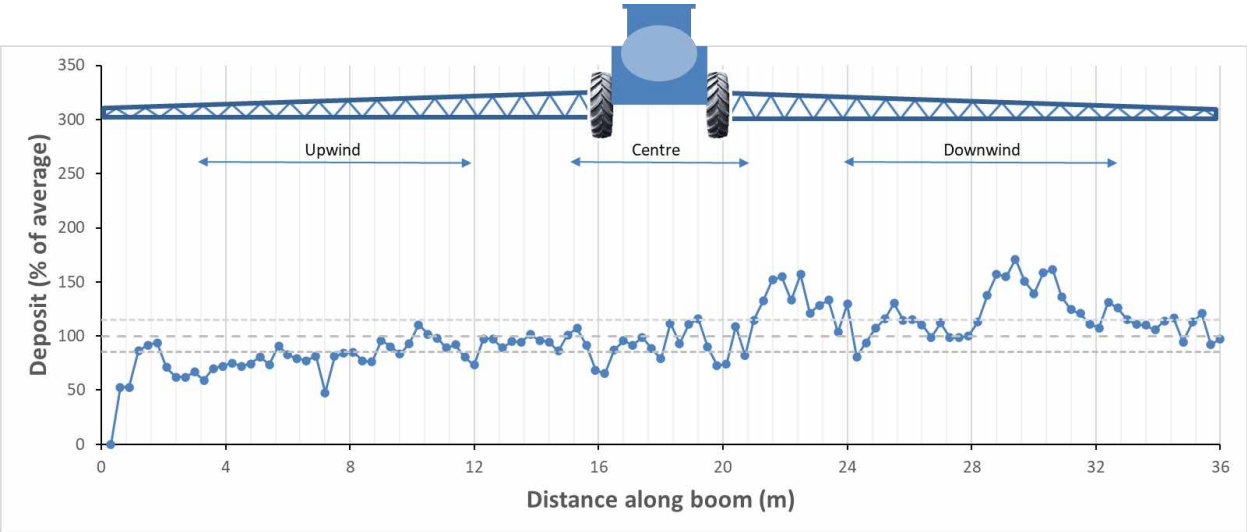

Figure 88: String N (LDX11004, 25" 7.5 mph)

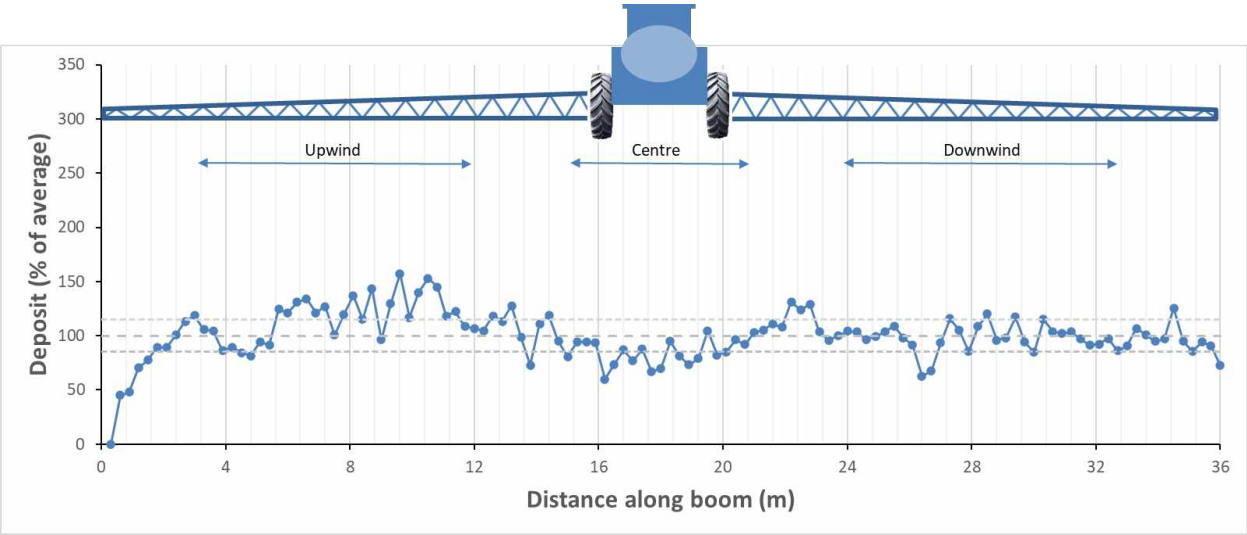

Figure 89: String O (LDX11004, 25" 7.5 mph)

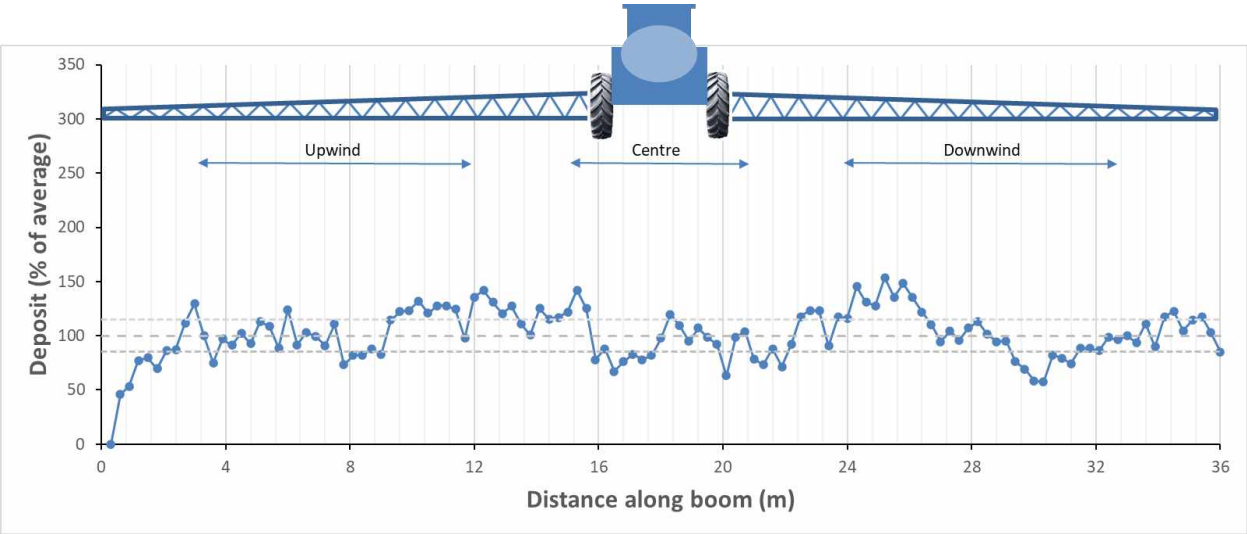

Figure 90: String Q (LDX11004, 35" 15 mph)

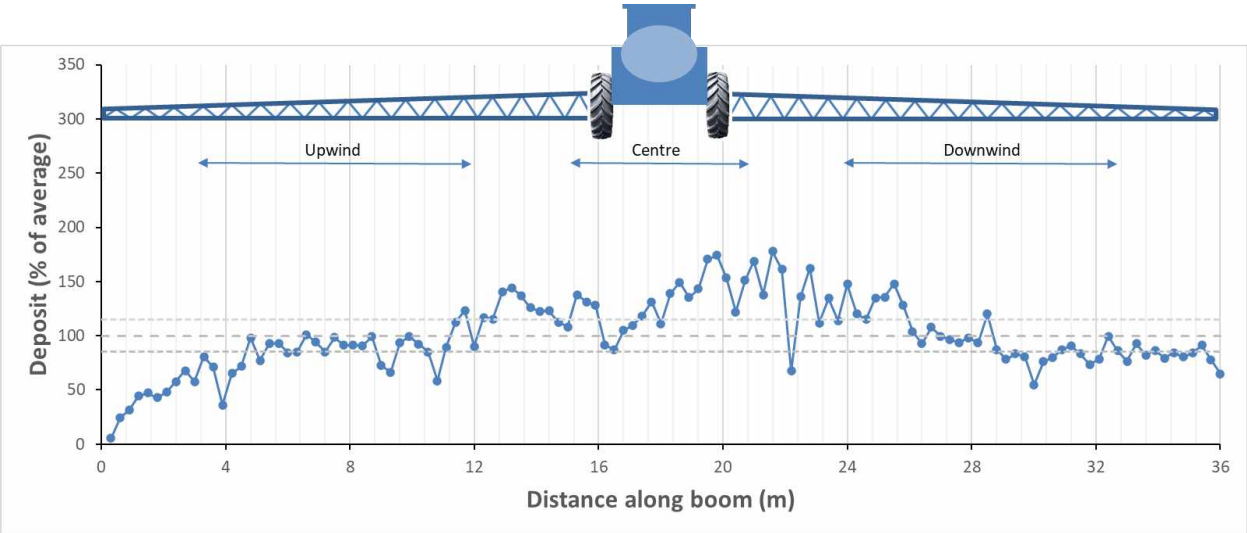

Figure 91: String T (LDX11004, 35" 15 mph)

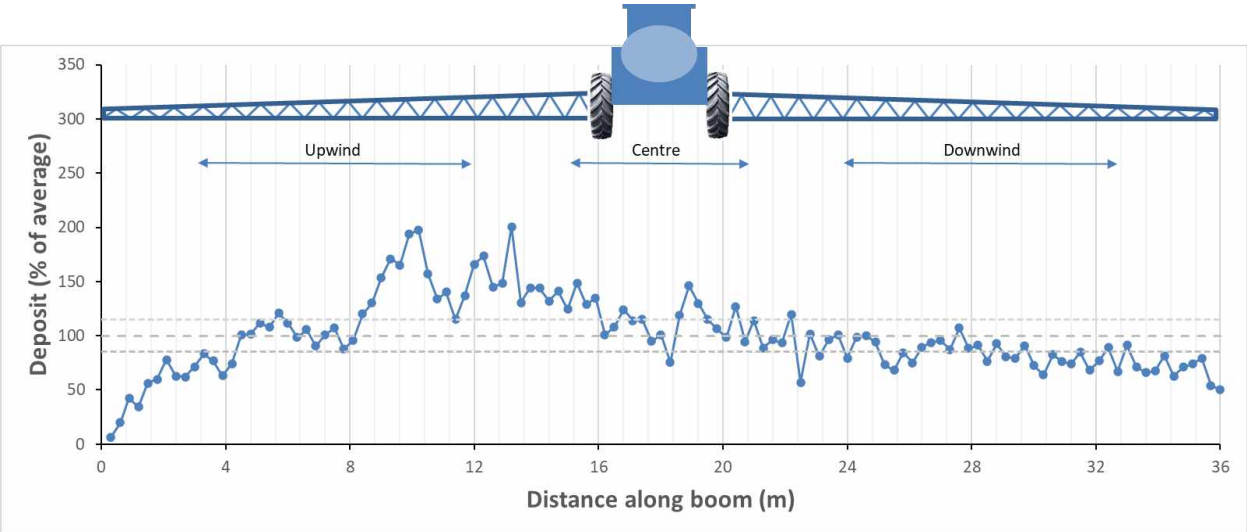

Figure 92: String V (LDX11004, 35" 15 mph)

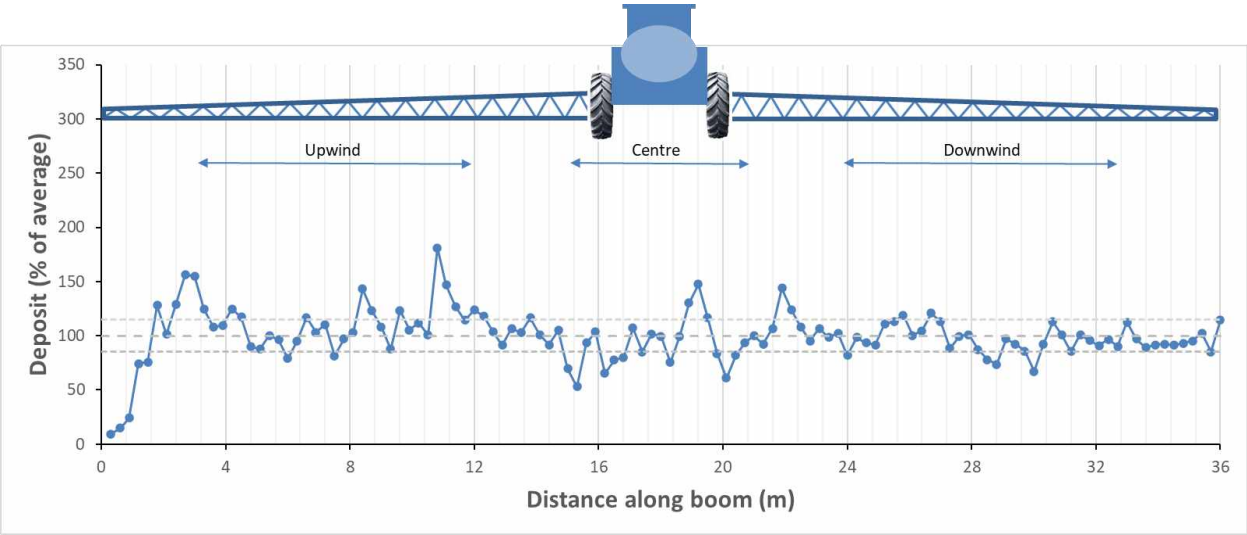

Figure 93: String R (ULD11004, 35" 15 mph)

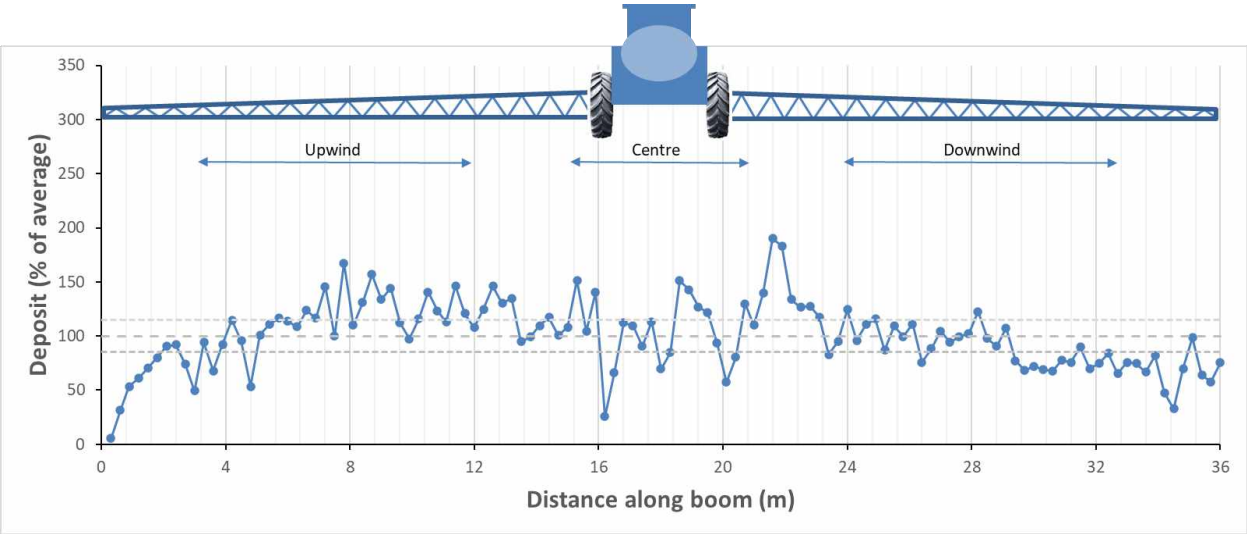

Figure 94: String S (ULD11004, 35" 15 mph)

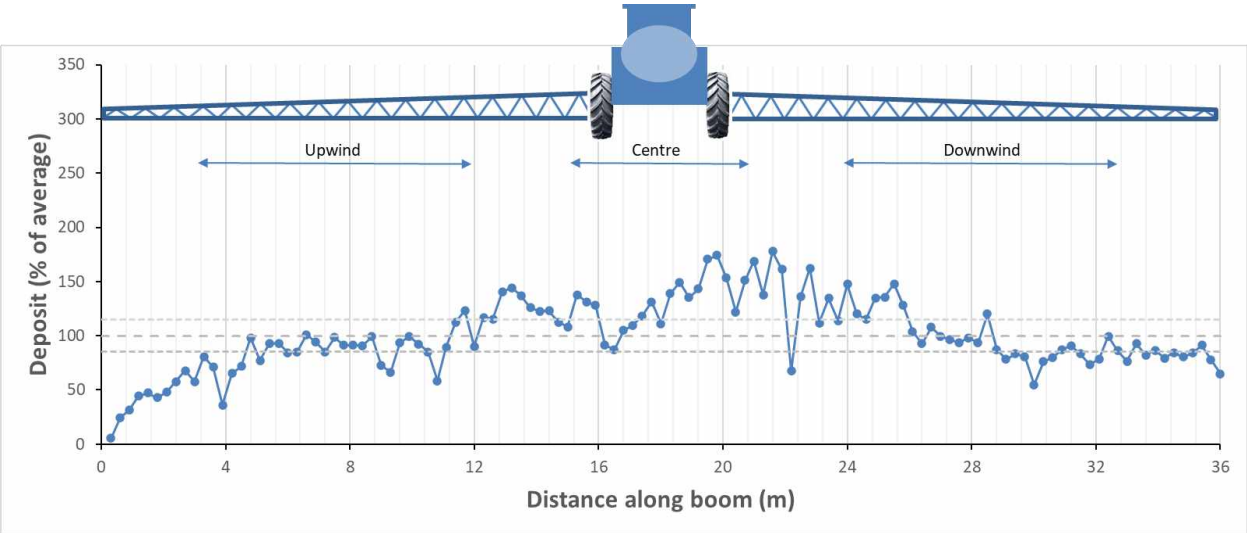

Figure 95: String U (ULD11004, 35" 15 mph)

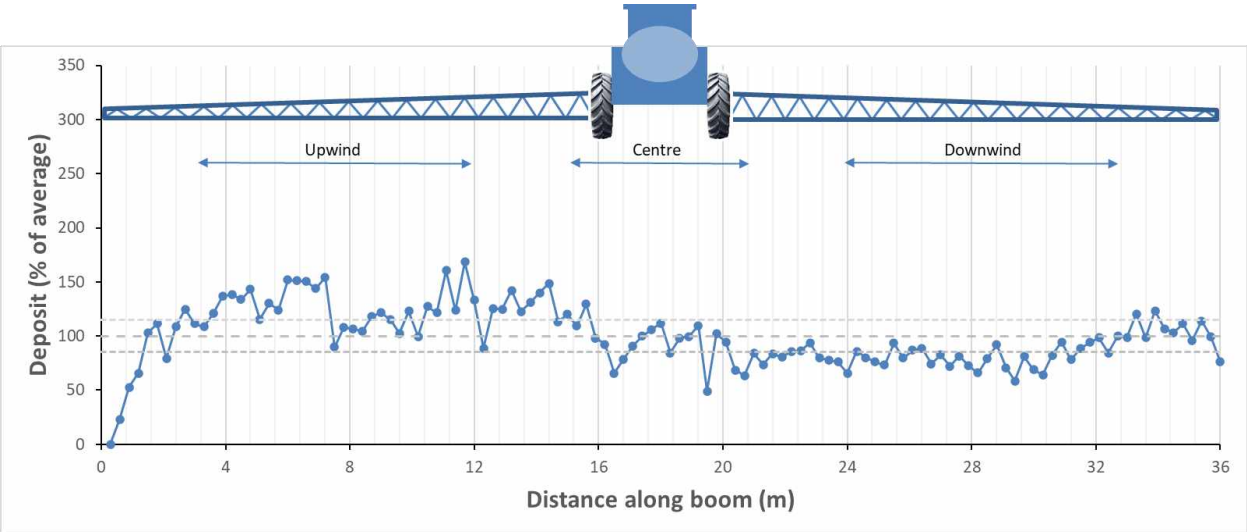

Figure 96: String F (ULD11004, 25" 15 mph)

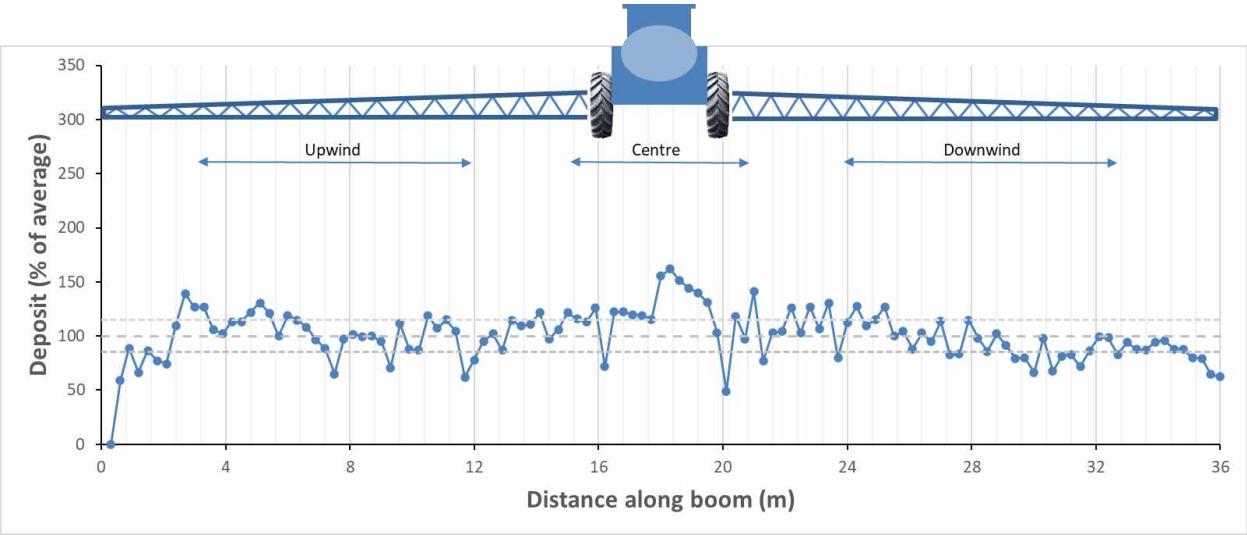

Figure 97: String L (LDX11004, 25" 15 mph)

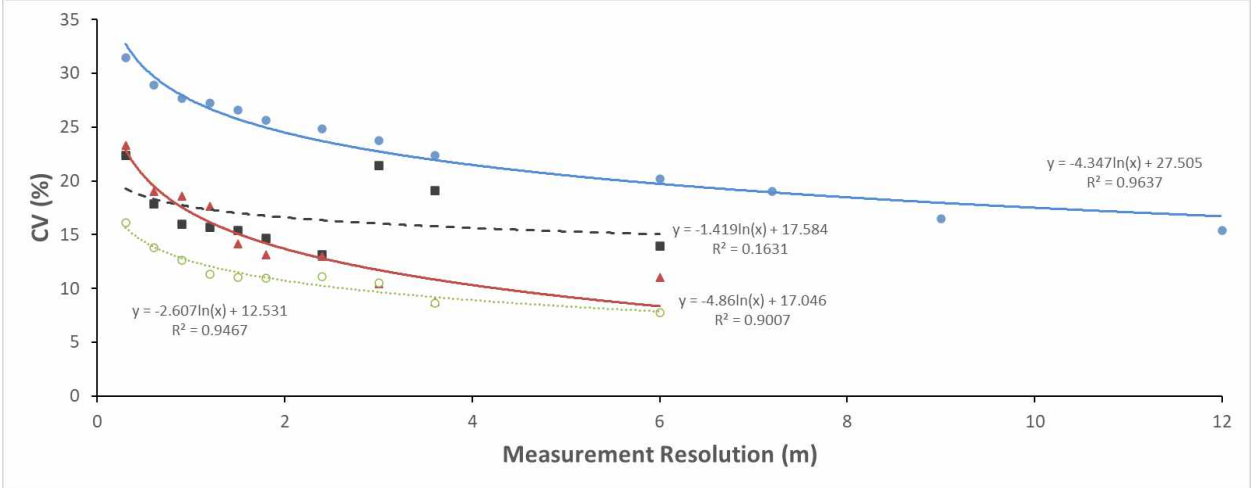

Figure 98: Spray boom CV as affected by measurement resolution (averaged over 15 treatments).

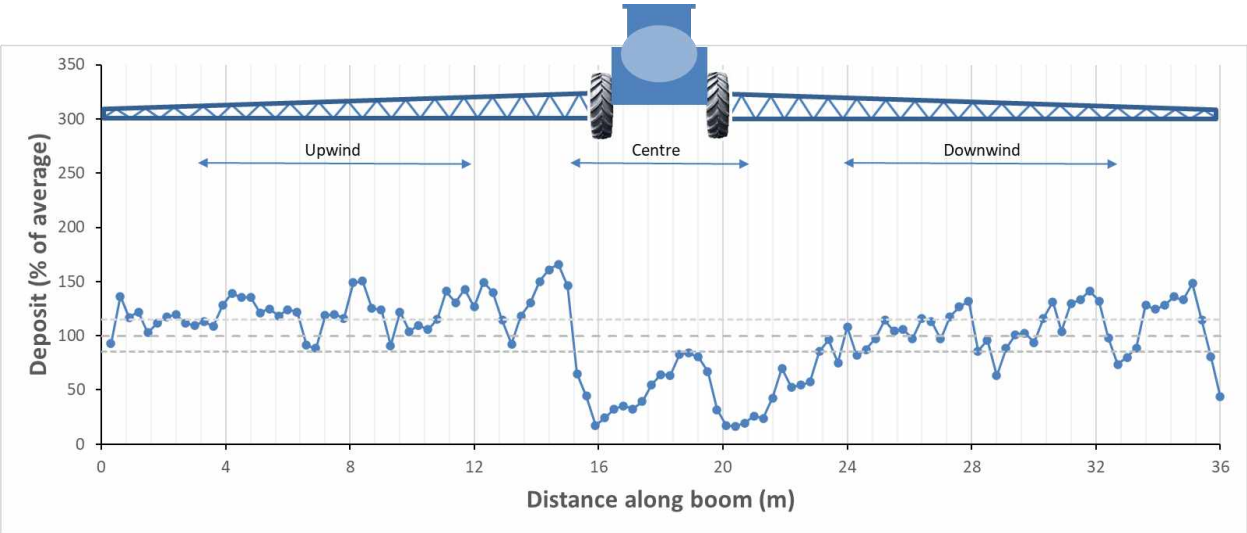

Figure 99: 19-02 L1 (LDX11004, 24", 17 mph)

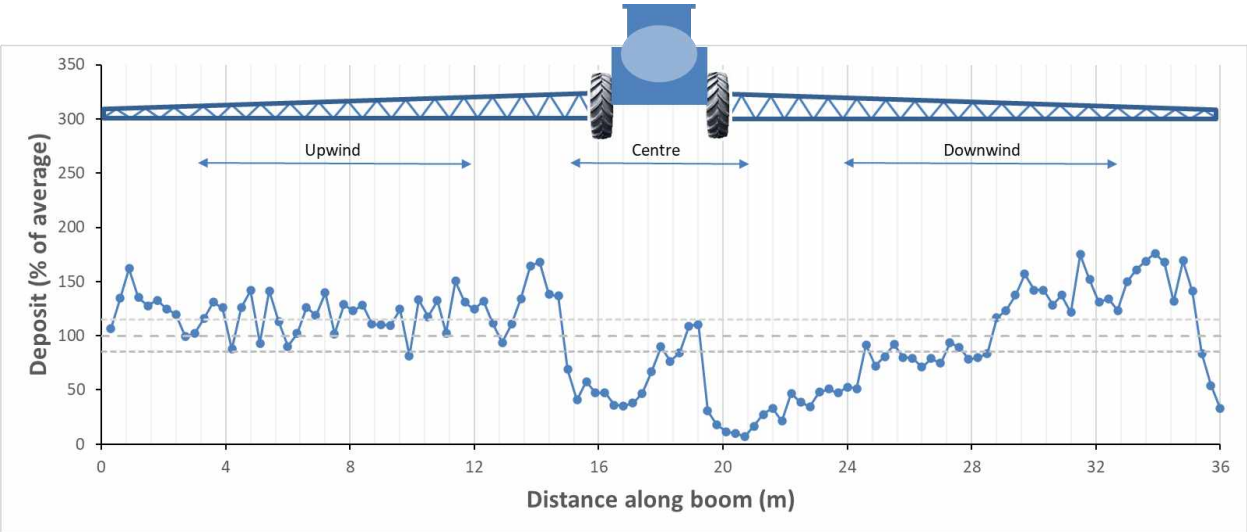

Figure 100: 19-02 L2 (LDX11004, 24", 17 mph)

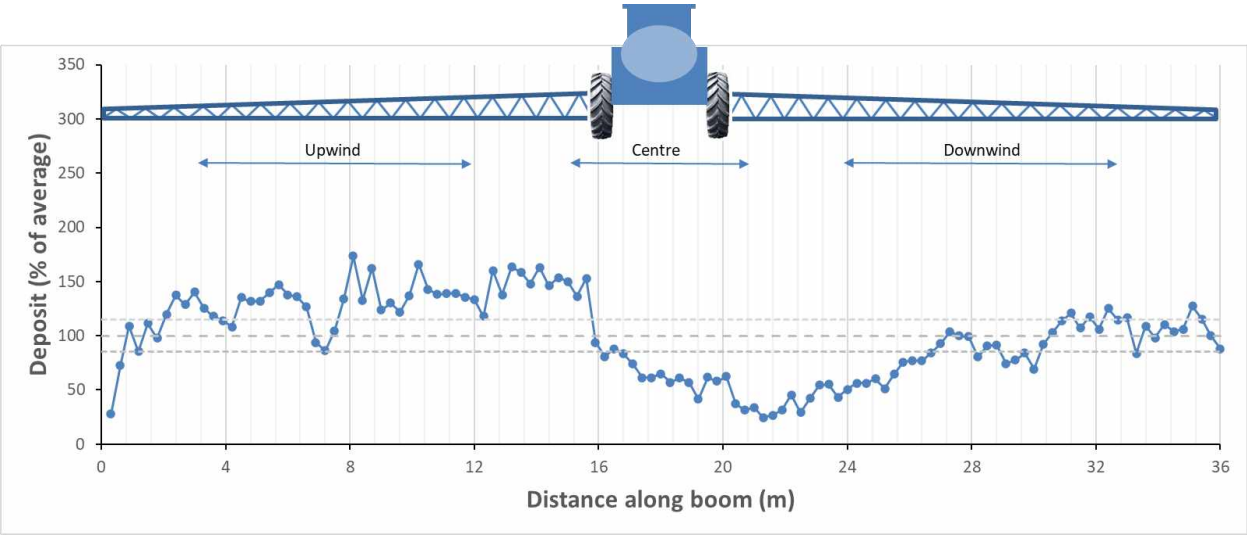

Figure 101: 19-02 L3 (LDX11004, 24", 17 mph)

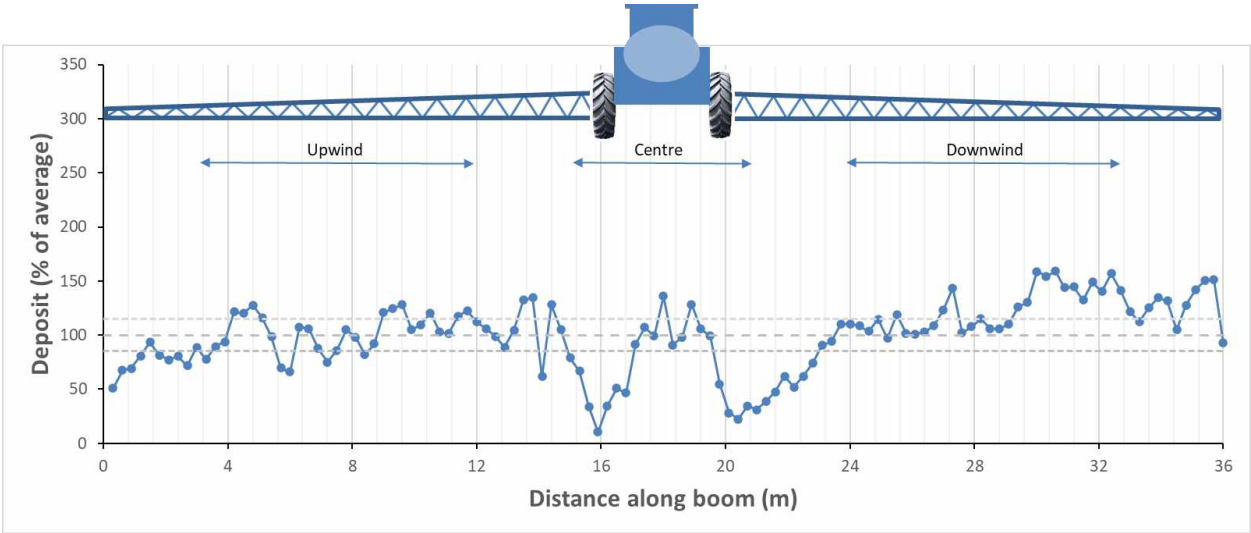

Figure 102: 19-03 L1 (LDX11004, 24", 17 mph)

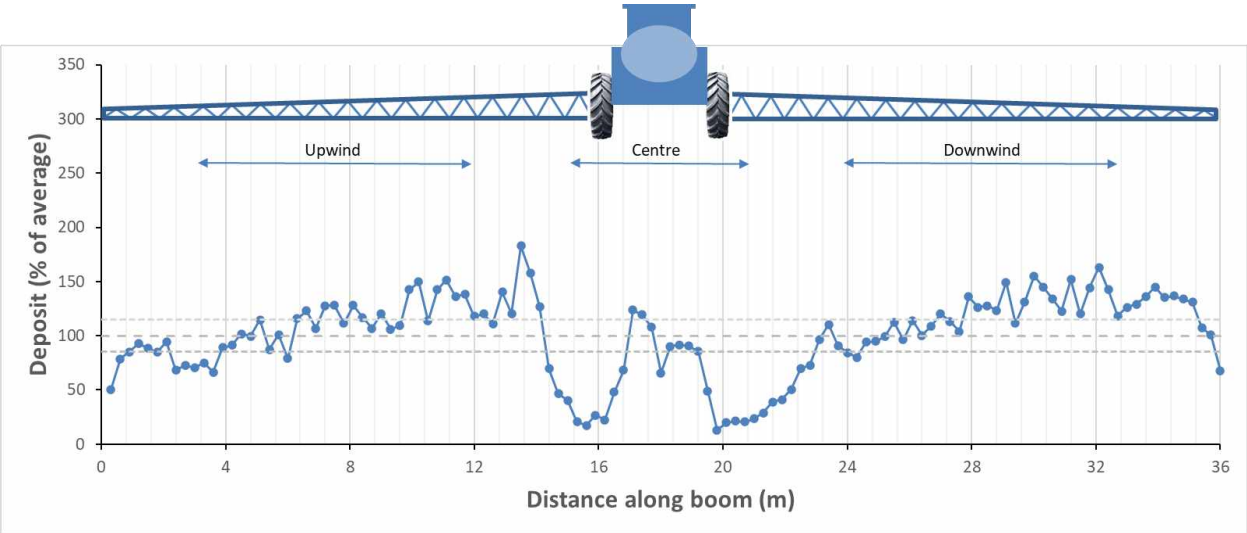

Figure 103: 19-03 L2 (LDX11004, 24", 17 mph)

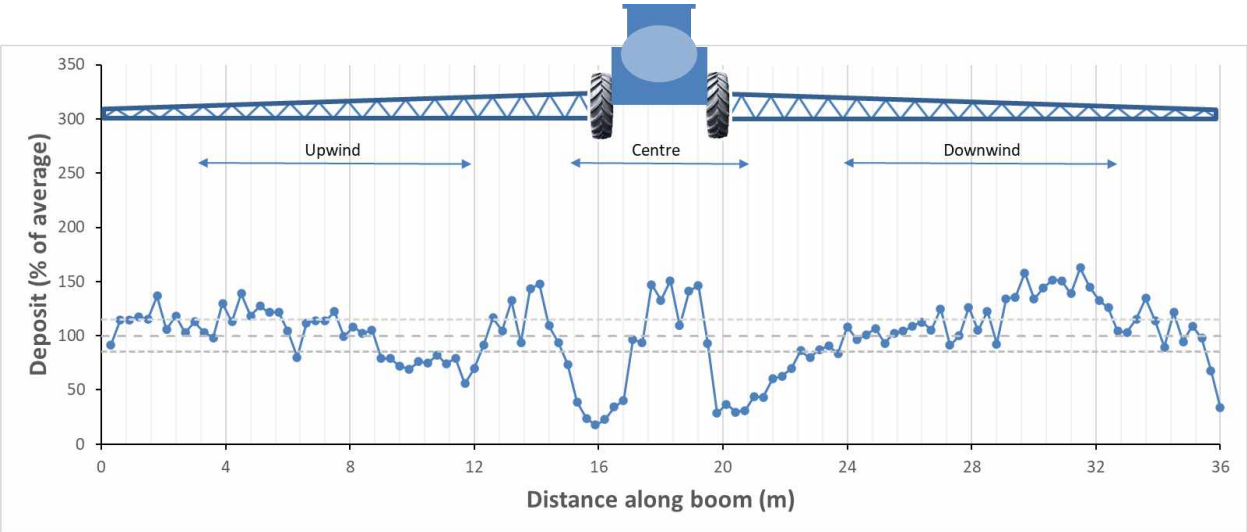

Figure 104: 19-03 L3 (LDX11004, 24", 17 mph)

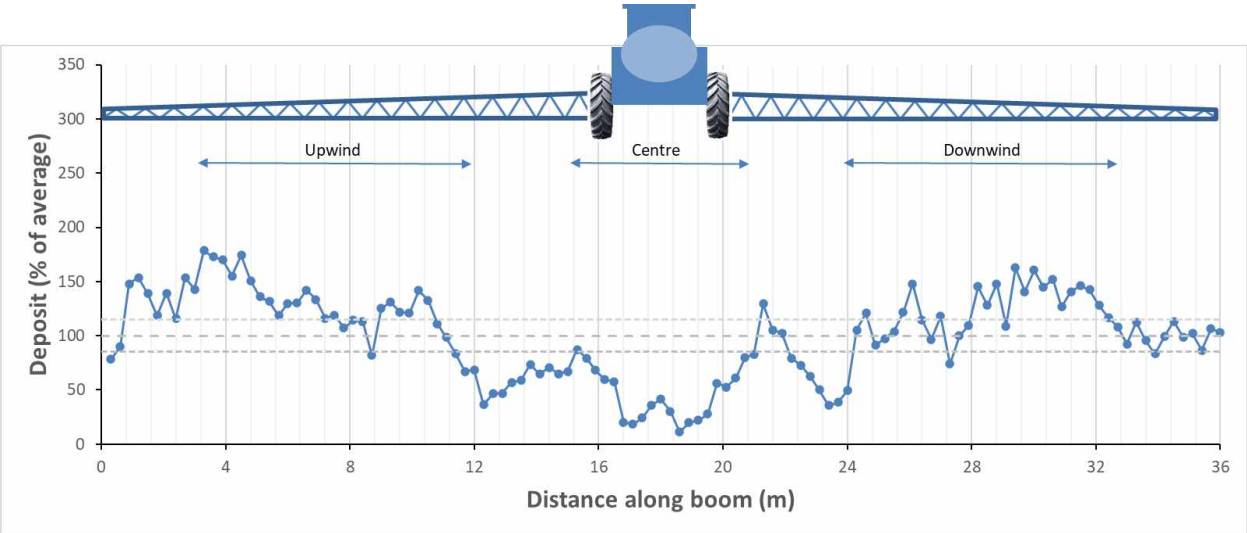

Figure 105: 19-04 L1 (LDX11004, 40", 17 mph)

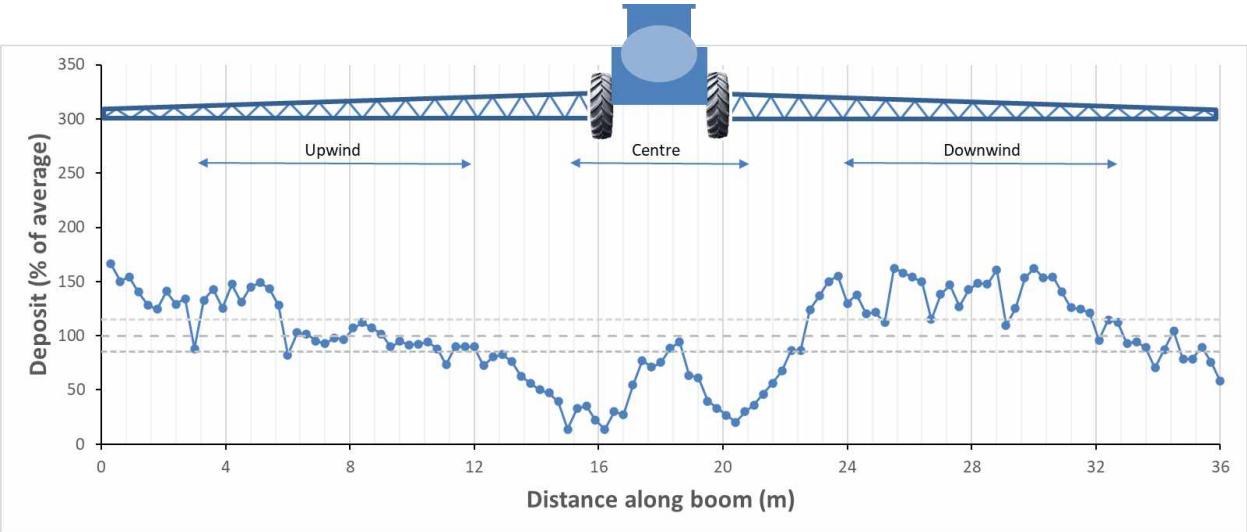

Figure 106: 19-04 L2 (LDX11004, 40", 17 mph)

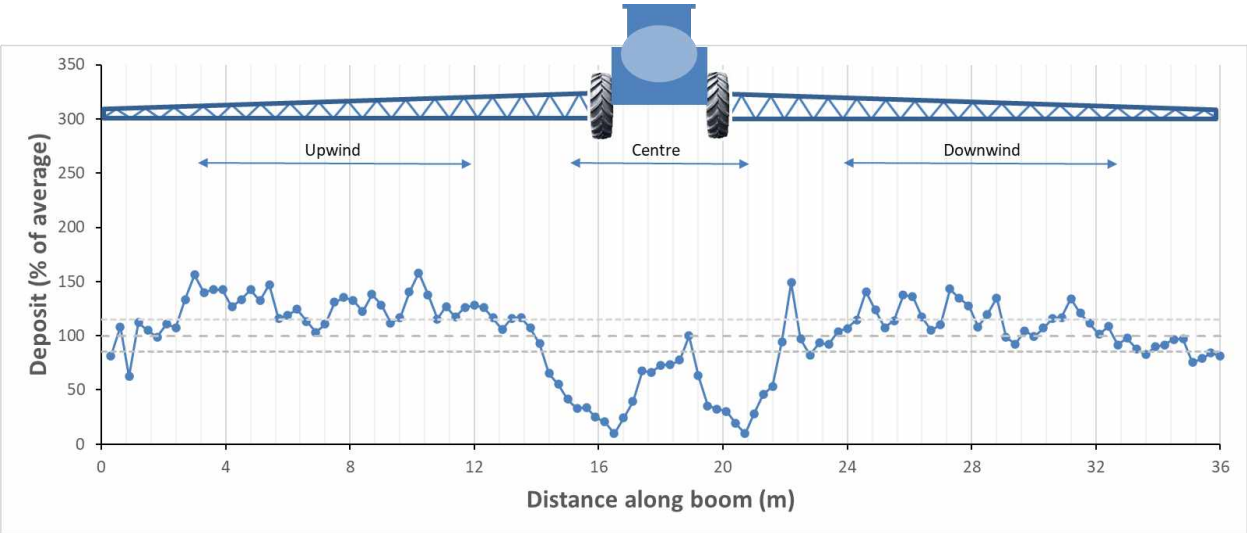

Figure 107: 19-04 L3 (LDX11004, 40", 17 mph)

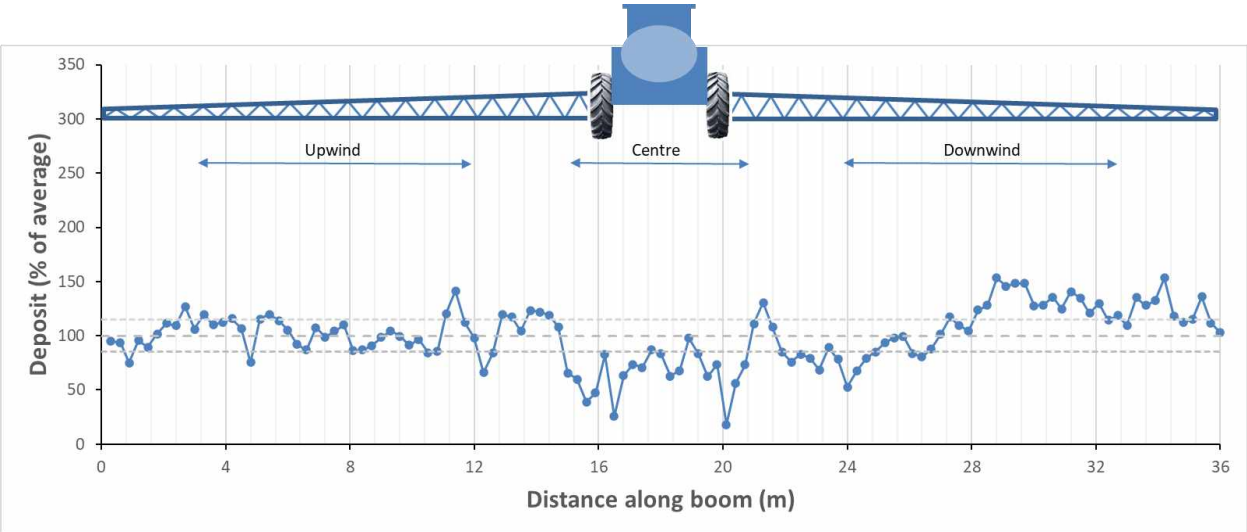

Figure 108: 19-05 L1 (LDX11004, 40", 7.3 mph)

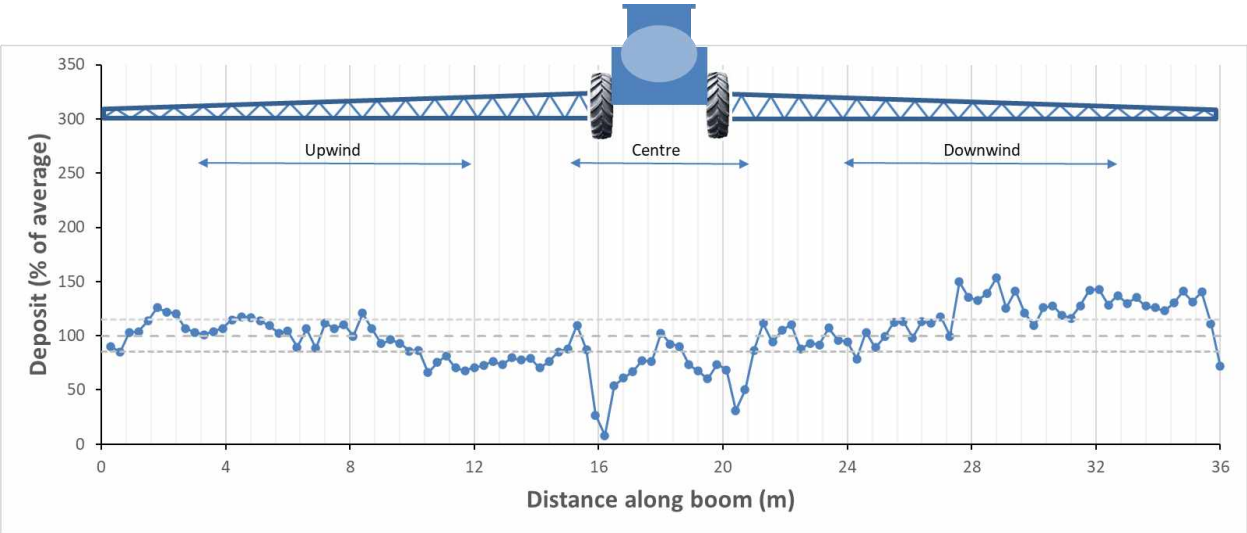

Figure 109: 19-05 L2 (LDX11004, 40", 7.3 mph)

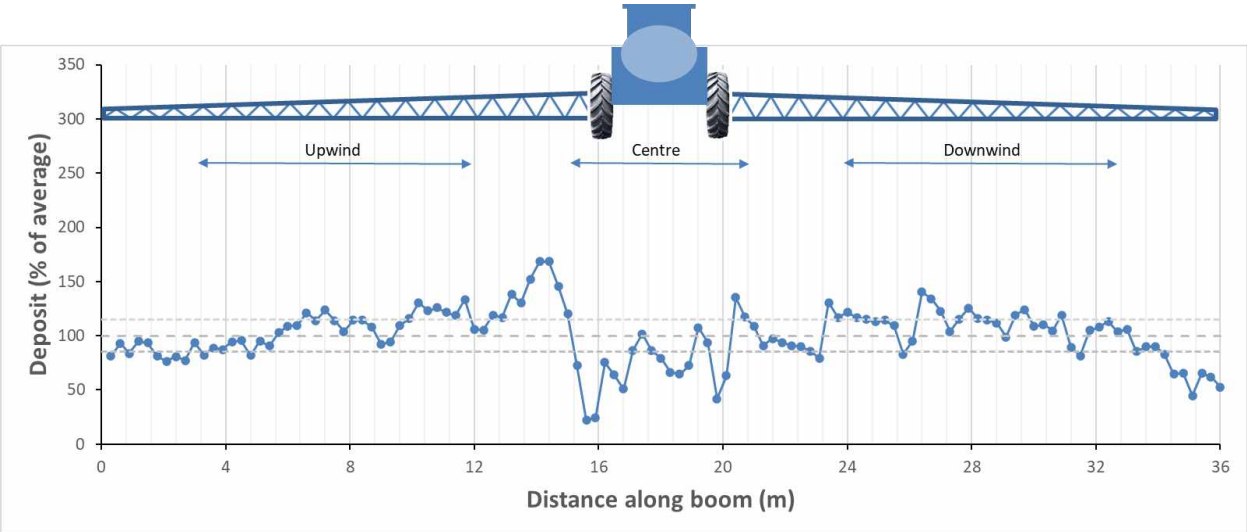

Figure 110: 19-05 L3 (LDX11004, 40", 7.3 mph)

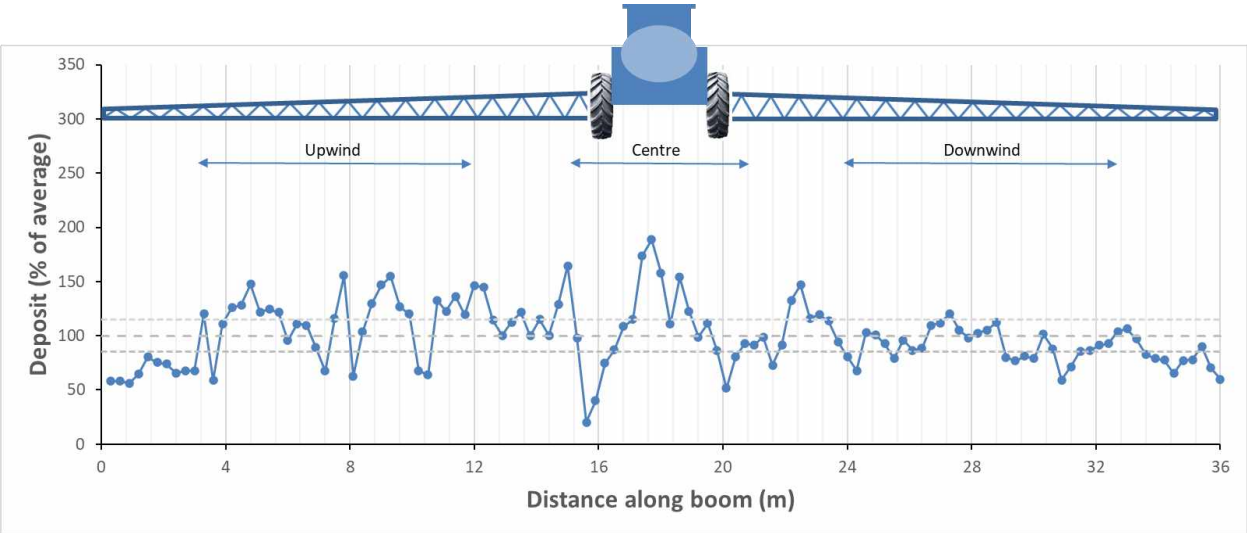

Figure 111: 19-06 L1 (LDX11004, 24", 7.3 mph)

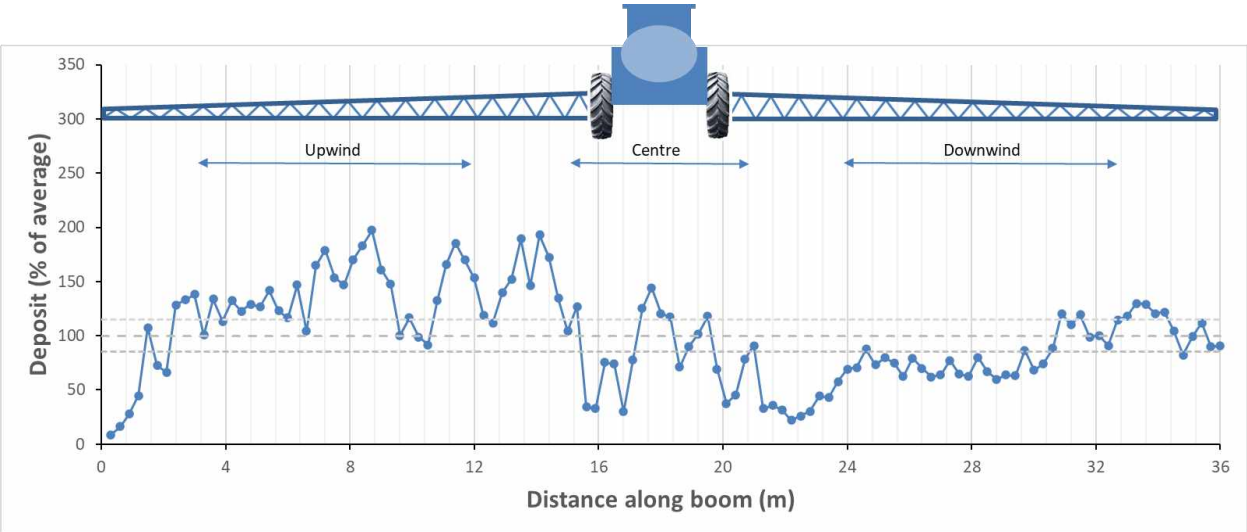

Figure 112: 19-06 L2 (LDX11004, 24", 7.3 mph)

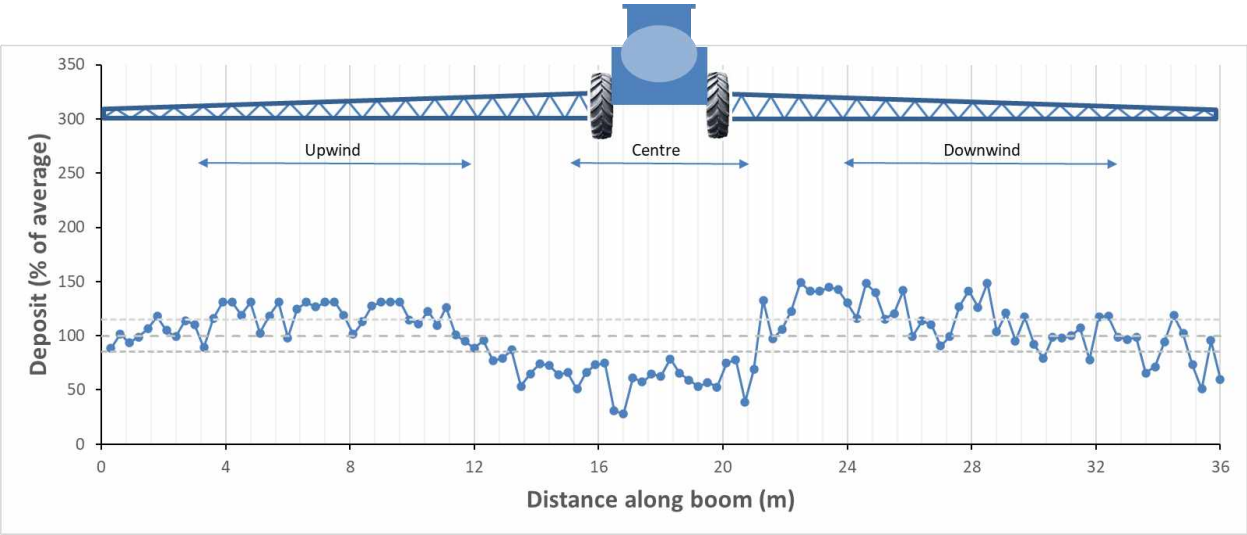

Figure 113: 19-06 L3 (LDX11004, 24", 7.3 mph)

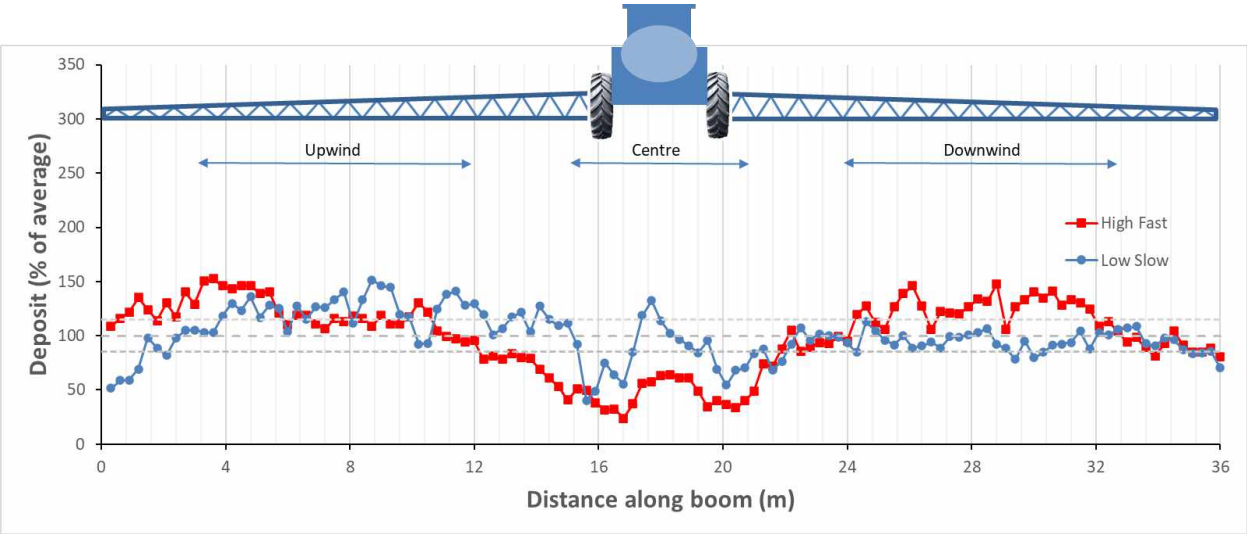

Figure 114: Average of replicate lines for "High & Fast" and "Low & Slow", 2019

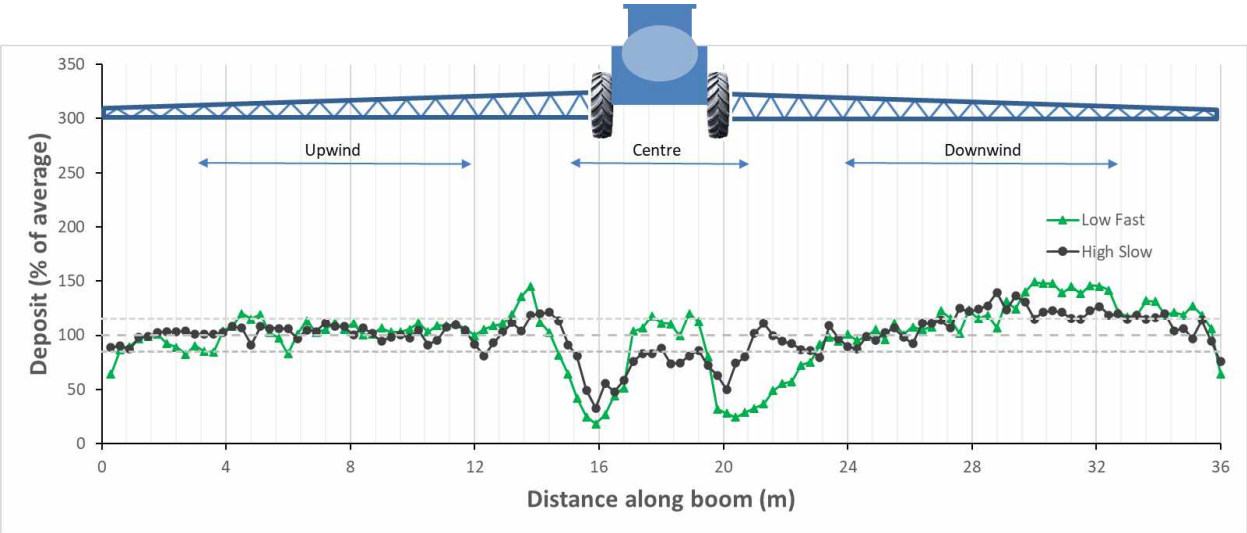

Figure 115: Average of replicate lines for "Low & Fast" and "High & Slow", 2019

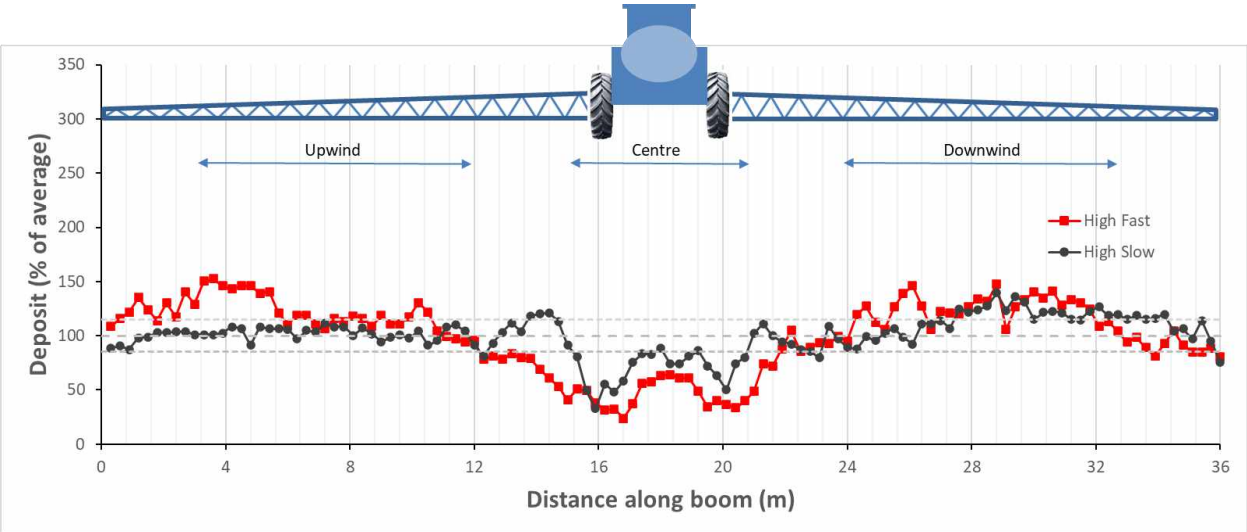

Figure 116: Average of replicate lines for "High & Fast" and "High & Slow", 2019

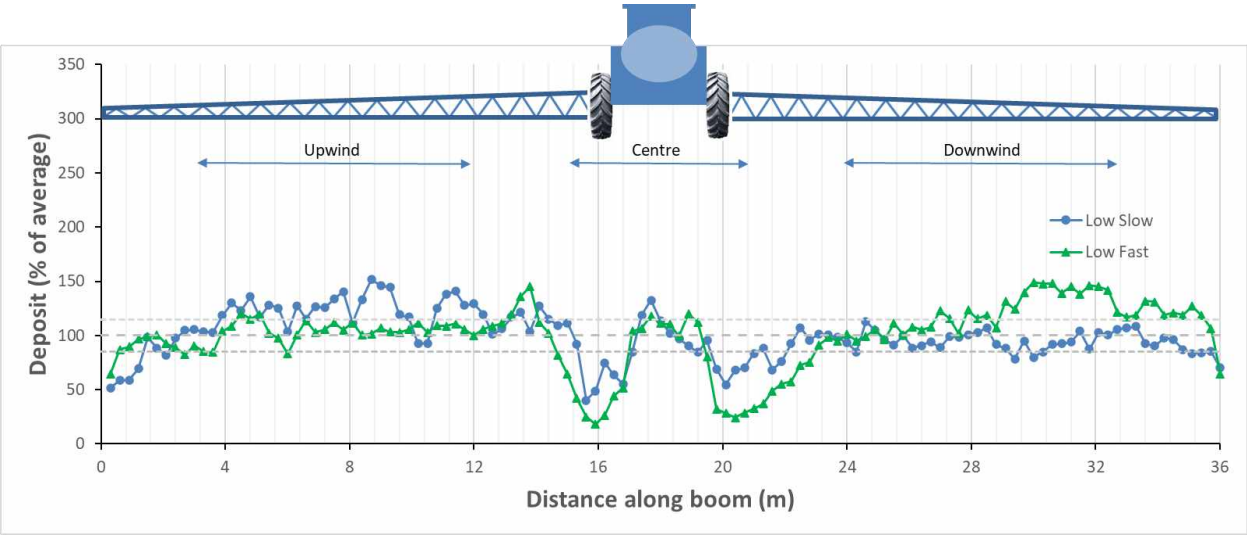

Figure 117: Average of replicate lines for "Low & Fast" and "Low & Fast", 2019

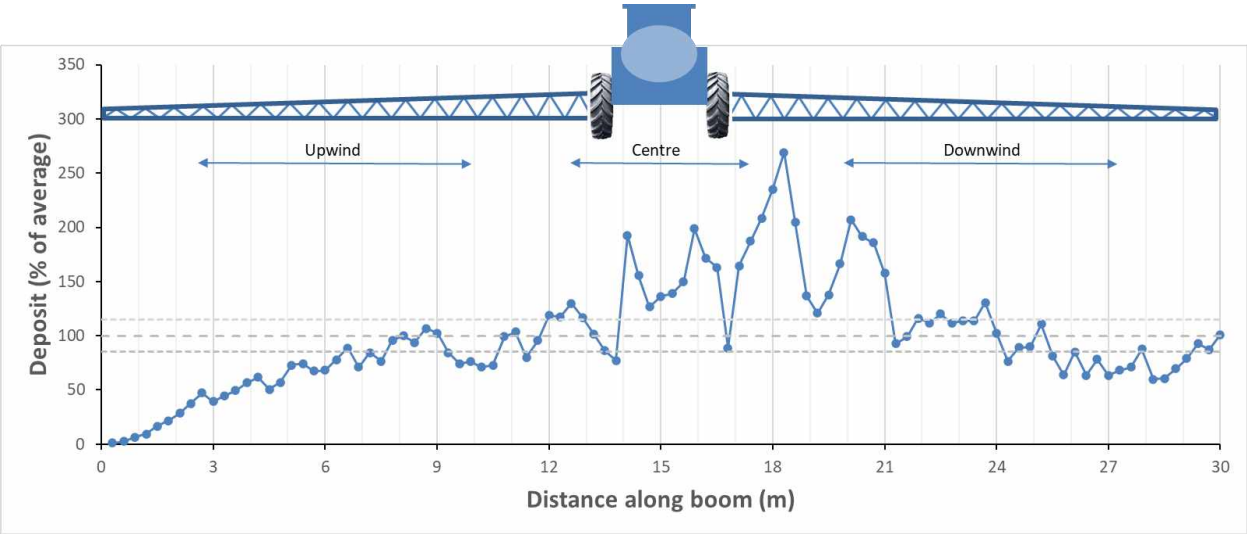

Figure 118: 20-01 L2 (LDA120035, 35", 18 mph)

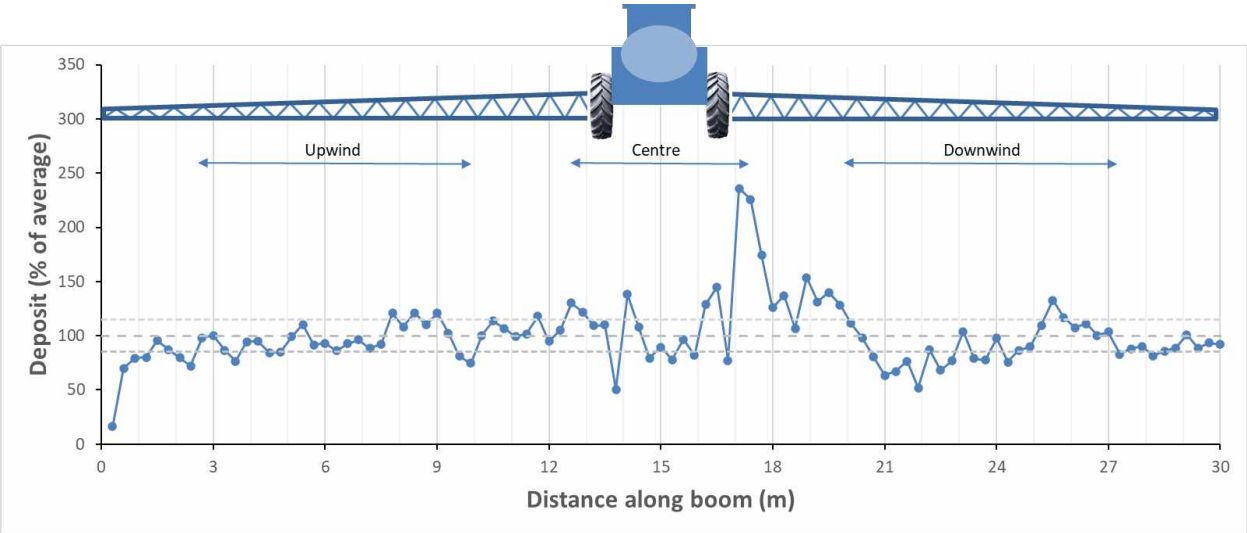

Figure 119: 20-01 L3 (LDA120035, 35", 18 mph)

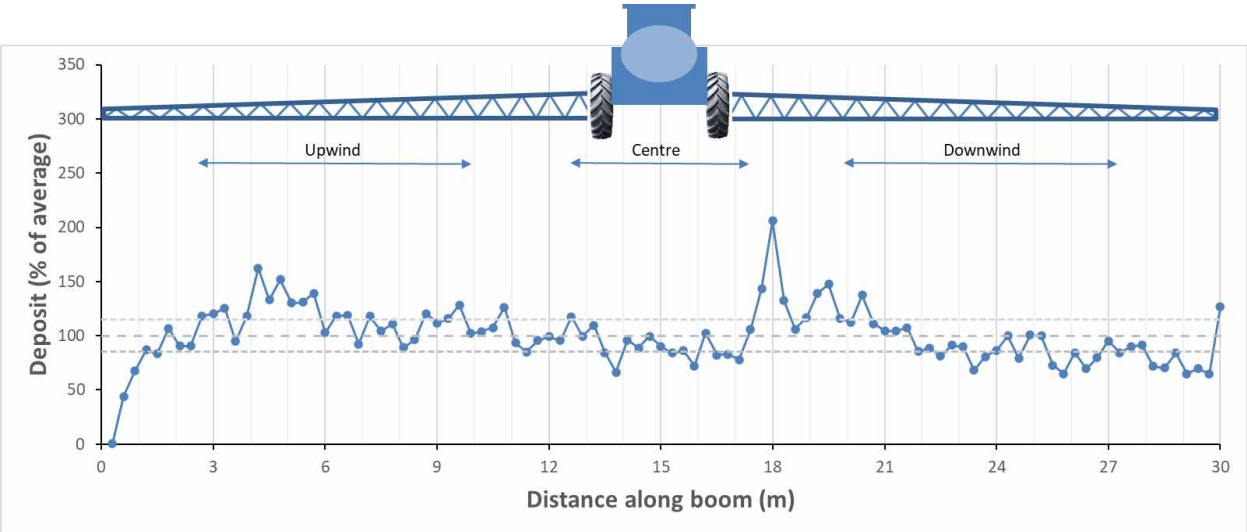

Figure 120: 20-02 L1 (LDA120035, 20", 9 mph)

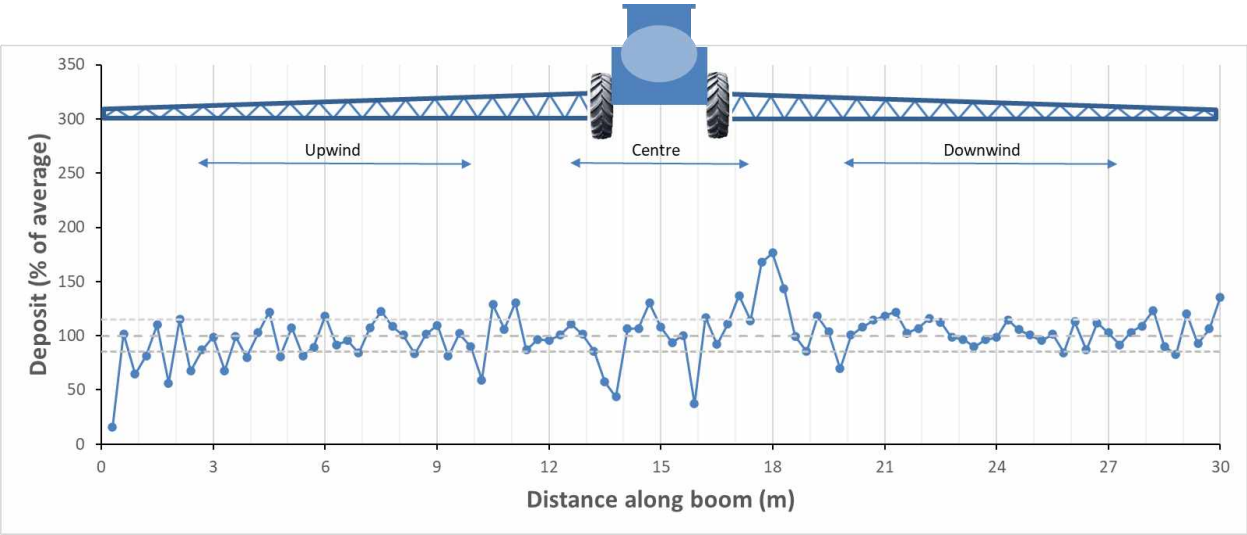

Figure 121: 20-02 L3 (LDA120035, 20", 9 mph)

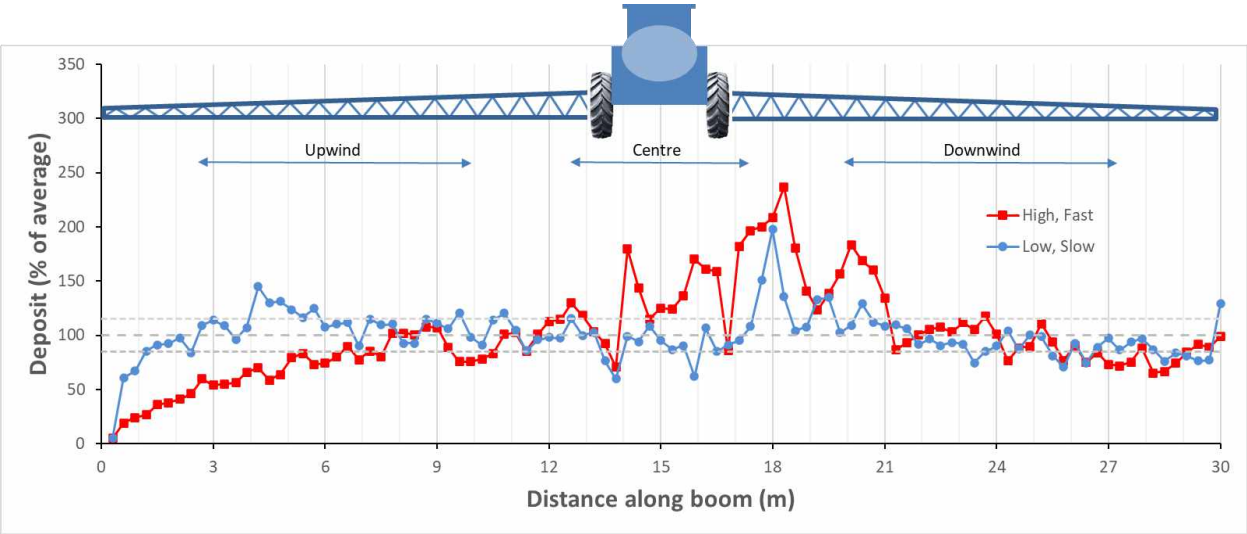

Figure 122: Average of 2 lines for 20-01 and 20-02 (LDA120035, "High & Fast" vs "Low & Slow")

Table 26: Summary statistics for string deposits along direction of travel

Trial	Spray Quality	Speed (mph)	Height (in)	Wind (km/h)	Mean	Range (Max-Min)	Ratio (Max / Min)	CV (%)	10th	50th	90th	Span
17-15 A	XC	15	25	7.9	139	114	2.6	17	110	141	170	0.43
17-16 B	XC	15	25	7.9	113	93	2.4	21	78	118	143	0.55
17-17 C	XC	15	25	7.9	107	83	2.3	18	77	108	135	0.54
17-18 D	XC	15	25	7.9	118	117	3.1	18	95	115	148	0.46
17-19 E	XC	15	25	7.9	101	72	2.1	17	75	100	125	0.50
17-21 G	C	15	25	20	229	207	2.6	20	173	214	293	0.56
17-22 H	C	15	25	20	186	162	2.3	21	135	181	237	0.56
17-23 I	C	15	25	20	155	83	1.7	12	130	154	183	0.34
17-24 J	C	15	25	20	143	100	2.0	15	113	141	171	0.41
17-25 K	C	15	25	20	124	70	1.8	12	103	124	145	0.34
Average		15	25	14	141	110	2.3	17	109	140	175	0.47

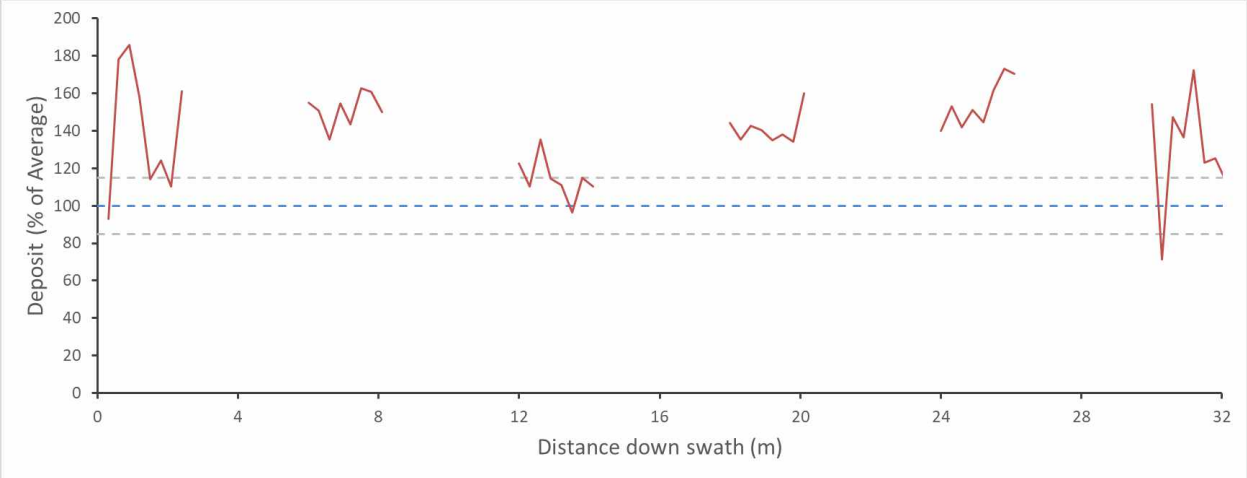

Figure 123: Spray deposits of Extremely Coarse spray in direction of travel, 4 m downwind from upwind edge of spray boom.

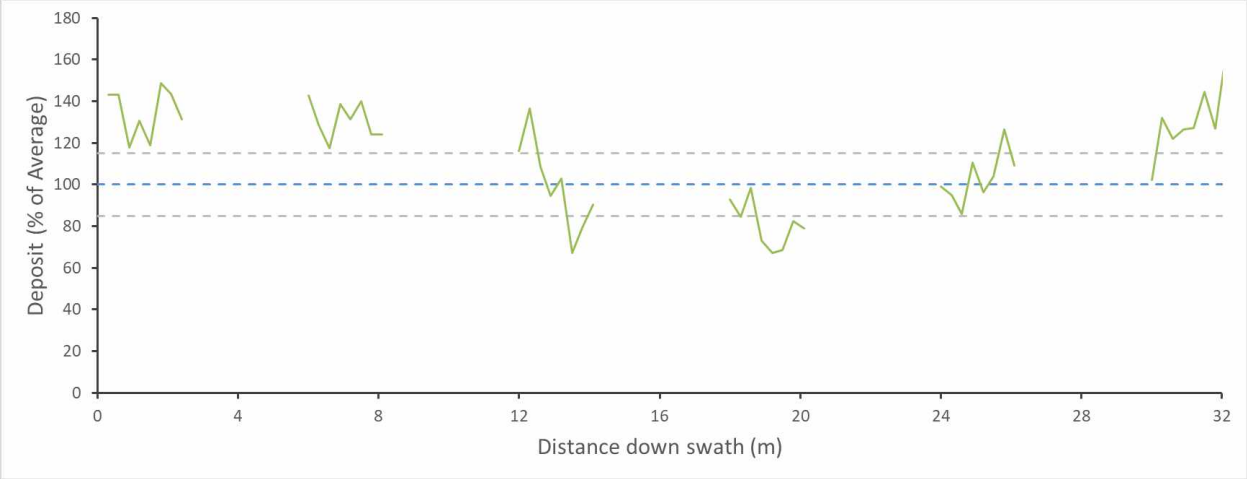

Figure 124: Spray deposits of Extremely Coarse spray in direction of travel, 11 m downwind from upwind edge of spray boom.

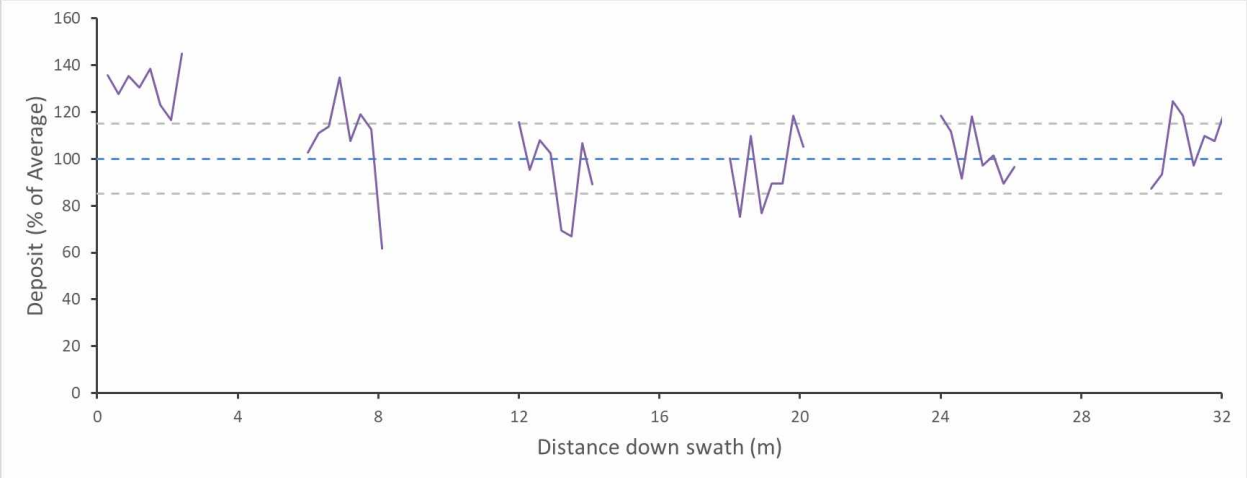

Figure 125: Spray deposits of Extremely Coarse spray in direction of travel, 15.5 m downwind from upwind edge of spray boom (0.5 m upwind of left wheel).

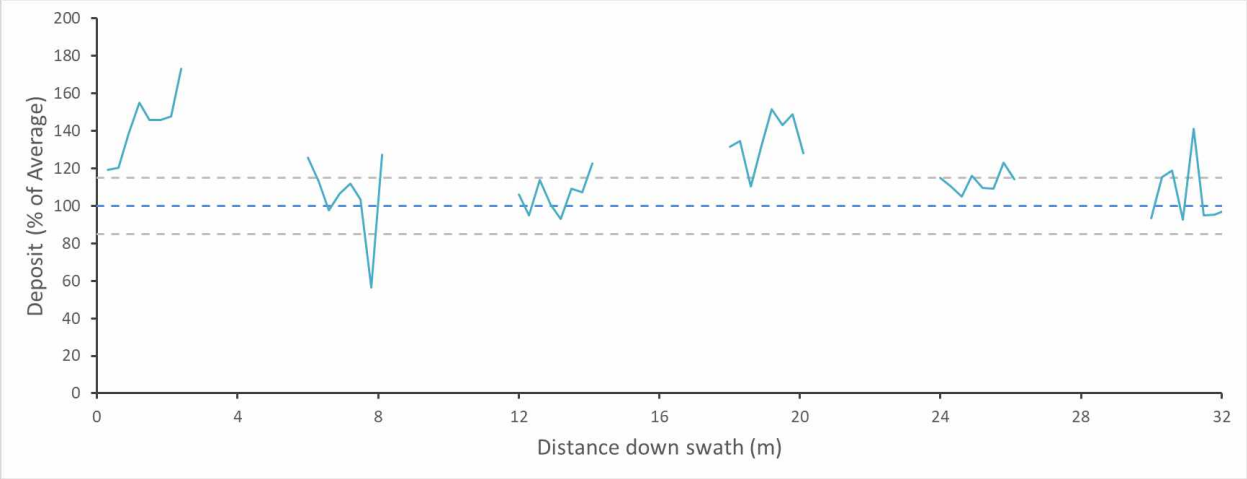

Figure 126: Spray deposits of Extremely Coarse spray in direction of travel, 18 m downwind from upwind edge of spray boom (centre of sprayer)).

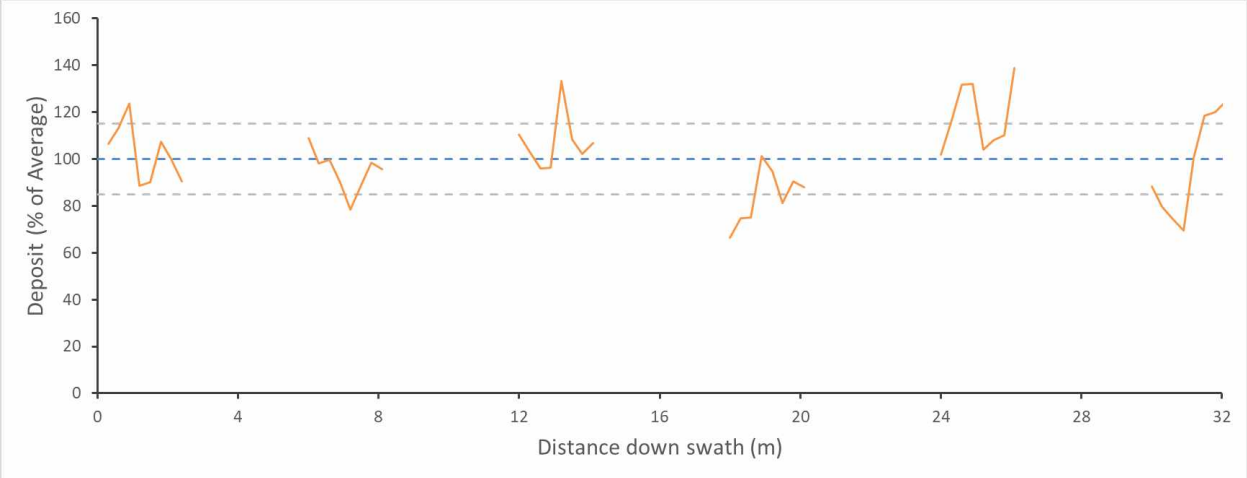

Figure 127: Spray deposits of Extremely Coarse spray in direction of travel, 20.5 m downwind from upwind edge of spray boom (0.5 m downwind of right wheel)

Appendix B

Budget

Cost Element (CDN $)	Year 1	Expenditure	Variance	Year 2	Expenditure	Variance	Year 3	Expenditure	Variance	TOTAL	Expenditure	Variance
Labour	$			$			$					
Professional (Agrimetrix)	14,750.00	14,750.00	-	16,000.00	16,000.00	-	15,750.00	15,750.00	-	46,500.00	46,500.00	-
Professional (PAMI)			-			-	36,000.00	36,158.25	158.25	36,000.00	36,158.25	158.25
Technical (Agrimetrix)	14,750.00	14,750.00	-	16,000.00	16,000.00	-	15,750.00	15,750.00	-	46,500.00	46,500.00	-
Technical (PAMI)												
Graduate Student(s)												
Other												
Equipment, Materials, Supplies & Incidentals												
Equipment	10,000.00	10,173.95	173.95	5,000.00	2,463.97	-2,536.03	5,000.00	7,604.50	2,604.50	20,000.00	20,242.42	242.42
Materials, Supplies & Incidentals	10,000.00	7,828.20	-2,171.80	5,000.00	6,621.55	1,621.55	10,000.00	11,381.24	1,381.24	25,000.00	25,830.99	830.99
Travel	7,000.00	7,008.46	8.46	7,000.00	7,357.11	357.11	5,000.00	3,473.27	-1,526.73	19,000.00	17,838.84	-1,161.16
Publication							2,000.00	1,900.00	- 100.00	2,000.00	1,900.00	- 100.00
Total Annual Costs	**56,500.00**	**54,510.61**	**-1,989.39**	**49,000.00**	**48,442.63**	**- 557.37**	**89,500.00**	**92,017.26**	**2,517.26**	**195,000.00**	**194,970.50**	**-29.50**